Geo-Bio Interfaces (2025), **2**, e10, 1–25
doi:10.1180/gbi.2025.10003

CAMBRIDGE UNIVERSITY PRESS

Review

The aerobic biosphere as an O_2 sink before the Great Oxygenation Event: geobiological feedback to solid Earth and surface oxidation

Eric Runge[1,2], Sara Vulpius[3], Daniel Herwartz[4], Andreas Pack[1], Caroline Brachmann[3,5] and Lena Noack[3]

[1]Geoscience Center, University of Göttingen, Göttingen, Germany; [2]Department of Biology and Environmental Science, Linnaeus University, Kalmar, Sweden; [3]Institute of Geological Sciences, Freie Universität Berlin, Berlin, Germany; [4]Department of Geosciences, Ruhr University Bochum, Bochum, Germany; and [5]German Aerospace Center, Berlin, Germany

Abstract

Microbial O_2 production via oxygenic photosynthesis was vital in oxygenating the Earth's surface environment during the Great Oxygenation Event (GOE) ca. 2.5 to 2.3 billion years ago. However, geochemical, paleontological and genomic data suggest the emergence of oxygenic photosynthesis precedes the GOE by at least 500 million years. This demonstrates that the first appearance of microbial O_2 in the environment cannot explain the timing of atmospheric oxygenation. Instead, the GOE was facilitated by Earth's geodynamic evolution, expanding cyanobacterial habitats and the changing redox state of the mantle, decreasing the abundance of reduced surface rocks, volcanic gases and aqueous solutes. These trends ultimately resulted in magnified O_2 production rates and diminished O_2 consumption rates. Thus, the GOE can be understood as a misbalance between O_2 sources and sinks. One of the most critical O_2 sinks on modern Earth is microbial O_2 consumption via aerobic respiration, and accumulating evidence suggests its emergence well before the GOE. However, the role of aerobic microorganisms as an O_2 sink delaying the GOE remains poorly explored. Here, we review the redox evolution of Earth's mantle and surface environments, as well as the Archean evolution of aerobic microbial metabolisms. Oxygenic photosynthesis released O_2 to the environment, but the secular oxidation of the solid Earth was critical in allowing O_2 accumulation. Aerobic respiration expanded in response to the GOE, but our survey suggests it could have been a critical O_2 sink even earlier. Hence, aerobic respiration can be seen as geobiological feedback to changes in the Earth system from deep in the mantle up to the surface. However, the timing and rate of O_2 consumption by aerobic respiration before the GOE remain poorly constrained. We conclude by highlighting open questions and future research directions to understand the role of the aerobic O_2 sink in delaying the GOE.

Keywords: Great Oxygenation Event; early Earth; habitability; biogeosphere; redox

(Received 13 November 2024; revised 21 May 2025; manuscript accepted: 22 May 2025)

Introduction

The Great Oxygenation Event (GOE) occurred 2.5 to 2.3 billion years ago (Ga) and was one of the most significant revolutions in the Earth system. It was marked by an increase in atmospheric O_2 by several orders of magnitude sourced from oxygenic photosynthesis (Lyons *et al.*, 2021) (Table 1). The accumulation of atmospheric O_2 changed the redox state of Earth's surface environment (Lyons *et al.*, 2014; Ostrander *et al.*, 2021), the mineralogical composition of the Earth (Hazen *et al.*, 2008) and allowed for major biological innovations, including the much later evolution of eukaryotic organisms and the Cambrian explosion (David and Alm, 2011; Zhang *et al.*, 2014; Mills *et al.*, 2022). This also has astrobiological implications because high O_2 concentrations in an exoplanet's atmosphere could point to the existence of an oxygenic biosphere, although alternative abiotic explanations for O_2 production exist (Meadows *et al.*, 2018; Schwieterman *et al.*, 2018). For these reasons, understanding the driving mechanisms of the GOE is important across various disciplines within the Earth and life sciences.

Much attention has been given to dating the emergence of oxygenic photosynthesis. Attempts at doing so included various putative biosignatures, like stromatolites in photic paleoenvironments, microfossils of cyanobacteria, carbon isotope signatures of photoautotrophic carbon fixation, lipid biomarkers in Archean rocks, as well as biogeochemical models (e.g. Buick, 1992; Schopf, 1993; Mojzsis *et al.*, 1996; Hofmann *et al.*, 1999; Brocks, 1999; Schidlowski, 2001; Kopp *et al.*, 2005). Many of these approaches are regarded as controversial (Brasier *et al.*, 2005; Rasmussen *et al.*, 2008; French *et al.*, 2015). These controversies have yielded a broad timespan for the possible emergence of oxygenic photosynthesis (ca. 3.5 to ca. 2.4 Ga). Molecular clock studies add a relatively recent approach to the problem. Using calibration points from the rock record, these studies point to an emergence of oxygenic photosynthesis at ca. 3.0 Ga, i.e. several hundred million years (m.y.) before the GOE (Schirrmeister *et al.*, 2015; Sánchez-Baracaldo, 2015; Cardona *et al.*, 2019; Garcia-Pichel *et al.*, 2019; Jabłońska and

Corresponding author: Eric Runge; Email: eric.runge@lnu.se
Cite this article: Runge E., Vulpius S., Herwartz D., Pack A., Brachmann C., & Noack L. (2025). The aerobic biosphere as an O_2 sink before the Great Oxygenation Event: geobiological feedback to solid Earth and surface oxidation. *Geo-Bio Interfaces* **2**, e10, 1–25. https://doi.org/10.1180/gbi.2025.10003

Table 1. Net reactions of microbial metabolism discussed in this paper (Konhauser, 2007).

Metabolism	Net reaction
Oxygenic photosynthesis	$CO_2 + H_2O \rightarrow CH_2O + O_2$
Aerobic respiration	$CH_2O + O_2 \rightarrow CO_2 + H_2O$
Methanogenesis (hydrogenotrophic) Methanogenesis (acetoclastic)	$4H_2 + CO_2 \rightarrow CH_4 + 2H_2O$ $CH_3COOH \rightarrow CH_4 + CO_2$
Aerobic methanotrophy	$CH_4 + O_2 \rightarrow CO_2 + H_2$
Aerobic NH_4^+ oxidation (nitrification)	$NH_4^+ + 1.5O_2 \rightarrow NO_2^- + H_2O + 2H^+$ $NO_2^- + 0.5O_2 \rightarrow NO_3^-$
Anaerobic NH_4^+ oxidation (anammox)	$NO_2^- + NH_4^+ \rightarrow N_2 + 2H_2O$
Microaerophilic Fe oxidation	$4Fe^{2+} + 0.5O_2 + 2H^+ \rightarrow 2Fe^{3+} + H_2O$
Microbial Mn oxidation	$Mn^{2+} + 0.5O_2 + H_2O \rightarrow Mn(IV)O_2 + 2H^+$
Microaerophilic S oxidation	$H_2S + 0.5O_2 \rightarrow S^0 + H_2O$ $S^0 + 1.5O_2 + H_2O \rightarrow H_2SO_4$

Tawfik, 2021; Fournier *et al.*, 2021; Boden *et al.*, 2024; but see Soo *et al.*, 2017). This timing is compatible with geochemical proxies indicating oxidative weathering *in situ* benthic microbial mats, local O_2 levels of few to few tens of μM, or transient "whiffs" of O_2 (reviewed in Ostrander et al., 2021). Apparently, Earth's atmosphere remained anoxic for at least 500 m.y. while oxygenic photosynthesis was already occurring. This delay of the GOE is one of its central conundrums.

Suggested ideas to solve this problem involve either an increasing rate of biological O_2 production or a decreasing O_2 consumption rate during the 500 m.y. preceding the GOE (e.g. Konhauser *et al.*, 2017; Catling and Zahnle, 2020; Lyons *et al.*, 2024). Thus, the GOE can be understood as the tipping point reached when O_2 production rates by oxygenic photosynthesis exceeded the O_2 consumption rates of all sinks. These sinks include reduced species such as volcanic gases in the atmosphere (e.g. H_2, CH_4), aqueous solutes (e.g. Fe^{2+}, Mn^{2+}), minerals in surface rocks (e.g. pyrite, uraninite) or sedimentary organic matter. The capacities of these sinks are, to a large degree, constrained by the redox evolution of the solid Earth. However, microorganisms have modulated the balance of Earth's redox buffers by catalysing otherwise inhibited chemical reactions since life emerged more than 3.5 Ga (e.g. Falkowski *et al.*, 2008; Knoll *et al.*, 2016; Ostrander *et al.*, 2021; Runge *et al.*, 2023). Thus, the Earth's buffering capacity against oxygenation can only be understood by integrating abiotic and biotic processes from deep in the mantle to the surface. Notably, advances in experimental microbiology and microbial ecology showed that microorganisms in diverse environments consume O_2 below the canonical lower limit for aerobic respiration (i.e. the 'Pasteur point', 2.2 μM O_2 at 25°C in seawater, e.g. Stolper *et al.*, 2010; Berg *et al.*, 2019; Ruff *et al.*, 2023) (Table 1). Given the emergence of oxygenic photosynthesis at ca. 3.0 Ga, it seems plausible that the early production of biological O_2 created aerobic niches since the mid-Archean. Nevertheless, the role of aerobic microorganisms as an O_2 sink delaying the GOE remains poorly understood.

Here, we review the redox evolution of the solid Earth and its surface environments from planetary accretion to the GOE, aiming to explore the role of microbial O_2 sinks in the Archean Earth. First, we reconstruct the solid Earth's redox evolution, which constrains the capacity of its abiotic redox buffers and sets the stage on which microbial life proliferates. Then, we address the oxygenation of Earth's surface environments, including the atmosphere and hydrosphere. Finally, we review evidence for the role of microbial O_2 sources and sinks in the Archean. We highlight the complex interplay of abiotic and biotic processes in the substantial delay from the first biological O_2 production to the onset of atmospheric oxygenation. Our survey suggests that the Earth's aerobic biosphere is a crucial yet poorly understood Archean O_2 sink that must be better quantified to unravel the delay of the GOE.

The delayed GOE: asynchronous solid Earth and surface oxidation

The Earth's atmosphere and hydrosphere evolved from outgassing and condensation of volatiles from the mantle, therefore the solid Earth sets the stage for the evolution of the surface reservoir. It represents the reservoir from which the lithosphere, atmosphere, hydrosphere and biosphere evolved, thereby defining the Earth's overall buffering capacity against oxygenation. However, the subsequent evolution of Earth's redox state is also closely coupled to the evolution of life in its surface environments. This section reviews the deep-time redox evolution of Earth's interior and surface reservoirs.

The evolving redox state of the solid Earth in deep time

The fO_2 of Earth's present-day upper mantle is QFM ± 2 (Fig. 1, see Box 1), but it decreases with depth (e.g. Haggerty, 1978; Christie *et al.*, 1986; O'Neill and Wall, 1987; Wood and Virgo, 1989; Wood *et al.*, 1990; Ballhaus *et al.*, 1991; O'Neill, 1991; Holloway *et al.*, 1992; Kasting, 1993; McCammon, 2005; Frost and McCammon, 2008; Cottrell and Kelley, 2011; Trail *et al.*, 2011; Ardia *et al.*, 2013; Gaillard *et al.*, 2021; Yang *et al.*, 2022) (Fig. 2). The transition zone is assumed to have an fO_2 of about QFM – 4 (McCammon, 2005; Frost and McCammon, 2008; Ardia *et al.*, 2013; Yang *et al.*, 2022) and the lower mantle is supposed to have an fO_2 below QFM – 5 (Frost *et al.*, 2004; McCammon, 2005; Ardia *et al.*, 2013; Yang *et al.*, 2022).

In contrast to the present day, it is commonly thought that the Earth was initially reduced, with an fO_2 of IW – 2 (ca. QFM – 5.7) as a maximum value during core formation (before that, the fO_2 could have been even as low as IW – 5 or about QFM – 8.7; Wade and Wood, 2001, 2005; Rubie *et al.*, 2011, 2015; Scaillet and Gaillard,

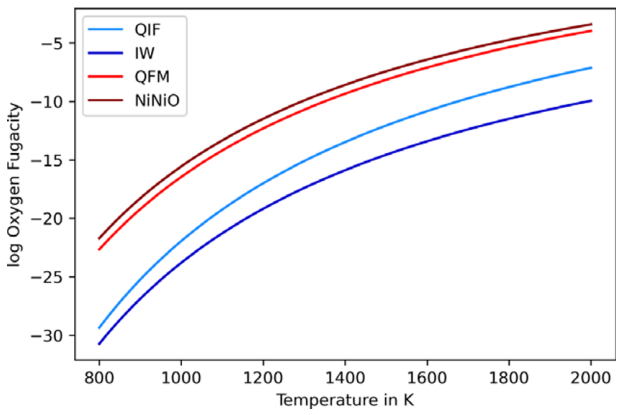

Figure 1. Commonly used mineral redox buffers and their relationship to fO_2 plotted over temperature. Quartz-fayalite-magnetite QFM) and nickel-nickel-oxide (NiNiO) depict oxidised conditions, while iron-wustite (IW) and quartz-iron-fayalite (QIF) represent reduced conditions.

https://doi.org/10.1180/gbi.2025.10003 Published online by Cambridge University Press

Box 1: Definition of the redox state and related terms

The term 'redox state' describes the oxidation potential of a system. In the context of this study, the system is the Earth mantle, crust, hydrosphere and atmosphere. 'Oxidising conditions' mean that elements, which occur in different oxidation states (e.g. Fe, Mn, Cr, S, C) predominantly occur in the oxidised state, e.g. Fe^{3+} or Mn^{4+}, whereas under 'reducing conditions', Fe predominantly occurs as Fe^{2+} and Mn as Mn^{2+}. The oxidation state can quantitatively be expressed in form of the oxygen fugacity fO_2, which is approximately equal to the equilibrium oxygen partial pressure pO_2. In reducing systems, fO_2 is low; in oxidising systems, fO_2 is high. Because the absolute numbers for fO_2 are very low (e.g. 10^{-10}), one expresses fO_2 as $\log_{10}(fO_2)$. An important buffer for the O_2 fugacity within planets is the Fe–FeO ('iron-wüstite', IW) buffer with:

$$Fe + \frac{1}{2}O_2 = FeO$$

Metallic iron (Fe) occurs in Fe–Ni alloys and FeO as a component in many silicate minerals. As long as Fe and FeO are present, fO_2 is fixed. For the reaction shown, the fO_2 would be fixed by the IW buffer. The absolute fO_2 varies with temperature and pressure. Oxygen fugacities that deviate from the fO_2 buffered by the IW buffer are conventionally expressed as fO_2 deviating in $\log_{10}$ units from fO_2 buffered by the IW buffer. An fO_2 that is two orders of magnitude lower (factor of 0.01) than buffered by the IW buffer at a given temperature would be termed $\log_{10}(fO_2) = IW - 2$. Other O_2 buffers exist, such as the quartz-fayalite-magnetite (QFM) buffer. However, the redox state is conventionally expressed in $\log_{10}$ units relative to fO_2 buffered by the IW buffer. The most reduced system known is the H_2-dominated solar nebula, where the fO_2 was buffered by the H_2–H_2O equilibrium to IW – 7. Modern rocks have a redox state in the range buffered by the QFM buffer, which is at about IW + 3.7.

The fO_2 determines the speciation of volatiles. If the fO_2 is low, the system is reducing, meaning that reduced species such as H_2, CO, CH_4, H_2S and NH_3 prevail. In contrast, if the fO_2 is high, the system is oxidising and oxidised species like H_2O, CO_2, SO_2 and N_2 are dominant (Kasting, 1993; Kasting *et al.*, 1993; Ballhaus and Frost, 1994; Holloway and Blank, 1994; Delano, 2001; Burgisser and Scaillet, 2007; Trail *et al.*, 2011; Gaillard *et al.*, 2015, 2021; Ortenzi *et al.*, 2020; Yang *et al.*, 2022). This demonstrates that the redox state is a fundamentally important parameter for the evolution of the Earth interior and surface system.

2011; Cartier *et al.*, 2014; Fischer *et al.*, 2015; Schaefer and Elkins-Tanton, 2018; Gaillard *et al.*, 2021) (Fig. 2). One argument for a reducing start of the Earth is the assumption that it initially accreted from highly reduced, volatile-depleted material (like enstatite chondrites). Another argument is that the metal–silicate equilibrium required for core formation suggests a considerably low fO_2. A low fO_2 enhances the siderophile behaviour of certain elements like nickel, cobalt, manganese, chromium, vanadium and silicon (Gessmann *et al.*, 1999; Wade and Wood, 2001, 2005; Rubie *et al.*, 2011, 2015; Scaillet and Gaillard, 2011; Siebert *et al.*, 2013; Cartier *et al.*, 2014; Fischer *et al.*, 2015; Schaefer and Elkins-Tanton, 2018; Gaillard *et al.*, 2021; but see Badro *et al.* (2015) for an alternative viewpoint).

Assuming reduced conditions early in Earth's history, its relatively oxidised state today requires oxidation over time (e.g. Wade and Wood, 2005; Cartier *et al.*, 2014; Schaefer and Elkins-Tanton, 2018; Gaillard *et al.*, 2021). Pahlevan *et al.* (2019) found that if the magma ocean was initially reduced, it must have evolved to a higher fO_2 (>IW + 1 or ~QFM – 2.7) during its final stages based on the D/H ratio. Moreover, Deng *et al.* (2020) suggested that the magma ocean had a vertical gradient in fO_2, with the upper layer reaching IW + 2 (~QFM – 1.7). However, it was also proposed that more oxidised, volatile-rich material (e.g. CI chondrites) was delivered during the last stages of accretion and core formation (e.g. Wänke *et al.*, 1984; Javoy, 1995; Wade and Wood, 2005; Schönbächler *et al.*, 2010; Rubie *et al.*, 2011; Scaillet and Gaillard, 2011; Marty, 2012; Cartier *et al.*, 2014; Fischer *et al.*, 2015; Dauphas, 2017; Fischer-Gödde and Kleine, 2017; Lammer *et al.*, 2018; Grewal *et al.*, 2019; Budde *et al.*, 2019; Fischer-Gödde *et al.*, 2020; Gaillard *et al.*, 2021). Rubie *et al.* (2011) concluded that 30–40% of the final mass accreted was rather oxidised, therefore the evolution towards a more oxidised planet probably occurred already during the formation of the Earth.

Besides the variation in the delivered material, the change in the Earth´s redox state during accretion can also be explained by the increasing size of the Earth (Wade and Wood, 2005). It was proposed that due to the higher pressures associated with the growth of the Earth, perovskite $(Mg,Fe,Al)(Al,Si)O_3$ becomes the dominant phase of the lower mantle (stable below 660 km depth in present-day Earth). Perovskite formation drives Fe(II) disproportionation to Fe(III) and Fe(0) via Eq. (1):

$$3Fe^{2+}O + Al_2O_3 = 2Fe^{3+}AlO_3 + Fe^0 \quad (1)$$

Because Fe(0) has been sequestered into the core, the lower mantle became relatively enriched in Fe(III). It was suggested that the upper mantle became enriched over time due to convection (Mao and Bell, 1977; Frost *et al.*, 2004, 2008; Wade and Wood,

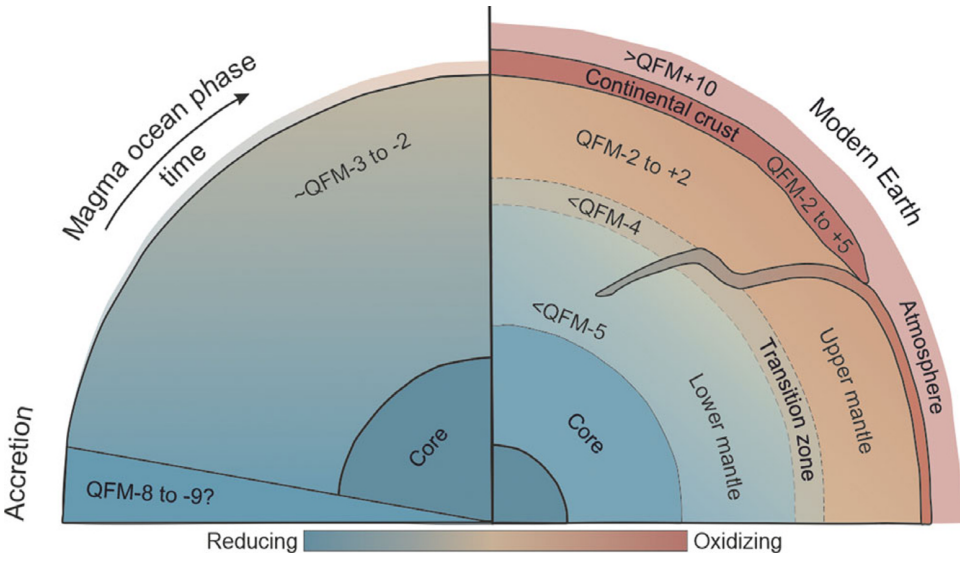

Figure 2. Evolution of the Earth´s redox state for different formation stages. The changing fO_2 is indicated by the deviation in log units from the quartz-fayalite-magnetite (QFM) buffer and is explained in the text. The colours range from blue (reduced) to red (oxidised). The Earth is assumed to become more oxidised with time, with the most reduced values during the accretion period before core formation. It is thought that during the magma ocean period, fO_2 evolved towards more oxidised values. The modern Earth is comparatively oxidised, with a decreasing redox state with depth (after McCammon, 2005). See the text for references on the redox state of the early Earth.

https://doi.org/10.1180/gbi.2025.10003 Published online by Cambridge University Press

2005). This transfer of Fe(III) from the lower to the upper mantle is also known as the 'oxygen pump' (Frost *et al.*, 2004, 2008; Wade and Wood, 2005). This process would also explain why the Martian mantle is more reduced than Earth (Righter and Drake, 1996; Herd *et al.*, 2001, 2002; Wadhwa, 2001, 2008; Wade and Wood, 2005; Righter *et al.*, 2008), even though Mars is enriched in volatiles and FeO. Perovskite is unstable in the Martian mantle due to its smaller size, resulting in lower lithostatic pressures, thus the self-oxidation of the mantle via perovskite formation could not occur on Mars (Wade and Wood, 2005). It was proposed that the preferential partitioning of Fe(III) into the liquid phase enhances the equilibration of the redox state between the lower and upper mantle by mixing processes (Carmichael, 1991; Scaillet and Gaillard, 2011). In addition, FeO and $FeO_{1.5}$ have different molar volumes and densities, further favouring a more oxidised upper mantle and a more reduced lower mantle (Deng *et al.*, 2020).

Alternatively, it was suggested that the oxidation of the mantle occurred directly during the magma ocean state (Schaefer and Elkins-Tanton, 2018; Pahlevan *et al.*, 2019). Accordingly, the sink and sequestration of iron metal into the core would leave behind an oxidised mantle without requiring crystallisation and whole-scale mantle mixing (Schaefer and Elkins-Tanton, 2018; Pahlevan *et al.*, 2019). In particular, the crystallising magma ocean would become progressively oxidised over time (Scaillet and Gaillard, 2011). Similar arguments have been brought forward for a carbon pump leading to the formation of diamonds in the lower mantle (causing oxidation) in case of a deep (potentially giant-impact-induced) magma ocean, which may explain the thick CO_2 atmosphere of Venus in the absence of a late giant impact (Armstrong *et al.*, 2019). Moreover, H_2 loss from the mantle by outgassing is also discussed as a mechanism for oxidising the upper mantle (Sharp *et al.*, 2013).

It has also been suggested that recycling of surface material could have oxidised the upper part of the mantle (Arculus, 1985; Kasting, 1993; Kasting *et al.*, 1993; Kump *et al.*, 2001; Smart *et al.*, 2016; Nicklas *et al.*, 2019; Stagno and Aulbach, 2021). At least today, the material transported with the subducting slab is more oxidised than the surrounding mantle (e.g. Wood *et al.*, 1990; Ballhaus *et al.*, 1991; Blundy *et al.*, 1991). Mikhail and Sverjensky (2014) found that under oxidising conditions, N_2 is the dominant nitrogen species over NH_4^+. They argue that, during subduction, the increased fO_2 of the mantle wedges, compared to the surrounding upper mantle, results in N_2-rich fluids. The ascent and outgassing of such fluids allow an enhanced N_2 outgassing. Plate tectonics would, therefore, not only favour oxidised mantles and atmospheres but would also be needed for nitrogen-rich atmospheres like the Earth's.

Duncan and Dasgupta (2017) turned the argument around: if reduced material (like organic carbon) was subducted, then this may have led to a transient increase of biological O_2 in the atmosphere by removing reducing power from the surface reservoir. At the same time, it would lead to a reducing effect on the mantle (unless permanently sequestered into a hidden reservoir) and result in releasing reducing gases into the atmosphere on melting.

The estimates on when the upper mantle was oxidised to near-modern values range from 4.4 to 2.7 Ga (e.g. Canil, 1997; Delano, 2001; Lee *et al.*, 2003; Li and Lee, 2004; Foley, 2011; Scaillet and Gaillard, 2011; Trail *et al.*, 2011; Aulbach and Stagno, 2016; Rollinson *et al.*, 2017; Nicklas *et al.*, 2018, 2019) (Figs 3, 4a). An important archive for understanding the redox state of the early Earth's mantle is the cerium concentration in zircons ($ZrSiO_4$) (Loucks *et al.*, 2020). Cerium exists in both tri- and quadrivalent states in silicate melts. Zircons crystallising from these melts preferentially incorporate Ce^{4+} over Ce^{3+}, substituting for Zr^{4+} in the

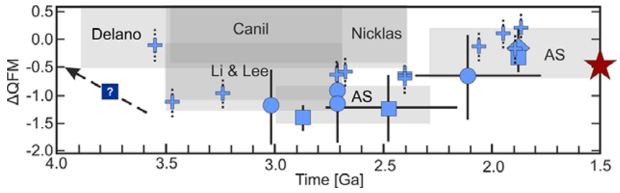

Figure 3. Literature estimates regarding the fO_2 of the upper mantle on early Earth (after Aulbach and Stagno, 2016; Schaefer and Elkins-Tanton, 2018; Stagno and Aulbach, 2021). The shaded rectangles represent the results of the fO_2 estimated from individual studies (normalised to the QFM buffer) over the respective ages of the samples examined. The references for the horizontal rectangles are Canil (1997), Delano (2001), Li and Lee (2004), Nicklas *et al.* (2018, 2019), Aulbach and Stagno (2016) (AS), Aulbach *et al.* (2017). The crosses are data points from Nicklas *et al.* (2018) and Nicklas *et al.* (2019) that represent an estimated fO_2 based on the redox-dependent partitioning of vanadium between liquidus olivine and melt. The squares are orogenic eclogites, the circles are mantle eclogites and the diamond is a mid-ocean ridge ophiolite from Aulbach and Stagno (2016). The symbols display the fO_2 (corrected to 1 GPa) calculated from V/Sc ratios. The vertical error bars are predicted 1σ errors of the V/Sc ratios (representing 1σ of the mean per sample suite) and the horizontal error bars show age ranges or 1σ errors for isochron ages from the literature. The red star shows the calculated fO_2 of the modern MORB and the arrow points toward the estimated fO_2 of the uppermost mantle according to Trail *et al.* (2011) of samples from 4.4 Ga. QFM, quartz-fayalite-magnetite.

zircon crystal structure. The ratio of Ce^{4+} to Ce^{3+} is influenced by the fO_2 of the melt. As a result, the cerium concentration in magmatic zircons can indicate the oxygen content in the magma (Trail *et al.*, 2011). Trail *et al.* (2011) calibrated the relationship between the zircon/melt partitioning coefficient of cerium and the fO_2 of the melt. Using their different oxygen isotopic compositions, Trail *et al.* (2011) distinguished zircons derived from the mantle ($\delta^{18}O$ = +5.3‰) and those from the crust. The cerium concentration data of both populations indicated that the host magmas had similar fO_2 to the modern mantle, which has QFM ± 2 (Yang *et al.*, 2022). It was observed that the primary mantle melts were not saturated in zircon, but rather, the 'mantle' zircons crystallised in melt residues. The $\delta^{18}O$ values of these residues would still closely resemble the composition of the host mantle. At such fO_2 values, the outgassing of CO_2, N_2, H_2O, and SO_2 would dominate over more reduced species like CO, H_2, NH_3 and H_2O (Frost and McCammon, 2008).

The oxygen isotope ratios in these up to 4.4 Ga zircons have provided valuable insights into the history of early Earth's water cycle. Studies by Peck *et al.* (2001), Valley *et al.* (2002) and Cavosie *et al.* (2005) also examined oxygen isotope ratios in Hadean zircon, some of which yield elevated $\delta^{18}O$ values consistent with the assimilation of sediments or crustal material derived from low-temperature water–rock interactions. The isotopic signatures found in these zircons thus suggest the presence of liquid water on the Earth's surface during the Hadean as early as 4.4 Ga. These findings support the presence of a hydrosphere on Earth at that time. If correct, the $\delta^{18}O$ of the hydrosphere needs to be considered because the $\delta^{18}O$ of the early oceans may have been lower than the present oceans (Wallmann, 2001; Sengupta and Pack, 2018; Herwartz *et al.*, 2021; Tatzel *et al.*, 2022; Isson and Rauzi, 2024) and meteoric water generally comprises lower $\delta^{18}O$ than seawater. Due to the variability of $\delta^{18}O$ in the hydrosphere, water–rock interaction at high and low temperatures can result in a large range of silicate $\delta^{18}O$, and assimilation of such altered material is also known to generate low $\delta^{18}O$ magmas (Bindeman *et al.*, 2010; Herwartz *et al.*, 2015; Zakharov *et al.*, 2019). In general, assimilation of the altered mafic crust may not lead to elevated $\delta^{18}O$ of magmas from which the zircons crystallised, therefore a mantle-like $\delta^{18}O$ of Hadean zircons

https://doi.org/10.1180/gbi.2025.10003 Published online by Cambridge University Press

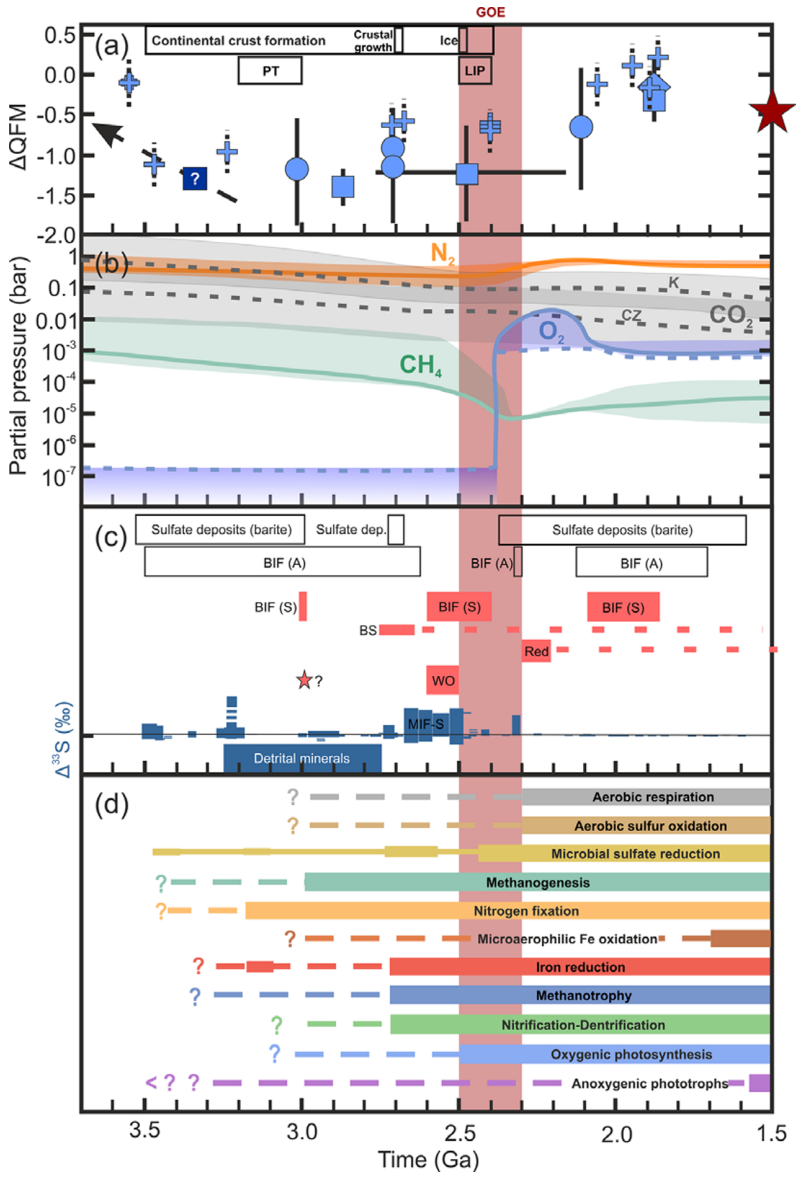

Figure 4. Oxidation and oxygenation of the upper mantle and the surface environment over time. (a) Calculated fO_2 of samples derived from the upper mantle after Aulbach and Stagno (2016) and Stagno and Aulbach (2021) (see Fig. 3 for the legend). The rectangles at the top of the figure display some important geodynamic events: extensive formation of continental crust ca. 3.5–2.4 Ga (Collerson and Kamber, 1999; Huston and Logan, 2004), onset of modern style plate tectonics (PT) ca. 3.2–3.0 Ga (Smithies *et al.*, 2005; Van Kranendonk *et al.*, 2007; Van Kranendonk, 2011; Duncan and Dasgupta, 2017; Kuang *et al.*, 2023), major crustal growth ca. 2.7 Ga (Gaillard *et al.*, 2011), intrusion of large igneous provinces (LIPs) 2.5–2.4 Ga (Ernst and Bleeker, 2010; Gumsley *et al.*, 2017), first glaciations (Ice) ca. 2.4 Ga (Kirschvink *et al.*, 2000; Gumsley *et al.*, 2017). (b) Partial pressure of specific gas species over time after Catling and Zahnle (2020). The two grey dashed lines indicate the partial pressure of CO_2. The upper line (K) is after Kasting (1987) and Herwartz *et al.* (2021), and the lower line (CZ) is after Catling and Zahnle (2020). (c) Geological evidence for oxygenation of the surface environment is explained in detail in the text. The red star indicates early whiffs of oxygen at 3.0 Ga. WO, more abundant later whiffs of oxygen; BS, black shales; Red, red beds (see the main text for references). Mass-independent sulfur isotope fractionation (MIF-S) marks the positive and negative excursions of $\Delta^{33}S$ in ‰ (after Ono, 2017; see also the main text). The data for banded iron formations (BIFs) (S, = superior-type; A, algoma-type) and sulfate deposits (barite) is from Huston and Logan (2004). Reddish colours display evidence of oxygenation, while blueish colours indicate reduced conditions. The boxes without colours are deposits discussed in the literature as possible hints for redox conditions, even though the general opinion is that they cannot be used as redox proxies. (d) Timetable for the emergence of the microbial metabolic processes discussed in this review. Solid lines represent well-established timeframes. Dashed lines represent tentative timeframes. Question marks signify highly uncertain periods. Adapted from Lepot (2020) and modified based on references in the text. The red bar across the whole figure indicates the timing of the GOE (2.5–2.3 Ga; see text for references). GOE, Great Oxygenation Event; QFM, quartz-fayalite-magnetite

may be taken cautiously as an argument for the mantle origin of the zircons. An origin from the crust, however, would not allow any conclusions to be drawn about the redox state of the mantle.

Indeed, Hopkins *et al.* (2008) suggested that the Hadean zircons they studied (which contained mineral inclusions) formed in a crustal setting. Based on the derived formation pressure and temperature (700°C, 7 kbar), they concluded that the surface heat flow from 4.2 to 4.0 Ga was only 75 mW/m^2. Additionally, they proposed that the crustal zircon host melts may have formed above a subduction-like setting, where the subducting slab cools the underlying lithosphere. A similar conclusion was reached by Harrison *et al.* (2008), who suggested that Hadean zircons formed through crystallisation from crustal magmas. The negative ε(Hf,T) values observed in the set of zircons studied by Harrison *et al.* (2008) imply formation in a reservoir with sub-chondritic Lu/Hf (i.e. felsic crust), which may have formed as early as 4.5 Ga. Zircons that crystallise from a residual mantle melt should have positive ε(Hf,T) values.

Others used redox-sensitive elements like vanadium and chromium (e.g. Canil, 1997; Delano, 2001; Lee *et al.*, 2003; Li and Lee, 2004; Aulbach and Viljoen, 2015; Nicklas *et al.*, 2016, 2018, 2019; Aulbach and Stagno, 2016) or the $Fe^{3+}/(Fe^{3+} + Fe^{2+})$ ratio (Rollinson *et al.*, 2017; Aulbach *et al.*, 2017) to determine the redox state of early Earth's mantle. Applying these methods, it was claimed that oxidation occurred early because since 3.9 to 3.5 Ga samples exhibit fO_2 similar to modern mid-ocean ridge basalts (MORBs; Canil, 1997; Delano, 2001; Li and Lee, 2004; Rollinson *et al.*, 2017). In contrast, more recent studies observed that Archean samples are still relatively reduced (QFM – 1.19 ± 0.33) compared to the post-Archean samples (including MORB: QFM – 0.26 ± 0.44). This observation hints at a transition from a relatively reduced towards an oxidised upper mantle during the mid or late Archean (Lee *et al.*, 2003; Aulbach and Viljoen, 2015; Aulbach and Stagno, 2016; Aulbach *et al.*, 2017; Stagno and Fei, 2020) (Figs 3, 4a), which would have direct consequences on the volcanic outgassing efficiency and atmospheric evolution (Guimond *et al.*, 2021).

The data shown in Fig. 3 suggest a gradual increase in the fO_2 of the upper mantle observed from 3.0 to 2.0 Ga, which contrasts with a sudden increase proposed by previous studies (Canil, 1997;

https://doi.org/10.1180/gbi.2025.10003 Published online by Cambridge University Press

Delano, 2001; Li and Lee, 2004; Scaillet and Gaillard, 2011; Rollinson *et al.*, 2017). This discrepancy between a gradual and sudden increase in the redox sate is explained by heterogeneity of the early upper mantle due to incomplete mixing with the lower mantle, the addition of reduced meteoritic material or inherited from magma ocean processes (Ringwood, 1979; Arculus, 1985; Nicklas *et al.*, 2019; Stagno and Fei, 2020; Stagno and Aulbach, 2021). Gu *et al.* (2016) experimentally demonstrated that oxidised lower mantle material is less dense than reduced lower mantle material. This enhances the ascent probability, leading to an efficient mixing between the lower and upper mantle. According to Gu *et al.* (2016), the upper mantle could have been oxidised within 800 m.y. via this mixing process. However, the process was probably prolonged due to the effect of the strength of bridgmanite (which is about three orders of magnitude higher compared to ferropericlase) on the mantle viscosity and, thus, on the mixing behaviour (Girard *et al.*, 2016; Ballmer *et al.*, 2017; O'Neill and Aulbach, 2022). Another reason for a delayed mantle mixing could have been a larger grain size resulting from hotter early Earth conditions. This larger grain size could have led to stronger plate boundaries, decreasing convective motion (Foley and Rizo, 2017). An inefficient mixing of the material from the lower mantle with the upper mantle would explain the preservation of primordial reservoirs suggested to explain observed isotope anomalies (e.g. Mukhopadhyay, 2012; Debaille *et al.*, 2013; Rizo *et al.*, 2013, 2016b, 2016a; Girard *et al.*, 2016; Ballmer *et al.*, 2017; Mundl *et al.*, 2017; Horan *et al.*, 2018; Tusch *et al.*, 2021, 2022).

Furthermore, Aulbach and Stagno (2016) propose that, in contrast to their suite of samples, the rocks measured by previous studies were not derived from the convective mantle. They argue that the latter intruded into a cratonic setting and thus experienced mixing with the sublithospheric mantle. An oxidised mantle at the end of the Archean has also been suggested due to an increase of mantle mixing gradually over time (O'Neill and Aulbach, 2022), by a change in interior convection patterns from two-layered to one-layered mantle convection (Breuer and Spohn, 1995) or by the onset of plate tectonics (Debaille *et al.*, 2013; Andrault *et al.*, 2018). The main argument for mantle mixing due to plate tectonics is to allow the more oxidised, bridgmanite-rich lower mantle (Mao and Bell, 1977; Frost *et al.*, 2004, 2008; Wade and Wood, 2005) to efficiently mix with the more reducing upper mantle material due to slabs penetrating and stirring up the lower mantle. The mechanisms resulting in mantle mixing could explain the observed rise in upper mantle fO_2 between 3.0 and 2.0 Ga (Figs 3, 4a; Aulbach and Viljoen, 2015; Aulbach and Stagno, 2016; Aulbach *et al.*, 2017; Stagno and Fei, 2020; O'Neill and Aulbach, 2022).

First hints of locally oxidised surface environments around 3.0 Ga: implications from stable isotopes

The first geochemical evidence for locally oxidised conditions in marginal marine basins comes from measurements of stable isotopes (e.g. chromium, molybdenum, uranium) of marine black shales (e.g. Anbar *et al.*, 2007; Scott *et al.*, 2008; Lyons *et al.*, 2014; Planavsky *et al.*, 2014; Kendall *et al.*, 2015; Ossa Ossa *et al.*, 2016, 2018; Wang *et al.*, 2018, 2020; Brüske *et al.*, 2020; Kendall, 2021). Earth's mantle and crustal rocks contain chromium in a trivalent state. In modern surface environments, Cr(III) is oxidised to soluble Cr(VI), which is preferentially enriched in heavy isotopes ($\delta^{53}Cr > 0$). The oxidation occurs by the reaction of Cr(III) with Mn(IV) oxides, which require free O_2 exceeding 0.1–1% of the present atmospheric level (PAL) (Planavsky *et al.*, 2014); therefore heavy chromium isotopes are a proxy for the presence of free O_2 in the surface environment. Molybdenum isotopes are another tracer for the presence of free O_2. Molybdenum adsorbs on Mn(IV) oxide surfaces, a reaction with strong mass-dependent fractionation toward lighter isotopes, therefore low $\delta^{98/95}Mo$ values hint towards the existence of Mn(IV) oxides, which require free O_2 to form.

No chromium isotope fractionation has been observed in 3.8 Ga banded iron formations (BIFs) from Isua (Frei *et al.*, 2009), which is taken as evidence for atmospheric O_2 pressures below 0.02–0.2 bar (i.e. 0.1–1% PAL) (Fig. 4b). This can be regarded as an indication that oxygenation of the surface reservoir had not yet initiated at 3.8 Ga. The earliest hints of locally oxidised conditions are currently recorded in the 3.0 Ga Sinqeni Formation of the Mozaan Group in South Africa (Planavsky *et al.*, 2014; Ossa Ossa *et al.*, 2016, 2018; Smith and Beukes, 2023) (Fig. 4c). Contemporaneous oxidative weathering in soils was suggested based on the extensive mobilisation of redox-sensitive elements and fractionation of the redox-sensitive $\delta^{53}Cr$ value. Crowe *et al.* (2013) reported marked negative $\delta^{53}Cr$ from the 3.0 Ga Nsuze paleosol and small positive $\delta^{53}Cr$ from contemporaneous Ijzermyn iron formation (both from the Pongola Supergroup, South Africa). They concluded that free O_2 exceeding 0.1% PAL existed in the Mesoarchean, some 600 m.y. before the GOE. However, modern weathering was identified at this site and may have altered the chromium isotope ratios (Albut *et al.*, 2018, 2019). Post-depositional alteration as the cause for the measured chromium isotope fractionation was supported by Heard *et al.* (2021). They could not confirm the fractionation of chromium isotopes in the Pongola Supergroup paleosol and concluded that the Mesoarchean was anoxic. Irrespective of these arguments, Smith and Beukes (2023) combined evidence from detailed stratigraphy, mineralogy, petrography and carbonate mineral chemistry with isotopic evidence from $\delta^{13}C$ to conclude that the local surface ocean within this basin was oxidised supporting previous $\delta^{56}Fe$ and $\delta^{98}Mo$ data. They suggest microaerophilic chemolithoautotrophs were responsible for iron and manganese oxidation, which would require the presence of free oxygen in the water column, but not the atmosphere. Thus, at least concerning O_2, the chemical exchange between the hydrosphere and atmosphere can be suppressed. In the following, evidence for a persistently anoxic Archean atmosphere is summarised.

Atmospheric O_2 content remains low between 3.25 and 2.75 Ga: implications from mineral archives

In addition to stable isotopes, indirect proxies such as certain mineral deposits can be used as oxygen barometers. Many minerals that are stable in the subsurface environment become oxidised when exposed to the O_2-rich modern atmosphere. Notable among these minerals are sulfides like pyrite (FeS_2), uraninite (UO_2]) or siderite ($FeCO_3$). In the presence of O_2, pyrite is oxidised to Fe(III) (oxyhydr)oxides (rust), uraninite to soluble hexavalent species and siderite to Fe(III) (oxyhydr)oxides. Fluvial uraninite and pyrite detritus were described, e.g. by Ramdohr (1958) and Schidlowski (1981), in Archean sedimentary rocks from the Witwatersrand basin (South Africa). The rounded shape of the mineral grains and absence of oxidation rims suggest that they once occurred as river sand in an O_2-free Archean environment. Detrital pyrite, gersdorffite [NiAsS], uraninite and siderite were described by Rasmussen and Buick (1999) from Archean (3.25–2.75 Ga) fluvial sediments from Pilbara (Australia) and later by Hofmann *et al.*, (2009) from South Africa (3.2–2.7 Ga; Fig. 4c). These minerals can be used as oxygen barometers. For instance, the stability of

https://doi.org/10.1180/gbi.2025.10003 Published online by Cambridge University Press

uraninite in the surface environment is limited to atmospheric O_2 levels below 10^{-2} times the PAL (Grandstaff, 1980). Detailed thermodynamic modelling resulted in an upper $p(O_2)$ limit of 3.2×10^{-5} bar (1.4×10^{-4} times the PAL) (Johnson *et al.*, 2014). The presence of detrital siderite puts an upper limit not only on free O_2 but also on H_2S. Abundant H_2S would lead to the pyritisation of siderite, which is not observed in the Archean sediments studied by Rasmussen and Buick (1999). They concluded that the Archean atmosphere was poor in H_2S, with levels below 10^{-5} bar.

Hexavalent sulfur S(VI), as present in sulfate (SO_4^{2-}), should not exist in the reduced Archean environment. Instead, S(IV), S(0), or S (–II) should be the dominating sulfur oxidation states in equilibrium with the lithosphere and atmosphere. However, sedimentary and hydrothermal barite ($BaSO_4$) exists in Paleo- and Mesoarchean rocks from Australia (e.g. Dresser Formation) and South Africa (Barberton Greenstone Belt) (Heinrichs and Reimer, 1977; Thorpe, 1979; Walter *et al.*, 1980; Lowe *et al.*, 2019) (Fig. 4c). The presence of oxidised sulfate within at least some surface waters is regarded as disequilibrium sulfate, i.e. it is produced by local processes but is not in thermodynamic equilibrium with the entire reduced environment (Olson *et al.*, 2022). Thus, the presence of sulfate minerals (such as barite) in the geological record is generally not regarded as representative of the redox state of the Archean ocean (Huston and Logan, 2004).

One process to obtain the S(VI) to form barite is the UV-induced photodissociation and disproportionation of SO_2 from volcanic degassing into reduced elemental sulfur S(0) and oxidised sulfate S(VI). Indeed, the Paleo- and Mesoarchean sulfate comprises sulfur isotope signatures revealing at least a partial origin from the atmosphere (Bao *et al.*, 2007; Ueno *et al.*, 2008). Triple oxygen isotope data reveal at least two distinct sources of oxygen in sulfate. Apart from an atmospheric endmember, photooxidation of dissolved Fe^{2+} to Fe^{3+} could have acted as a sulfur oxidiser and microbial sulfur cycling may also have been significant (Olson *et al.*, 2022). Further suggestions include sulfate formation through the reaction between reduced S(IV, 0, –II) components and water at high temperatures of igneous systems and the disproportionation of SO_2 in hydrothermal systems (Halevy, 2013). Thus, sulfate does not require an oxidised environment but may result from very particular reactions involving SO_2 from volcanic emissions. All these processes form sulfate, which is in thermodynamic disequilibrium with the atmo-, hydro- and lithosphere and hence contains little information about the redox state of the Archean Earth.

Large-scale oxidation begins around 2.7 Ga: insights from iron formations

Iron formations (IFs) are iron- and silica-rich marine chemical sediments that commonly display a distinct banding (i.e. banded iron formations, BIFs) (e.g. Bekker *et al.*, 2010; Konhauser *et al.*, 2017; Mänd *et al.*, 2021; Aftabi *et al.*, 2021; Dreher *et al.*, 2021). Two main endmember types are distinguished. Algoma-type IFs are generally associated with volcanic provinces and comprise large positive europium anomalies inherited from anoxic vent fluids. These comparably small-scale deposits appear throughout the Archean and early Proterozoic (Barrett *et al.*, 1988; Bolhar *et al.*, 2005; Ohmoto *et al.*, 2006b; Bekker *et al.*, 2010; Pirajno and Yu, 2021). Superior-type IFs form on continental shelves covering extensive areas between 2.7 and 1.8 Ga (Fig. 4c), with a few occurrences already around 3.0 Ga (Huston and Logan, 2004; Smith and Beukes, 2023). Especially after 2.4 Ga, some of these formed above the storm wave base, destroying the banding and generating granular iron formations (GIFs). The depositional depth seems to be related to the depth of the photic zone (Herwartz and Viehmann, 2024). Superior-type IFs exhibit smaller europium anomalies, pointing to dominant contributions of rare earth elements derived from continental weathering or low-temperature alteration of oceanic crust rather than hydrothermal vents. The direct precipitation from open seawater makes superior-type IFs the prime target for reconstructing ambient seawater conditions (Bekker *et al.*, 2010; Konhauser *et al.*, 2017; Mänd *et al.*, 2021). Today, IFs comprise iron-rich phases, including hematite, magnetite, siderite and iron silicates with variable redox states (mean oxidation state of ~$Fe^{2.4+}$) and low (<<0.5 wt.%) organic carbon content (Klein and Beukes, 1992; Trendall, 2002). However, the mineralogy observed today does not represent the primary precipitates from an ancient ocean (Konhauser *et al.*, 2017; Muhling and Rasmussen, 2020). Most candidates for primary precipitates comprise Fe(III) (but see Muhling and Rasmussen, 2020). Hence, large-scale oxidation of soluble Fe(II) to insoluble Fe(III) is required to form IFs. Several abiotic and biotic mechanisms have been suggested, most of which are proposed to occur within the photic zone of ocean water.

In the absence of an ozone layer, UV irradiation reaches the Earth's surface, which induces photochemical oxidation of dissolved Fe^{2+} to Fe^{3+} (Cairns-Smith, 1978; Braterman *et al.*, 1983; Anbar and Holland, 1992). It is suggested that this process occurs at a sufficient rate to form IF deposits (François, 1986). In contrast, Konhauser *et al.* (2007a) argue that the photochemical contribution to solid-phase precipitation is negligible, as most of the Fe^{2+} quickly forms poorly crystalline precursor phases to Fe(II) silicates and/or Fe(II) carbonates. The rate of indirect photochemical oxidation via atmospheric H_2O_2 is found to be too low to account for depositional rates of IF (Pecoits *et al.*, 2015). Another source of H_2O_2 is the decay of primordial radioactive isotopes dissolved in seawater. Ershov (2021) estimates that the decay of highly soluble ^{40}K alone may account for the oxidation of 10^{21} g of iron within a period between 4.3 and 2.5 Ga. The aqueous oxidation of Fe^{2+} to Fe^{3+} is favourable at high pH because this reaction generates protons ($2Fe^{2+} + 4H_2O \rightarrow 2FeOOH + H_2 + 4H^+$). Shibuya *et al.* (2010) argue that high-temperature hydrothermal vent fluids, which are acidic today, had elevated pH in the Archean and comprised Fe^{3+}. Experimental results by Dodd *et al.* (2022) show that the decomposition of $Fe(OH)_2$ in Archean seawater analogues produces Fe^{3+} species. The $Fe(OH)_2$ compound is stable at elevated pH.

The spontaneous conversion of green rust ($Fe_4^{2+}Fe_2^{3+}(OH)_{12}SO_4 \bullet 8H_2O$) to magnetite ($Fe^{2+}Fe^{3+}{}_2O_4$) goes along with a net increase in Fe^{3+} (Tamaura *et al.*, 1984; Li *et al.*, 2017). Green rust is commonly considered a primary iron precipitate in Archean oceans (e.g. Sun *et al.*, 2022) which are, however, considered to be sulfate-poor, at least between 3.2 and 2.4 Ga (Huston and Logan, 2004). Archean seawater chemistry (including pH and ion concentrations) considerably affects the efficiency of abiotic iron oxidation pathways (e.g. Konhauser *et al.*, 2007a; Shibuya *et al.*, 2010). Therefore, the respective net contribution to individual BIF deposits remains unclear and may vary spatially and over time for each abiotic oxidation mechanism.

The proposed biotic iron oxidation mechanisms can be subdivided into indirect oxidation by free O_2 from oxygenic photosynthesis (Cloud, 1973; Klein and Beukes, 1992) and direct oxidation either by chemolithoautotrophic or anoxygenic photoautotrophic iron-oxidising bacteria (Konhauser *et al.*, 2002; Kappler and Newman, 2004; Kappler *et al.*, 2005). The relative proportions of these pathways can be approximated from reactive transport modelling (Ozaki *et al.*, 2019). This approach shows how variations between

https://doi.org/10.1180/gbi.2025.10003 Published online by Cambridge University Press

individual settings with variable nutrient and Fe^{2+} supply and the available light intensity within a given water mass control the dominating oxidation pathway (Ozaki *et al.*, 2019; Herwartz and Viehmann, 2024).

Manganese in IFs is a main tracer for the oxygenation of Earth's hydrosphere (Robbins *et al.*, 2023). Tetravalent Mn(IV) oxides form at redoxclines via consumption of dissolved molecular O_2 and are thus direct evidence for oxygenic photosynthesis (see Robbins *et al.*, 2023 for a review). Oxidised Mn^{4+}, Fe^{3+} and organic matter form particles that sink towards the seafloor. This process is observed in anoxic basins today and is known as the Fe–Mn shuttle (Dellwig *et al.*, 2010). While respective particles slowly sink below the chemocline into the anoxic water body, the Mn^{4+} is reduced again by dissolved Fe^{2+} (Dellwig *et al.*, 2010; Kurzweil et al., 2016; Ossa Ossa *et al.*, 2018). Deposition of such Mn^{4+} particles in the sediment is only viable at low Fe^{2+}, e.g. distal to the iron source (Smith and Beukes, 2023), or when oxygenic photosynthesis is so active that the flux of sinking Mn^{4+} particles outcompetes the upwelling flux of Fe^{2+}. During and in the aftermath of the GOE, enormous amounts of Mn^{4+} particles have been deposited on the seafloor, forming the world's largest manganese deposits (Gutzmer and Beukes, 1996; Tsikos *et al.*, 2003; Sekine *et al.*, 2011), reflecting the high productivity around that time. Elevated manganese contents are a prime indicator for "whiffs of oxygen" (Planavsky *et al.*, 2014; Ossa Ossa *et al.*, 2016; Smith and Beukes, 2023) and a general increase in manganese contents in IFs is observed at the onset of the GOE, e.g. in the Transvaal Supergroup of South Africa (Tsikos *et al.*, 2003; Schröder *et al.*, 2011; Kurzweil *et al.*, 2016; Smith, 2018).

Subsequent oxidation of organic matter in the sediment partially reduced Fe^{3+} and Mn^{4+} back to soluble Fe^{2+} and Mn^{2+}. Hence, diagenetic processes can be responsible for the variable mineralogy observed in IFs today. For instance, the Fe and Mn in siderite and rhodochrosite can be derived from the oxidation of organic matter by Fe^{3+} and Mn^{4+}, which precludes the use of IF mineralogy to reconstruct paleo-atmospheric gas concentrations (Reinhard and Planavsky, 2011). Identifying primary mineral phases and other features, such as the banding of BIFs, has been the main challenge in using these rocks as reliable archives (Mänd *et al.*, 2021; Mundl-Petermeier *et al.*, 2022; Bau *et al.*, 2022).

Abundant whiffs of oxygen between 2.6 and 2.5 Ga: implications from stable isotopes and black shales

Whiffs of oxygen in marine sediments become more abundant in the Neoarchean (2.6–2.5 Ga) towards the GOE (Anbar *et al.*, 2007; Scott *et al.*, 2008; Lyons *et al.*, 2014; Kendall *et al.*, 2015; Ostrander *et al.*, 2019; Brüske *et al.*, 2020) (Fig. 4c). Frei *et al.* (2009) reported on sedimentary rocks with marked positive $\delta^{53}Cr$, suggesting that O_2 rich oases existed before the GOE. These oases probably occurred near the shore, and rivers washed heavy Cr(VI) into the oceans, where chemical sediments preserved the isotope signature.

Significant volumes of black shales started forming at 2.7 Ga (Fig. 4c), indicating a substantial burial of organic carbon that was probably a response to increasing primary productivity via oxygenic photosynthesis (Condie, 2001; Lyons *et al.*, 2014). Oxygenic photosynthesis is assumed to be one of the primary mechanisms leading to the significant accumulation of O_2 in the oceans and the atmosphere. Additionally, O_2 accumulation is favoured by organic carbon burial (Lee *et al.*, 2016). Thus, black shales indirectly record the enhanced oxidation of the hydrosphere-atmosphere system.

Significant enrichment of free O_2 in the surface reservoir recorded by sediments and sulfur isotopes starting at 2.5 Ga

Widespread release of O_2 from an oxygenated surface ocean is evident after around 2.3 Ga when red beds emerge (Konhauser *et al.*, 2017) (Fig. 4c). Iron loss is observed during paleosol weathering (Rye and Holland, 1998) and detrital pyrite and uraninite disappearance, just like the MIF-S (mass-independent sulfur isotope fractionation) anomaly disappears with the rise of O_2 in the atmosphere (Bekker, 2001). The MIF-S signal is assumed to occur due to photolysis and/or photoexcitation of volcanogenic SO_2 by ultraviolet light in a reduced, anoxic atmosphere. Reduced sulfur species displaying a positive $\Delta^{33}S$ signature result from this photolytic process (e.g. Farquhar, 2000; Farquhar *et al.*, 2001; Ono *et al.*, 2003; Whitehill and Ono, 2012; Whitehill *et al.*, 2013). The sudden disappearance of the MIF-S signal at ca. 2.3 Ga is one of the most well-known and solid evidence for the accumulation of free O_2 above 10^{-5} PAL and thus marks the onset of the GOE (Fig. 4c) (e.g. Pavlov and Kasting, 2002; Ono *et al.*, 2003; Bekker *et al.*, 2004; Zahnle *et al.*, 2006; Domagal-Goldman *et al.*, 2008; Guo *et al.*, 2009; Luo *et al.*, 2016; Warke *et al.*, 2020; Poulton *et al.*, 2021). The positive $\Delta^{33}S$ signal in Archaean sedimentary sulfides is recognisable but comparatively low between 3.9 and 2.7 Ga (except for a peak between ca. 3.2 and 3.2 Ga). Between about 2.7 and 2.5 Ga a pronounced MIF-S spike is observed coinciding with the GOE (Farquhar, 2000; Mojzsis *et al.*, 2003; Ono *et al.*, 2003; Hu *et al.*, 2003; Bekker *et al.*, 2004; Whitehouse *et al.*, 2005; Papineau *et al.*, 2005; Jamieson *et al.*, 2006; Ohmoto *et al.*, 2006a; Ono *et al.*, 2006; Cates and Mojzsis, 2006; Johnston *et al.*, 2006; Kamber and Whitehouse, 2007; Papineau *et al.*, 2007; Philippot *et al.*, 2007; Kaufman *et al.*, 2007; Bao *et al.*, 2007; Farquhar *et al.*, 2007; Domagal-Goldman *et al.*, 2008; Partridge *et al.*, 2008; Johnston *et al.*, 2008; Ueno *et al.*, 2008; Ono *et al.*, 2009; Thomazo *et al.*, 2009a; Shen *et al.*, 2009; Guo *et al.*, 2009; Gaillard *et al.*, 2011; Lyons *et al.*, 2014; Ono, 2017; Kendall, 2021).

While the atmosphere, surface oceans and marginal basins are oxidised after the GOE (Lyons *et al.*, 2014), the deep ocean remains anoxic until 1.8 Ga (Huston and Logan, 2004). Deep ocean oxygenation requires Phanerozoic-like atmospheric O_2 levels and deep ocean convection (Reinhard and Planavsky, 2022). Therefore, fully oxidised oceans as we know them today do not appear until atmospheric O_2 levels approach modern levels in the late Proterozoic oxidation event (Reinhard and Planavsky, 2022; but see Xu *et al.*, 2023), and even then bottom-water anoxia seem to have been the rule rather than the exception until the mid-Paleozoic era (Stockey *et al.* 2024).

O_2 sources vs. sinks: balancing atmospheric oxygenation

Upper mantle oxidation to near modern fO_2 probably occurred between 3.0 and 2.0 Ga (Fig. 4). The first geochemical evidence for localised O_2 appears ca. 3.0 Ga, consistent with paleontological and phylogenetic evidence for the emergence of oxygenic photosynthesis (Anbar *et al.*, 2007; Planavsky *et al.*, 2014; Schirrmeister *et al.*, 2015; Sánchez-Baracaldo, 2015; Cardona *et al.*, 2019; Garcia-Pichel *et al.*, 2019; Jabłońska and Tawfik, 2021, 2021; Fournier *et al.*, 2021; Boden *et al.*, 2024) (Fig. 4d). Despite the constant chemical exchange between atmosphere and hydrosphere, mineralogical and geochemical evidence in the Earth's sedimentary rock records contrasting timelines for their respective oxygenation. Irrespective of this problem, atmospheric oxygenation only occurs at 2.5–2.3 Ga (e.g. Holland, 2002, 2006; Bekker *et al.*, 2004; Canfield, 2005;

https://doi.org/10.1180/gbi.2025.10003 Published online by Cambridge University Press

Kasting *et al.*, 2006; Guo *et al.*, 2009; Luo *et al.*, 2016; Gumsley *et al.*, 2017; Warke *et al.*, 2020; Ossa Ossa *et al.*, 2022). This indicates a delay between upper mantle oxidation, the emergence of oxygenic photosynthesis and the GOE by several hundred m.y. (Fig. 4). Thus, the onset of microbial O_2 production alone cannot satisfactorily explain the timing of the GOE.

Constraining the O_2 source-limited oxygenic photosynthesis?

One explanation for this delayed oxygenation of the Earth's surface environments is that the productivity of oxygenic photosynthesis in early cyanobacteria was limited, decreasing the microbial O_2 flux (see Dick *et al.*, 2018 for a detailed review). Cyanobacteria depend on bioavailable nitrogen and are major agents for nitrogen fixation in today's surface oceans (Field *et al.*, 1998; Zehr and Kudela, 2011). Nitrogen fixation is catalysed by the enzyme nitrogenase, which contains molybdenum (Postgate, 1998). Molybdenum may have been scarce in the reducing environments of the early Archean Earth, where it was poorly soluble (Williams and Fraústo Da Silva, 2003). Thus, it was suggested that nitrogen fixation in cyanobacteria was inhibited (Zerkle *et al.*, 2006). At the same time, O_2 output by oxygenic photosynthesis could have inhibited other nitrogen-fixing microorganisms, ultimately starving cyanobacteria of bioavailable nitrogen (Shi and Falkowski, 2008; Kasting and Canfield, 2012). Nitrogen fixation could have occurred via lightning-driven atmospheric reactions (Navarro-González *et al.*, 1998; Wong *et al.*, 2017). Still, the isotopic composition of most Archean sedimentary nitrogen isotope records suggests this process was not quantitatively important for sustaining primary production (Barth *et al.*, 2023). Instead, nitrogen isotope evidence is consistent with biological nitrogen fixation by at least 3.2 Ga (Stüeken *et al.*, 2015a, 2016). This is consistent with phylogenetic studies suggesting an early emergence of nitrogen fixation in cyanobacteria (Latysheva *et al.*, 2012). Hydrothermal sources may have sufficiently compensated the low supply of molybdenum for nitrogenase from oxidative weathering in the Archean (Evans *et al.*, 2023). Moreover, hydrothermal systems probably played a role in recycling sedimentary ammonium (Stüeken *et al.*, 2021; Martin *et al.*, 2024). Therefore, nitrogen may not have been a limiting factor for cyanobacterial productivity in the late Archean.

Bioavailable phosphorous, in the form of phosphate, is widely considered another limiting factor for primary productivity in the Archean and early Proterozoic ocean (Derry, 2015; Reinhard *et al.*, 2017; Ossa Ossa *et al.*, 2019; Walton *et al.*, 2023). This is despite its supply from continental weathering (Hao *et al.*, 2020; Watanabe and Tajika, 2021) and possible hydrothermal sources (Rasmussen *et al.*, 2021, 2023). For example, Ozaki *et al.* (2019) provide a model for open ocean settings and investigate the competition between O_2-producing cyanobacteria and photoferrotrophs, the latter being adapted to lower light levels, allowing them to thrive deeper in the water column. Accordingly, nutrients such as phosphate and Fe^{2+} from upwelling water masses are consumed by photoferrotrophs, leaving surface water starved in either phosphate or Fe^{2+} (Kappler *et al.*, 2005; Ozaki *et al.*, 2019). If oceanic iron/phosphate ratios are high, oxygenic photosynthesis in the upper water column is efficiently suppressed (Ozaki *et al.*, 2019). In coastal settings, where the water column is shallow and more nutrients are supplied from the continent, benthic microbial mats are observed that probably produce O_2 (Homann *et al.*, 2015; Homann, 2019), therefore the productivity of cyanobacteria probably varied spatially and over time (Konhauser *et al.*, 2018). Moreover, the bioavailability of phosphorous may have been limited due to inefficient remineralisation of organic matter (Kipp and Stüeken, 2017) or phosphate scavenging by Fe^{2+} and adsorption on or co-precipitation with (biogenic) Fe(III) minerals in ferruginous oceans (Bjerrum and Canfield, 2002; Laakso and Schrag, 2014; Derry, 2015). The efficiency of phosphate scavenging by Fe (III) minerals is debated (Konhauser *et al.*, 2007b; Jones *et al.*, 2015). Recent analyses of carbonate-associated phosphate in Archean rocks also challenge severe phosphate limitation in coeval waters (Ingalls *et al.*, 2022; Crockford and Halevy, 2022). Hence, the possible phosphate limitation of Archean cyanobacteria remains an open question.

Phylogenetic evidence suggests the earliest cyanobacteria were benthic freshwater strains that only diversified into brackish and marine habitats in the late Archean (Blank and Sánchez-Baracaldo, 2010; Schirrmeister *et al.*, 2016; Sánchez-Baracaldo *et al.*, 2017; Grettenberger *et al.*, 2025). Planktonic cyanobacteria may have only appeared in the Neoproterozoic, expanding their habitat to the open ocean (Sánchez-Baracaldo *et al.*, 2014, 2019; Sánchez-Baracaldo, 2015; Schirrmeister *et al.*, 2016). A benthic lifestyle, on the other hand, would have constrained the spatial extent of Archean cyanobacterial habitats to terrestrial or coastal areas, limiting their overall O_2 production (Sánchez-Baracaldo *et al.*, 2014, 2017; Lalonde and Konhauser, 2015; Sánchez-Baracaldo, 2015). Once cyanobacteria expanded to marine environments, they may have suffered from iron toxicity in the Archean oceans (Swanner *et al.*, 2015a, 2015b; Dreher *et al.*, 2021). If true, this was most probably due to reactive oxygen species produced during Fe(II) oxidation by photosynthetic O_2 (Rush and Bielski, 1985). However, more recent experiments did not observe such effects in open bottle cultures that allowed for gas exchange, limiting the accumulation of photosynthetic O_2 to concentrations assumed for Archean oxygen oases (≤10 μM; Herrmann *et al.*, 2021). In these sunlit environments, early cyanobacteria would have also been exposed to high levels of UV radiation due to the absence of an ozone shield (Mloszewska *et al.*, 2018). Recently, it has also been suggested that the net O_2 production in Archean cyanobacterial mats was lower than previously thought due to shorter day lengths (Klatt *et al.*, 2021) or an inefficient photosystem in early cyanobacteria (Grettenberger and Sumner, 2024). One or more of these factors could have limited the productivity of cyanobacteria in the late Archean. The increasing abundance of continental crust through the Archean (Fig. 4a) (Kemp and Hawkesworth, 2014; Smit and Mezger, 2017; Korenaga, 2018) may have helped overcome some of these limitations by supplying weathering-derived phosphate and creating shallow marine habitats, increasing the biological O_2 source. However, reliable primary productivity estimates depend on the magnitudes of these effects, which remain to be determined.

Critical O_2 sinks: reduced gases and solutes in Archean surface environments

Apart from limited biological O_2 production, low ambient O_2 levels could also be due to large fluxes into O_2 sinks. The most prominent O_2 sinks are reduced gases and aqueous solutes in the Archean atmosphere and oceans (e.g. Fe^{2+}, Mn^{2+}, H_2S, C_{org}) (Holland, 2002; Claire *et al.*, 2006; Gaillard *et al.*, 2011; Lyons *et al.*, 2014, 2024; Lee *et al.*, 2016; Catling and Zahnle, 2020). The sizes and capacities of these sinks are partly controlled by fluid–rock interactions and volcanic outgassing in chemical equilibrium with the redox state of the Earth's mantle and crust (Gaillard *et al.*, 2021). As discussed above, Earth supposedly accreted from relatively reduced material. However, the mantle subsequently experienced oxidation between 3.0 and 2.0 Ga (Fig. 4), shifting the redox state of volcanic gases toward more oxidised species (Claire *et al.*, 2006; Aulbach and

https://doi.org/10.1180/gbi.2025.10003 Published online by Cambridge University Press

Stagno, 2016; O'Neill and Aulbach, 2022). When the abundance of continental crust rose, magmatic outgassing was increasingly shallow and subaerial and, thus, more oxidised due to the pressure dependence of volatile speciation in magmatic systems (Holland, 2002; Kump and Barley, 2007; Gaillard *et al.*, 2011). Less mafic and ultramafic rocks at the surface meant fewer reduced solutes (e.g. Fe^{2+}, Mn^{2+}) in seawater (Kump *et al.*, 2001; Lee *et al.*, 2016) and fewer reduced species from serpentinisation (e.g. H_2) (Hoffmann, 2017; Smit and Mezger, 2017). More continental landmass increased the accommodation space for the burial of reduced sediments, removing these critical O_2 sinks from the surface environment (Canfield, 2005; Lee *et al.*, 2016; Zhao *et al.*, 2023).

Biotic processes like microbial methanogenesis also control the abundance of gaseous sinks in surface environments. Methanogens are strictly anaerobic archaea that form CH_4 either by reduction of a carbon substrate (e.g. hydrogenotrophic methanogenesis, CO_2 reduction with H_2 as the electron donor) or by disproportionation (i.e. fermentation) of organic compounds (e.g. acetoclastic methanogenesis, acetate disproportionation) (Head, 2016) (Table 1). Methane can contribute to O_2 consumption via photochemically generated CH_3 and OH radicals in the atmosphere (Pavlov *et al.*, 2001; Kasting and Siefert, 2002; Claire *et al.*, 2006; Daines and Lenton, 2016). A study on the ferruginous and sulfate-poor Lake Matano, an Archean ocean analogue site, showed a limitation of dissimilatory sulfate reduction in favour of methanogenesis (Crowe *et al.*, 2011). Methanogens could, therefore, also have been important agents for the remineralisation of organic matter from Archean primary production (e.g. Thompson *et al.*, 2019). Highly ^{13}C depleted CH_4 ($\delta^{13}C$ down to –56‰) from fluid inclusions in hydrothermal quartz of the 3.48 Ga Dresser Formation may represent the oldest direct evidence for methanogenesis (Ueno *et al.*, 2006). However, this CH_4 may originate from abiotic organic synthesis (Sherwood Lollar and McCollom, 2006). Carbon isotopic evidence for methanogenesis is also found in ca. 3.0 Ga fluviolacustrine Lalla Rokh Sandstone ($\delta^{13}C_{org}$ –30 to –38‰; Stüeken and Buick, 2018), and in the shallow marine or lacustrine 2.72 Ga Tumbiana Formation in Western Australia ($\delta^{13}C_{org}$ down to –56‰; Thomazo *et al.*, 2011), which are probably unaffected by hydrothermal CH_4. Indeed, recent molecular clock studies place the emergence of methanogenesis even ≥3.5 Ga (Wolfe and Fournier, 2018; but see Roger and Susko, 2018 for an alternative viewpoint). Assuming biogenic CH_4 fluxes similar to today, the Archean atmosphere could have maintained CH_4 concentrations of thousands of ppm (Pavlov *et al.*, 2001; Kasting and Siefert, 2002; Kharecha *et al.*, 2005). The CH_4 flux probably decreased when sufficient seawater sulfate was available and sulfate-reducing bacteria overtook methanogens in organic carbon mineralisation (Zahnle *et al.*, 2006). Declining oceanic nickel concentrations may have further inhibited methanogens (Konhauser *et al.*, 2009). It seems plausible that the late Archean decline of the atmospheric CH_4 pool was crucial for the subsequent rise of atmospheric O_2, rendering biogenic CH_4 an important O_2 sink in the Archean. Together with an increasing flux of biogenic O_2, these processes exhausted the capacity of Earth's gaseous and aqueous O_2 sinks throughout the Archean, paving the way for the GOE.

The Archean aerobic O_2 sink: insights from recent environments, ancient rocks and modern genomes

Another potential O_2 sink in the Archean is its reduction coupled to the oxidation of various electron donors (organic matter, CH_4, NH_4^+, NO_2, Mn(II), Fe(II), sulfide) for conserving energy (i.e. aerobic respiration) by microorganisms (Table 1). Aerobic respiration is associated with a greater energy yield compared to anaerobic (i.e. O_2-free) respiration, making it highly competitive in environments where O_2 is available. Indeed, it is the most competitive pathway for organic carbon remineralisation to CO_2 on modern Earth and a critical buffer against further atmospheric O_2 accumulation (Berner, 1989). Microbial oxidation of CH_4 to CO_2 using O_2 as the terminal electron acceptor (i.e. aerobic methanotrophy) is a critical CH_4 sink (Table 1). Ammonium oxidation to nitrite and nitrate by O_2 (i.e. nitrification; Table 1) is dominantly controlled by aerobic microorganisms like *Nitrosomonas* and *Nitrobacter* sp. in modern oceans (Falkowski, 1997; Stüeken *et al.*, 2024). Microbial manganese oxidation by O_2 (Table 1) is the main mechanism for Mn(IV) oxide production in modern oceans (Tebo *et al.*, 2005). This is because the microbially mediated oxidation of Mn(II) by O_2 is up to five orders of magnitude faster than its abiotic counterpart in seawater-like conditions (Nealson *et al.*, 1988; Tebo, 1991; Hansel, 2017; Yu and Leadbetter, 2020). Therefore, Mn(II) oxidation in the presence of O_2 is generally mediated by Mn-oxidising microorganisms, even at sub-micromolar O_2 concentrations (Tebo *et al.*, 2004, 2005; Schippers *et al.*, 2005; Clement *et al.*, 2009; Learman *et al.*, 2011). Microaerophilic Fe(II)-oxidising bacteria (e.g. *Gallionella*, *Leptothrix*, *Mariprofundus sp*) couple the oxidation of Fe(II) to the reduction of O_2 (Table 1). At neutral pH, the oxidation of reduced sulfur compounds (e.g. H_2S) to S^0 or sulfate can occur at micromolar O_2 concentrations using O_2 or nitrate as an electron acceptor (e.g. *Beggiatoa*; Hentschel and Felbeck, 1993; Jørgensen and Gallardo, 1999; Girguis *et al.*, 2000; Dahl *et al.*, 2008) (Table 1). In acidic environments (e.g. hydrothermal sulfide systems, acid rock drainage sites), microorganisms can exploit the aerobic oxidation of S^0 or sulfide minerals, such as pyrite (e.g. *Acidothiobacillus*; Segerer *et al.*, 1986; Dahl *et al.*, 2008). Microbial sulfide oxidation is orders of magnitude faster than abiotic sulfide oxidation in most sedimentary environments, particularly at low O_2 concentrations, highlighting its role in consuming O_2 in the environment (Luther *et al.*, 2011).

Despite the significance and diversity of microbial O_2 sinks in recent environments and previous suggestions for the antiquity of aerobic respiration ('respiration early hypothesis'; Castresana and Saraste, 1995), the role of biological O_2 consumption in the Archean is poorly explored. The proliferation of aerobic microorganisms is traditionally assumed to postdate the GOE due to the canonical lower limit for aerobic respiration (the 'Pasteur Point') of 2.2 μM O_2 in seawater at 25°C (Devol, 1978). However, the discovery of 'nanaerobic' life (Baughn and Malamy, 2004), respiring aerobically at nanomolar O_2 concentrations, challenges this paradigm. For instance, *Escherichia coli*, a well-studied model organism, grows aerobically at O_2 concentrations as low as 3 nM (Stolper *et al.*, 2010). Moreover, it is increasingly recognised that many microorganisms typically considered strict anaerobes can also respire aerobically at low O_2 concentrations (Cypionka, 2000; Lee *et al.*, 2019; Berg *et al.*, 2019). It was cautioned that aerobic growth rates under nanomolar O_2 concentrations are strongly muted, suggesting that anaerobic respiration (e.g. Fe(III) reducers) could outcompete aerobic microorganisms in the Archean (Ducluzeau *et al.*, 2014). However, advances in O_2 microsensing and metatranscriptomic analysis demonstrate that aerobic respiration is widespread in recent environments, even under apparent anoxia, where aerobic microorganisms may consume O_2 faster than it can accumulate (Berg *et al.*, 2022 and references therein).

https://doi.org/10.1180/gbi.2025.10003 Published online by Cambridge University Press

Recent oxygen minimum zones and stratified lakes parallel late Archean environments by their low O_2 concentrations within or below the photic zone, shedding light on the possible role of microbial communities and biogeochemical processes before the GOE. Aerobic methanotrophy (Table 1) has been identified as an efficient CH_4 sink coupled to cryptic O_2 from oxygenic photosynthesis in the photic zone of lakes (Oswald *et al.*, 2015; Milucka *et al.*, 2015). These conditions could have been widespread in Archean lakes and oceans, supporting the suggested role of aerobic methanotrophy in buffering atmospheric O_2 accumulation (Daines and Lenton, 2016). Nitrification is efficient in oxygen minimum zones, even at nanomolar O_2 concentrations (Kalvelage *et al.*, 2011, 2015; Füssel *et al.*, 2012; Thamdrup *et al.*, 2012; Beman *et al.*, 2013; Bristow *et al.*, 2016). Optimal rates of microaerophilic Fe(II) oxidation by *Sideroxydans* were observed at 5–20 μM O_2 (Maisch *et al.*, 2019), but the marine strain *Mariprofundus* can still grow at sub-micromolar O_2 concentrations (Chiu *et al.*, 2017; McAllister *et al.*, 2019). Most importantly, however, because the abiotic oxidation of Fe(II) is slow at neutral pH and low O_2 (Søgaard *et al.*, 2000), microaerophilic Fe(II) oxidation outcompetes abiotic oxidation at or below 50 μM O_2 (Druschel *et al.*, 2008). Aerobic sulfide oxidation also occurs in apparently anoxic environments of modern lakes and oxygen minimum zones when the influx and microbial consumption of O_2 are balanced, resulting in a cryptic O_2 cycle (Sommer *et al.*, 2017; Callbeck *et al.*, 2018; Berg *et al.*, 2019). The micromolar O_2 concentrations inferred for late Archean oxygen oases satisfy even conservative lower limits for aerobic respiration, demonstrating that aerobic respiration was viable in Neoarchean and, perhaps transiently, in Mesoarchean surface waters. Cryptic O_2 consumption in recent environments, resulting in O_2 concentrations below the detection limits of modern microsensors, suggests the downwelling and downward diffusion of oxygenated surface waters may have even allowed for aerobic metabolism in apparently anoxic deeper Archean settings.

Early studies suggested that aerobic respiration is required to mass-balance the preserved organic carbon in Archean black shales (Towe, 1990). It is difficult to verify this by investigating the rock record because isotope fractionation involved in heterotrophy is much less than during the initial autotrophic carbon fixation (Hayes, 2001). The resulting carbon species of aerobic methanotrophy are strongly depleted in ^{13}C and can be bound in carbonates or assimilated in microbial biomass, enabling the reconstruction of CH_4 oxidation in the geological record (Hayes, 2001; Eigenbrode and Freeman, 2006). The $\delta^{13}C$ values in sedimentary carbonaceous matter of down to –60‰ were interpreted as evidence for aerobic methanotrophs in the late Archean (Hayes, 1983, 1994; Hayes and Waldbauer, 2006). Eigenbrode and Freeman (2006) present indirect evidence for aerobic respiration based on $\delta^{13}C_{org}$ analysis of ≤2.7 Ga sedimentary rocks. They conclude that the more consistently ^{13}C-depleted deep versus shallow facies ($\delta^{13}C_{org}$ = –40 to –45‰ and –57 to –28‰, respectively) demonstrate a more prominent role of CH_4 cycling in anoxic deep water versus (aerobic) respiration of photosynthetic organic matter in oxic surface water. The presence of 3β-methylhopane biomarkers in the 2.7–2.5 Ga Transvaal Supergroup and Hamersley Group supports this (Brocks *et al.*, 2003; Eigenbrode *et al.*, 2008; Waldbauer *et al.*, 2009), but the syngeneity of biomarkers in these localities to their host rocks was contested (Brocks, 2011). Highly depleted $\delta^{13}C$ signatures in Archean carbonaceous matter could also be explained by anaerobic oxidation of methane (AOM) (Hinrichs, 2002; Thomazo *et al.*, 2009b; Guy *et al.*, 2012; Stüeken *et al.*, 2017; Flannery *et al.*, 2018; Lepot *et al.*, 2019), which is a major CH_4 sink on modern Earth (Knittel and Boetius, 2009). The quantitative importance of AOM may have been limited in the Archean due to low marine sulfate levels before the GOE (Catling *et al.*, 2007) but alternative electron acceptors like Fe(III) seem plausible (Knittel and Boetius, 2009; Stüeken and Buick, 2018).

Nitrification produces ^{15}N-enriched residual ammonium ($\delta^{15}N$ up to +35‰) that can be assimilated and recorded in sedimentary organic matter (Mariotti *et al.*, 1981; Casciotti, 2009; Mandernack *et al.*, 2009). Nitrite can be used to oxidise ammonium in the absence of excess O_2 (anaerobic ammonium oxidation, 'anammox'; Mulder *et al.*, 1995; Van De Graaf *et al.*, 1995; Lam *et al.*, 2009) (Table 1). However, the anammox reaction also requires O_2 because nitrite cannot be produced anaerobically (Stüeken *et al.*, 2016). Ammonium oxidation may also be coupled to the reduction of sulfate (i.e. sulfammox) or Fe(III) (i.e. feammox) (Clement *et al.*, 2005; Yang *et al.*, 2012; Rios-Del Toro *et al.*, 2018). The latter was suggested as the possibly dominant ammonium oxidation pathway in the early Archean when O_2 scarcity prevented nitrite and sulfate accumulation (Pellerin *et al.*, 2023). Both denitrification to N_2O or N_2 and anammox produce ^{15}N-enriched residual nitrate (Stüeken *et al.*, 2024). Notably, the $\delta^{15}N$ record in metasedimentary rocks can be further shifted to more positive values with increasing metamorphic grade due to the release of isotopically light ammonium or N_2 (Ader *et al.*, 2016). Ample nitrogen isotope evidence from low-grade metasedimentary rocks (greenschist facies and below) shows highly variable $\delta^{15}N$ signatures (ca. –11 to +50‰) and a secular increase of $\delta^{15}N$ of approximately 2‰ at ca. 2.8–2.6 Ga (Garvin *et al.*, 2009; Godfrey and Falkowski, 2009; Thomazo *et al.*, 2011; Busigny *et al.*, 2013; Stüeken *et al.*, 2015b, 2016; Koehler *et al.*, 2018; Pellerin *et al.*, 2024). The overall increase in sedimentary $\delta^{15}N$ values strongly suggests an increasing role of ammonium oxidation in marine environments. Sulfate was virtually unavailable as an electron acceptor during this time (e.g. Crowe *et al.*, 2014) and $\delta^{15}N$ values of up to +37.5‰ from marine sediments are inconsistent with feammox (Pellerin *et al.*, 2024). Therefore, this trend is best explained by the rise of nitrification, denitrification and/or anammox in the Meso- to Neoarchean (Garvin *et al.*, 2009; Godfrey and Falkowski, 2009; Thomazo *et al.*, 2011; Busigny *et al.*, 2013; Stüeken *et al.*, 2015b, 2016; Koehler *et al.*, 2018; Pellerin *et al.*, 2024), consistent with phylogenetic reconstructions (Parsons *et al.*, 2021). These processes, including the presence of nitrate, were probably transient and limited to settings with oxygenated surface waters.

Microaerophilic Fe(II)-oxidising bacteria commonly form characteristic mineral-organic structures that consist of Fe(III) (oxydr) oxide-encrusted stalks (Chan *et al.*, 2016), which show good potential for fossilisation (Picard *et al.*, 2015). The fossil record of these stalks in hydrothermal jaspers, where preservation of such delicate structures is most probable, extends back to at least 1.74 Ga (Little *et al.*, 2021). The oldest putative findings of such fossils are reported in 3.77 Ga hydrothermal vent deposits (Dodd *et al.*, 2017; Papineau *et al.*, 2022), although the biogenicity of these features would require free O_2 in Eoarchean seafloor hydrothermal systems or a different metabolic affinity. On modern Earth, microaerophilic Fe(II) oxidisers inhabit a limited niche at opposing gradients of O_2 and Fe^{2+} in marine and terrestrial environments like hydrothermal vents, sediment–water interfaces and soils (Kappler *et al.*, 2021). However, in Archean oxygen oases where O_2 was produced in the photic zone and Fe^{2+} was supplied from below, this niche could have been much larger (Holm, 1989; Konhauser *et al.*, 2002; Dreher *et al.*, 2021).

The presence of abundant Mn oxides in late Archean sedimentary rocks is another signature of aerobic metabolism. In the absence

https://doi.org/10.1180/gbi.2025.10003 Published online by Cambridge University Press

of O_2, Mn(II) may also be oxidised by a range of abiotic and other biotic mechanisms, including photooxidation by UV radiation, Mn-dependent anoxygenic photosynthesis and Mn oxidation coupled to alternative electron acceptors like nitrate (Luther *et al.*, 1997; Johnson *et al.*, 2013; Daye *et al.*, 2019; Liu *et al.*, 2020). However, the transfer of Mn oxides from the water column to the sediments and their preservation required an oxygenated depositional environment devoid of Fe(II) and H_2S, in which aerobic microorganisms dominate Mn(II) oxidation today (Jones *et al.*, 2011; Smith and Beukes, 2023; Robbins *et al.*, 2023; Mhlanga *et al.*, 2023).

Fossil evidence for the antiquity of aerobic sulfur oxidation is scarce, probably due to the metastable nature of the product S^0, the poor preservation potential of sulfur oxidiser cells upon silicification and a lack of distinct sulfur isotope signatures (Canfield, 2001; Cosmidis *et al.*, 2019; Nims *et al.*, 2021). Nevertheless, morphological characteristics (size, cell wall structure) combined with paleoecological considerations were used to interpret carbonaceous microstructures in the 2.52 Ga Gamohaan Formation (South Africa) as sulfur-oxidising bacteria similar to *Thiomargarita* (Czaja *et al.*, 2016). Microbial sulfur oxidation is also supported by multiple sulfur isotope compositions of 3.22 Ga sulfates (Nabhan *et al.*, 2020) and possible microbially induced corrosion features on ca. 3.4 Ga detrital pyrite (Wacey *et al.*, 2011). If true, this does not necessarily indicate an aerobic metabolism due to the potential coupling of sulfur oxidation with nitrate reduction. Chromium isotopes in Archean BIFs trace chromium mobilisation during the oxidative weathering of pyrite exposed on continents by 2.48 Ga (Konhauser *et al.*, 2011). It was suggested that this was due to the activity of acidophilic sulfide-oxidising bacteria (Konhauser *et al.*, 2011) or pyrite oxidation by photochemically generated Fe^{3+} (Hao *et al.*, 2022). In marine environments, aerobic sulfur oxidisers may have been limited to microbial mats, oxidising sulfide generated in underlying sediments (Konhauser, 2007). In the open ocean, sulfide was dominantly sourced from hydrothermal systems and probably scavenged by Fe^{2+} before it reached oxygenated surface waters (Canfield *et al.*, 2006), although euxinic conditions possibly prevailed locally in the late Archean (Reinhard *et al.*, 2009; Scott *et al.*, 2011). These examples highlight the fragmented nature of direct evidence for aerobic metabolism from the geological record.

Such biosignatures can be used as calibration points in phylogenetic studies exploring the emergence and diversification of aerobic microorganisms on early Earth. A Mesoarchean origin of aerobic respiration is supported by the emergence of enzymes involved in oxygen cycling to ≥2.9 Ga, i.e. at least ca. 500 m.y. before the GOE (David and Alm, 2011; Wang *et al.*, 2011; Kim *et al.*, 2012; Jabłońska and Tawfik, 2021; Boden *et al.*, 2021). Possibly, early enzymes catalysing O_2 reduction might be a detoxification mechanism for coping with oxidative stress ('aerotolerance') rather than aerobic respiration (Brochier-Armanet *et al.*, 2009; Gribaldo *et al.*, 2009; Jabłońska and Tawfik, 2021, 2022). Aerotolerance could be an adaptation to abiotic sources of reactive oxygen species and O_2 on early Earth (Haqq-Misra *et al.*, 2011; He *et al.*, 2021, 2023; Stone *et al.*, 2022). Nevertheless, the early origin of these enzymes is consistent with geochemical proxies suggesting locally or transiently sufficient O_2 for aerobic respiration (Anbar *et al.*, 2007; Ostrander *et al.*, 2021), current reconstructions of the emergence of oxygenic photosynthesis at ca. 3.0 Ga (Schirrmeister *et al.*, 2015; Sánchez-Baracaldo, 2015; Cardona *et al.*, 2019; Garcia-Pichel *et al.*, 2019; Jabłońska and Tawfik, 2021; Fournier *et al.*, 2021; Boden *et al.*, 2024) and the recent discovery of ancestral high redox potential quinones predating the emergence of cyanobacteria (Elling *et al.*, 2025). Notably, for O_2 to leave a proxy record, it must degas into the atmosphere (in the case of MIF-S) or affect the solubility of redox-sensitive elements (e.g. chromium, molybdenum). However, released O_2 may not reach concentrations reflected in O_2 proxies due to its consumption by various O_2 sinks, including aerobic microorganisms. Conversely, oxidative weathering within benthic microbial mats can produce O_2 proxy signals, even if O_2 does not accumulate in the environment due to microbial consumption (Lalonde and Konhauser, 2015). Therefore, aerobic microorganisms are a plausible O_2 sink after the emergence of oxygenic photosynthesis, even when seawater or atmospheric O_2 concentrations were too low to leave a proxy record. Aerobic microorganisms may thus have consumed O_2 produced by cyanobacteria, even if the O_2 flux was small due to the possible inhibition of oxygenic photosynthesis. Thus, as soon as oxygenic photosynthesis emerged ca. 3.0 Ga, an aerobic niche appeared for microorganisms to exploit. In concert, the current evidence renders it probable that the Archean aerobic biosphere represented an O_2 sink that helped delay the GOE.

Synthesis and future research directions

Earth presumably accreted from reduced material but the mantle oxidised early in its history due to core formation, late accretion of relatively oxidised material, Fe(III) transfer from the lower to the upper mantle and H_2 outgassing (e.g. Wade and Wood, 2001; Frost *et al.*, 2004; Rubie *et al.*, 2011; Sharp *et al.*, 2013; Pahlevan *et al.*, 2019). Between 3.0 and 2.0 Ga, the upper mantle probably evolved to near-modern fO_2 (e.g. Aulbach and Stagno, 2016; Stagno and Fei, 2020; O'Neill and Aulbach, 2022) (Figs 2, 3). The earliest putative evidence for localised and/or transient O_2 in Earth's surface environments appears at 3.0 Ga (Planavsky *et al.*, 2014; Ossa Ossa *et al.*, 2016, 2018; Smith and Beukes, 2023), coinciding with phylogenetic studies on the emergence of oxygenic photosynthesis (e.g. Schirrmeister *et al.*, 2015; Sánchez-Baracaldo, 2015; Fournier *et al.*, 2021) (Fig. 4). 'Whiffs of oxygen' inferred from manganese enrichments and stable isotopes become more abundant at 2.6–2.5 Ga, suggesting an expansion of oxygenated surface waters (e.g. Anbar *et al.*, 2007; Kendall *et al.*, 2015; Smith and Beukes, 2023). Atmospheric oxygenation is recorded by the disappearance of the MIF-S signal at ca. 2.3 Ga (e.g. Farquhar, 2000; Pavlov and Kasting, 2002; Bekker *et al.*, 2004; Poulton *et al.*, 2021) (Fig. 4). This timeline demonstrates a delay of several hundred million years between the first appearance of O_2 in Earth's surface environments and its atmospheric accumulation. Thus, the emergence of oxygenic photosynthesis alone cannot satisfactorily explain the timing of the GOE.

Various models were put forward to explain this delay. One set of ideas centres around a suppressed biological O_2 source due to phosphorous limitation, iron toxicity or ecological factors affecting the productivity of oxygenic photosynthesis in the Archean (e.g. Swanner *et al.*, 2015a; Sánchez-Baracaldo, 2015; Reinhard *et al.*, 2017). Other models focus on O_2 sinks, like reduced gases and aqueous solutes in surface environments, which acted as effective buffers against atmospheric oxygenation before their capacity diminished over time (e.g. Holland, 2002; Gaillard *et al.*, 2011; Lee *et al.*, 2016; O'Neill and Aulbach, 2022). However, the role of aerobic respiration, a critical O_2 sink today, seems less constrained for the Archean. Studies on recent environments and microbial incubation experiments increasingly show that aerobic growth occurs at O_2 concentrations inferred for late Archean oases or even

https://doi.org/10.1180/gbi.2025.10003 Published online by Cambridge University Press

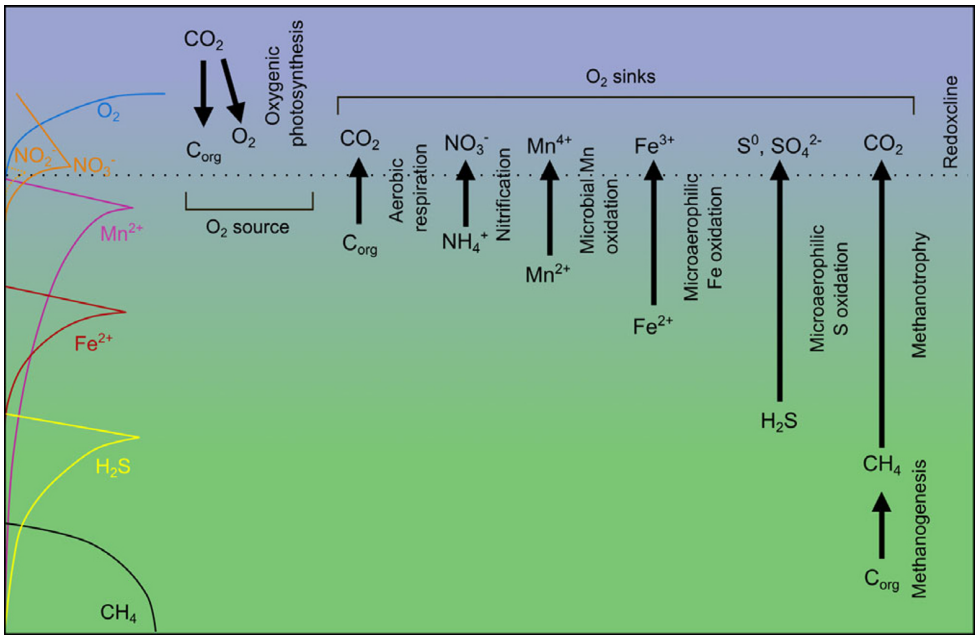

Figure 5. Schematic of microbial O_2 sources and sinks on the late Archean Earth. Oxygenic photosynthesis is the major O_2 source. Biomass from primary productivity, anaerobic respiration (i.e. dissimilatory reduction of NO_3^-, Mn(IV), Fe(III), SO_4^{2-}), methanogenesis and abiotic sources (not indicated) yield diverse O_2 sinks (i.e. C_{org}, NH_4^+, Mn(II), Fe(II), H_2S, CH_4). Aerobic microorganisms couple the oxidation of these sinks to the reduction of O_2, forming the microbial O_2 sink. The geochemical zonation on the left was redrawn from Canfield and Thamdrup (2009). Note that this zonation reflects the decreasing energy yield of the corresponding respiration process and may strongly overlap in natural environments, therefore it does not necessarily match the depth profile of the indicated chemical species.

under apparently anoxic conditions (e.g. Stolper *et al.*, 2010; Milucka *et al.*, 2015; Berg *et al.*, 2019). Combined evidence from biosignatures and phylogenetic reconstructions suggests the presence of an aerobic biosphere at least since the emergence of oxygenic photosynthesis (e.g. Godfrey and Falkowski, 2009; David and Alm, 2011; Jabłońska and Tawfik, 2021). These aerobic microorganisms could have lived closely associated with early cyanobacteria, helping to prevent environmental oxygenation since 3.0 Ga (Berg *et al.*, 2022). Microbial O_2 consumption was probably coupled to the oxidation of organic matter, CH_4, iron, manganese and sulfur before the end of the Archean (Fig. 5). The importance of this sink must have increased over time as a direct response to progressive oxygenation of Earth's surface environments. This, in turn, was facilitated by the solid Earth's redox evolution, shifting volcanic gases and aqueous solutes to more oxidised species. Viewed this way, the expansion of the aerobic biosphere represents geobiological feedback to solid Earth and surface oxidation, helping to delay the GOE for several hundred M.y. after the emergence of oxygenic photosynthesis.

Still, several questions remain concerning the efficacy of the aerobic biosphere as an O_2 sink. It was previously noted that the advent of aerobic metabolisms under Archean Earth conditions does not necessarily demonstrate their environmental impact (Lyons *et al.*, 2024). Indeed, the degree to which aerobic respiration could buffer O_2 production by oxygenic photosynthesis is currently unknown. This highlights the need for an improved mechanistic and quantitative assessment of the aerobic biosphere as an O_2 sink in the Archean. When and in what sequence did the various aerobic metabolisms emerge? What was the environmental distribution of aerobic microorganisms and how much O_2 could they consume under conditions in Archean aquatic settings? How did competition between aerobic microorganisms for resources impact their activity and what are the relative roles of microbial versus abiotic O_2 consumption in the environment?

A critical prerequisite for quantifying the role of the aerobic O_2 sink is constraining the O_2 flux. Despite significant advances, the productivity of cyanobacteria before the GOE and the spatial distribution of oxygenated environments remain open questions. Reconstructing whether the earliest molecular mechanisms for O_2 reduction were coupled to energy conservation rather than just detoxification would help identify when the biosphere became a more efficient O_2 sink. Protocols for biosignature detection must improve to pinpoint the earliest evidence of the various aerobic metabolisms in the geological record and serve as calibration points for phylogenetic studies on the genomes of modern (nan)aerobic microorganisms. This will help refine the evolutionary history of Earth's aerobic biosphere. Moreover, the environmental prevalence of aerobic growth at nanomolar O_2 concentrations is poorly constrained on modern Earth but may have been larger in the Archean (Berg *et al.*, 2022). Broad surveys of modern apparently anoxic environments, integrating geochemical and genomic evidence, will be crucial in constraining the prevalence of nanaerobic life. Co-culturing experiments of cyanobacteria and different aerobic microorganisms under Archean ocean conditions, including reduced species like Fe^{2+}, may better constrain the past activity of aerobic respiration. These data are critical for quantitative models on Archean microbial O_2 consumption, which previously did not account for the metabolic diversity of the aerobic biosphere (Goldblatt *et al.*, 2006; Claire *et al.*, 2006; Catling *et al.*, 2007; Daines and Lenton, 2016), possibly underestimating the capacity of the microbial O_2 sink. Addressing these issues will help answer which aerobic microorganisms consumed how much O_2, when and where in Archean environments and improve our understanding of why the GOE happened when it did.

Acknowledgements. The authors thank the associate editor and two anonymous reviewers for their insightful comments, which improved the manuscript. Jan-Peter Duda is thanked for his input on an early draft of this manuscript. Eric Runge was supported by the Emmy Noether program of the Deutsche Forschungsgemeinschaft (DFG; grant to Jan-Peter Duda; DU 1450/7-1). Sara Vulpius was funded by the DFG within the SPP 1833 "Building a Habitable Earth" project number NO 1324/2-1 and partly funded by the STRUCTURE program of Freie Universität Berlin (FUB). Daniel Herwartz was supported by the Heisenberg Program of the DFG (HE 6357/4-1). This study was also funded by the Project-ID 263649064–TRR 170 as well as by the European Union (ERC, DIVERSE, 101087755). Views and opinions expressed are, however, those of the author(s) only and do not necessarily reflect those of

the European Union or the European Research Council Executive Agency. Neither the European Union nor the granting authority can be held responsible.

Competing interests. The authors declare none.

References

Ader M. Thomazo C., Sansjofre P., Busigny V., Papineau D., Laffont R., Cartigny P. and Halverson, G.P. (2016) Interpretation of the nitrogen isotopic composition of Precambrian sedimentary rocks: Assumptions and perspectives. *Chemical Geology*, **429**, 93–110, doi:10.1016/j.chemgeo.2016.02.010.

Aftabi A., Atapour H., Mohseni S. and Babaki A. (2021) Geochemical discrimination among different types of banded iron formations (BIFs): A comparative review. *Ore Geology Reviews*, **136**, 104244, doi:10.1016/j.oregeore2021.104244.

Albut G., Babechuk M.G., Kleinhanns I.C., Benger M., Beukes N.J., Steinhilber B., Smith A.J.B., Kruger S.J. and Schoenberg R. (2018) Modern rather than Mesoarchaean oxidative weathering responsible for the heavy stable Cr isotopic signatures of the 2.95 Ga old Ijzermijn iron formation (South Africa). *Geochimica et Cosmochimica Acta*, **228**, 157–189, doi:10.1016/j.gca.2018.02.034.

Albut G., Kamber B.S., Brüske A., Beukes N.J., Smith A.J.B. and Schoenberg R. (2019) Modern weathering in outcrop samples versus ancient paleoredox information in drill core samples from a Mesoarchaean marine oxygen oasis in Pongola Supergroup, South Africa. *Geochimica et Cosmochimica Acta*, **265**, 330–353, doi:10.1016/j.gca.2019.09.001.

Anbar A.D. *et al.* (2007) A Whiff of Oxygen Before the Great Oxidation Event? *Science*, **317**, 1903–1906, doi:10.1126/science.1140325.

Anbar A.D. and Holland H.D. (1992) The photochemistry of manganese and the origin of banded iron formations. *Geochimica et Cosmochimica Acta*, **56**, 2595–2603, doi:10.1016/0016-7037(92)90346-K.

Andrault D., Muñoz M., Pesce G., Cerantola V., Chumakov, A., Kantor I., Pascarelli S., Rüffer R. and Hennet L. (2018) Large oxygen excess in the primitive mantle could be the source of the Great Oxygenation Event. *Geochemical Perspectives Letters*, **6**, 5–10, doi:10.7185/geochemlet.1801.

Arculus R.J. (1985) Oxidation status of the mantle: past and present. *Annual Review of Earth and Planetary Sciences*, **13**, 75–95.

Ardia P., Hirschmann M.M., Withers A.C. and Stanley B.D. (2013) Solubility of CH_4 in a synthetic basaltic melt, with applications to atmosphere–magma ocean–core partitioning of volatiles and to the evolution of the Martian atmosphere. *Geochimica et Cosmochimica Acta*, **114**, 52–71, doi:10.1016/j.gca.2013.03.028.

Armstrong K., Frost D.J., McCammon C.A., Rubie D.C. and Boffa Ballaran T. (2019) Deep magma ocean formation set the oxidation state of Earth's mantle. *Science*, **365**, 903–906, doi:10.1126/science.aax8376.

Aulbach S. and Stagno V. (2016) Evidence for a reducing Archean ambient mantle and its effects on the carbon cycle. *Geology*, **44**, 751–754, doi:10.1130/G38070.1.

Aulbach S. and Viljoen K.S. (2015) Eclogite xenoliths from the Lace kimberlite, Kaapvaal craton: From convecting mantle source to palaeo-ocean floor and back. *Earth and Planetary Science Letters*, **431**, 274–286, doi:10.1016/j.epsl.2015.08.039.

Aulbach S., Woodland A.B., Vasilyev P., Galvez M.E. and Viljoen K.S. (2017) Effects of low-pressure igneous processes and subduction on $Fe^{3+}/\Sigma Fe$ and redox state of mantle eclogites from Lace (Kaapvaal craton). *Earth and Planetary Science Letters*, **474**, 283–295, doi:10.1016/j.epsl.2017.06.030.

Badro J., Brodholt J.P., Piet H., Siebert J. and Ryerson F.J. (2015) Core formation and core composition from coupled geochemical and geophysical constraints. *Proceedings of the National Academy of Sciences*, **112**, 12310–12314, doi:10.1073/pnas.1505672112.

Ballhaus C., Berry R.F. and Green D.H. (1991) High pressure experimental calibration of the olivine-orthopyroxene-spinel oxygen geobarometer: implications for the oxidation state of the upper mantle. *Contributions to Mineralogy and Petrology*, **107**, 27–40.

Ballhaus C. and Frost B.R. (1994) The generation of oxidized CO_2-bearing basaltic melts from reduced CH_4-bearing upper mantle sources. *Geochimica et Cosmochimica Acta*, **58**, 4931–4940, doi:10.1016/0016-7037(94)90222-4.

Ballmer M.D., Houser C., Hernlund J.W., Wentzcovitch R.M. and Hirose K. (2017) Persistence of strong silica-enriched domains in the Earth's lower mantle. *Nature Geoscience*, **10**, 236–240, doi:10.1038/ngeo2898.

Bao H., Rumble D. and Lowe D.R. (2007) The five stable isotope compositions of Fig Tree barites: Implications on sulfur cycle in ca. 3.2Ga oceans. *Geochimica et Cosmochimica Acta*, **71**, 4868–4879, doi:10.1016/j.gca.2007.05.032.

Barrett T.J., Fralick P.W. and Jarvis I. (1988) Rare-earth-element geochemistry of some Archean iron formations north of Lake Superior, Ontario. *Canadian Journal of Earth Sciences*, **25**, 570–580, doi:10.1139/e88-055.

Barth P., Stüeken E.E., Helling C., Rossmanith L., Peng Y., Walters W. and Claire M. (2023) Isotopic constraints on lightning as a source of fixed nitrogen in Earth's early biosphere: *Nature Geoscience*, **16**, 478–484, doi:10.1038/s41561-023-01187-2.

Bau M., Frei R., Garbe-Schönberg D. and Viehmann S. (2022) High-resolution Ge-Si-Fe, Cr isotope and Th-U data for the Neoarchean Temagami BIF, Canada, suggest primary origin of BIF bands and oxidative terrestrial weathering 2.7 Ga ago. *Earth and Planetary Science Letters*, **589**, 117579, doi:10.1016/j.epsl.2022.117579.

Baughn A.D. and Malamy M.H. (2004) The strict anaerobe Bacteroides fragilis grows in and benefits from nanomolar concentrations of oxygen. *Nature*, **427**, 441–444, doi:10.1038/nature02285.

Bekker A. (2001) Chemostratigraphy of the Paleoproterozoic Duitschland Formation, South Africa: implications for coupled climate change and carbon cycling. *American Journal of Science*, **301**, 261–285, doi:10.2475/ajs.301.3.261.

Bekker A., Holland H.D., Wang P.-L., Rumble D., Stein H.J., Hannah J.L., Coetzee L.L. and Beukes N.J. (2004) Dating the rise of atmospheric oxygen. *Nature*, **427**, 117–120, doi:10.1038/nature02260.

Bekker A., Slack J.F., Planavsky N., Krapez B., Hofmann A., Konhauser K.O. and Rouxel O.J. (2010) Iron formation: the sedimentary product of a complex interplay among mantle, tectonic, oceanic, and biospheric processes. *Economic Geology*, **105**, 467–508, doi:10.2113/gsecongeo.105.3.467.

Beman J.M., Leilei Shih J. and Popp B.N. (2013) Nitrite oxidation in the upper water column and oxygen minimum zone of the eastern tropical North Pacific Ocean. *The ISME Journal*, **7**, 2192–2205, doi:10.1038/ismej.2013.96.

Berg J.S. *et al.* (2019) Dark aerobic sulfide oxidation by anoxygenic phototrophs in anoxic waters. *Environmental Microbiology*, **21**, 1611–1626, doi:10.1111/1462-2920.14543.

Berg J.S., Ahmerkamp S., Pjevac P., Hausmann B., Milucka J. and Kuypers M.M.M. (2022) How low can they go? Aerobic respiration by microorganisms under apparent anoxia. *FEMS Microbiology Reviews*, **46**, fuac006, doi:10.1093/femsre/fuac006.

Berner R.A. (1989) Biogeochemical cycles of carbon and sulfur and their effect on atmospheric oxygen over Phanerozoic time. *Global and Planetary Change*, **75**, 97–122.

Bindeman I.N., Schmitt A.K. and Evans D.A.D. (2010) Limits of hydrosphere-lithosphere interaction: Origin of the lowest-known $\delta^{18}O$ silicate rock on Earth in the Paleoproterozoic Karelian rift. *Geology*, **38**, 631–634, doi:10.1130/G30968.1.

Bjerrum C.J. and Canfield D.E. (2002) Ocean productivity before about 1.9 Gyr ago limited by phosphorus adsorption onto iron oxides. *Nature*, **417**, 159–162, doi:10.1038/417159a.

Blank C.E. and Sánchez-Baracaldo P. (2010) Timing of morphological and ecological innovations in the cyanobacteria – a key to understanding the rise in atmospheric oxygen. *Geobiology*, **8**, 1–23, doi:10.1111/j.1472-4669.2009.00220.x.

Blundy J.D., Brodholt J.P. and Wood B.J. (1991) Carbon–fluid equilibria and the oxidation state of the upper mantle. *Nature*, **349**, 321–324, doi:10.1038/349321a0.

Boden J.S., Konhauser K.O., Robbins L.J. and Sánchez-Baracaldo P. (2021) Timing the evolution of antioxidant enzymes in cyanobacteria. *Nature Communications*, **12**, 4742, doi:10.1038/s41467-021-24396-y.

Boden J.S., Zhong J., Anderson R.E. and Stüeken E.E. (2024) Timing the evolution of phosphorus-cycling enzymes through geological time using phylogenomics. *Nature Communications*, **15**, 3703, doi:10.1038/s41467-024-47914-0.

Bolhar R., Van Kranendonk M.J. and Kamber B.S. (2005) A trace element study of siderite–jasper banded iron formation in the 3.45Ga Warrawoona Group, Pilbara Craton—Formation from hydrothermal fluids and shallow seawater. *Precambrian Research*, **137**, 93–114, doi:10.1016/j.precamres.2005.02.001.

Brasier M., Green O., Lindsay J., Mcloughlin N., Steele A. and Stoakes C. (2005) Critical testing of Earth's oldest putative fossil assemblage from the ~3.5Ga Apex chert, Chinaman Creek, Western Australia. *Precambrian Research*, **140**, 55–102, doi:10.1016/j.precamres.2005.06.008.

Braterman P.S., Cairns-Smith A.G. and Sloper R.W. (1983) Photo-oxidation of hydrated Fe^{2+}—significance for banded iron formations. *Nature*, **303**, 163–164, doi:10.1038/303163a0.

Breuer D. and Spohn T. (1995) Possible flush instability in mantle convection at the Archaean–Proterozoic transition. *Nature*, **378**, 608–610, doi:10.1038/378608a0.

Bristow L.A. *et al.* (2016) Ammonium and nitrite oxidation at nanomolar oxygen concentrations in oxygen minimum zone waters. *Proceedings of the National Academy of Sciences*, **113**, 10601–10606, doi:10.1073/pnas.1600359113.

Brochier-Armanet C., Talla E. and Gribaldo S. (2009) The multiple evolutionary histories of dioxygen reductases: implications for the origin and evolution of aerobic respiration. *Molecular Biology and Evolution*, **26**, 285–297, doi:10.1093/molbev/msn246.

Brocks J.J. (1999) Archean molecular fossils and the early rise of eukaryotes. *Science*, **285**, 1033–1036, doi:10.1126/science.285.5430.1033.

Brocks J.J. (2011) Millimeter-scale concentration gradients of hydrocarbons in Archean shales: Live-oil escape or fingerprint of contamination? *Geochimica et Cosmochimica Acta*, **75**, 3196–3213, doi:10.1016/j.gca.2011.03.014.

Brocks, J.J. Buick, R. Logan G.A. and Summons R.E. (2003) Composition and syngeneity of molecular fossils from the 2.78 to 2.45 billion-year-old Mount Bruce Supergroup, Pilbara Craton, Western Australia. *Geochimica et Cosmochimica Acta*, **67**(21), 4289 – 4319.

Brüske A. *et al.* (2020) The onset of oxidative weathering traced by uranium isotopes. *Precambrian Research*, **338**, 105583, doi:10.1016/j.precamres.2019.105583.

Budde G., Burkhardt C. and Kleine T. (2019) Molybdenum isotopic evidence for the late accretion of outer Solar System material to Earth. *Nature Astronomy*, **3**, 736–741, doi:10.1038/s41550-019-0779-y.

Buick R. (1992) The antiquity of oxygenic photosynthesis: evidence from stromatolites in sulphate-deficient Archaean lakes. *Science*, **255**, 74–77, doi:10.1126/science.11536492.

Burgisser A. and Scaillet B. (2007) Redox evolution of a degassing magma rising to the surface. *Nature*, **445**, 194–197, doi:10.1038/nature05509.

Busigny V., Lebeau O., Ader M., Krapež B. and Bekker A. (2013) Nitrogen cycle in the Late Archean ferruginous ocean. *Chemical Geology*, **362**, 115–130, doi:10.1016/j.chemgeo.2013.06.023.

Cairns-Smith A.G. (1978) Precambrian solution photochemistry, inverse segregation, and banded iron formations. *Nature*, **276**, 807–808, doi:10.1038/276807a0.

Callbeck C.M. *et al.* (2018) Oxygen minimum zone cryptic sulfur cycling sustained by offshore transport of key sulfur oxidizing bacteria. *Nature Communications*, **9**, 1729, doi:10.1038/s41467-018-04041-x.

Canfield D.E. (2001) Biogeochemistry of sulfur isotopes. Pp. 607 – 636 in: *Reviews in Mineralogy and Geochemistry*, Vol. **43**(1) (J.W. Valley and D.R. Cole, editors). Mineralogical Society of America.

Canfield D.E. (2005) The early history of atmospheric oxygen: Homage to Robert M. *Garrels.* Annual Review of Earth and Planetary Sciences, **33**, 1–36, doi:10.1146/annureearth.33.092203.122711.

Canfield D.E., Rosing M.T. and Bjerrum C. (2006) Early anaerobic metabolisms. *Philosophical Transactions of the Royal Society B: Biological Sciences*, **361**, 1819–1836, doi:10.1098/rstb.2006.1906.

Canfield D.E. and Thamdrup B. (2009) Towards a consistent classification scheme for geochemical environments, or, why we wish the term 'suboxic' would go away. *Geobiology*, **7**, 385–392, doi:10.1111/j.1472-4669.2009.00214.x.

Canil D. (1997) Vanadium partitioning and the oxidation state of Archaean komatiite magmas. *Nature*, **389**, 842–845, doi:10.1038/39860.

Cardona T., Sánchez-Baracaldo P., Rutherford A.W. and Larkum A.W. (2019) Early Archean origin of Photosystem II. *Geobiology*, **17**, 127–150, doi:10.1111/gbi.12322.

Carmichael I.S.E. (1991) The redox states of basic and silicic magmas: a reflection of their source regions? *Contributions to Mineralogy and Petrology*, **106**, 129–141, doi:10.1007/BF00306429.

Cartier C., Hammouda T., Boyet M., Bouhifd M.A. and Devidal J.-L. (2014) Redox control of the fractionation of niobium and tantalum during planetary accretion and core formation. *Nature Geoscience*, **7**, 573–576, doi:10.1038/ngeo2195.

Casciotti K.L. (2009) Inverse kinetic isotope fractionation during bacterial nitrite oxidation. *Geochimica et Cosmochimica Acta*, **73**, 2061–2076, doi:10.1016/j.gca.2008.12.022.

Castresana J. and Saraste M. (1995) Evolution of energetic metabolism: the respiration-early hypothesis. *Trends in Biochemical Sciences*, **20**, 443–448.

Cates N.L. and Mojzsis S.J. (2006) Chemical and isotopic evidence for widespread Eoarchean metasedimentary enclaves in southern West Greenland. *Geochimica et Cosmochimica Acta*, **70**, 4229–4257, doi:10.1016/j.gca.2006.05.014.

Catling D.C., Claire M.W. and Zahnle K.J. (2007) Anaerobic methanotrophy and the rise of atmospheric oxygen. *Philosophical Transactions of the Royal Society A: Mathematical, Physical and Engineering Sciences*, **365**, 1867–1888, doi:10.1098/rsta.2007.2047.

Catling D.C. and Zahnle K.J. (2020) The Archean atmosphere. *Science Advances*, **6**, eaax1420, doi:10.1126/sciadaax1420.

Cavosie A.J., Valley J.W., Wilde S.A. and E.I.M.F. (2005) Magmatic $\delta^{18}O$ in 4400–3900 Ma detrital zircons: A record of the alteration and recycling of crust in the Early Archean. *Earth and Planetary Science Letters*, **235**, 663–681, doi:10.1016/j.epsl.2005.04.028.

Chan C.S., Emerson D. and Luther G.W. (2016) The role of microaerophilic Fe-oxidizing micro-organisms in producing banded iron formations. *Geobiology*, **14**, 509–528, doi:10.1111/gbi.12192.

Chiu B.K., Kato S., McAllister S.M., Field E.K. and Chan C.S. (2017) Novel pelagic iron-oxidizing zetaproteobacteria from the Chesapeake Bay oxic–anoxic transition zone. *Frontiers in Microbiology*, **8**, 1280, doi:10.3389/fmicb.2017.01280.

Christie D.M., Carmichael I.S.E. and Langmuir C.H. (1986) Oxidation states of mid-ocean ridge basalt glasses. *Earth and Planetary Science Letters*, **79**, 397–411, doi:10.1016/0012-821X(86)90195-0.

Claire M.W., Catling D.C. and Zahnle K.J. (2006) Biogeochemical modelling of the rise in atmospheric oxygen. *Geobiology*, **4**, 239–269, doi:10.1111/j.1472-4669.2006.00084.x.

Clement B.G., Luther G.W. and Tebo B.M. (2009) Rapid, oxygen-dependent microbial Mn(II) oxidation kinetics at sub-micromolar oxygen concentrations in the Black Sea suboxic zone. *Geochimica et Cosmochimica Acta*, **73**, 1878–1889, doi:10.1016/j.gca.2008.12.023.

Clement J., Shrestha J., Ehrenfeld J. and Jaffe P. (2005) Ammonium oxidation coupled to dissimilatory reduction of iron under anaerobic conditions in wetland soils. *Soil Biology and Biochemistry*, **37**, 2323–2328, doi:10.1016/j.soilbio.2005.03.027.

Cloud P. (1973) Paleoecological significance of the banded iron-formation. *Economic Geology*, **68**, 1135–1143, doi:10.2113/gsecongeo.68.7.1135.

Collerson K.D. and Kamber B.S. (1999) Evolution of the continents and the atmosphere inferred from Th-U-Nb systematics of the depleted mantle. *Science*, **283**, 1519–1522, doi:10.1126/science.283.5407.1519.

Condie K. (2001) Precambrian superplumes and supercontinents: a record in black shales, carbon isotopes, and paleoclimates? *Precambrian Research*, **106**, 239–260, doi:10.1016/S0301-9268(00)00097-8.

Cosmidis J., Nims C.W., Diercks D. and Templeton A.S. (2019) Formation and stabilization of elemental sulfur through organomineralization. *Geochimica et Cosmochimica Acta*, **247**, 59–82, doi:10.1016/j.gca.2018.12.025.

Cottrell E. and Kelley K.A. (2011) The oxidation state of Fe in MORB glasses and the oxygen fugacity of the upper mantle. *Earth and Planetary Science Letters*, **305**, 270–282, doi:10.1016/j.epsl.2011.03.014.

Crockford P. and Halevy I. (2022) Questioning the paradigm of a phosphate-limited Archean biosphere. *Geophysical Research Letters*, **49**, e2022GL099818, doi:10.1029/2022GL099818.

Crowe S.A. *et al.* (2014) Sulfate was a trace constituent of Archean seawater. *Science*, **346**, 735–739.

Crowe S.A. *et al.* (2011) The methane cycle in ferruginous Lake Matano: methane cycle in ferruginous Lake Matano. *Geobiology*, **9**, 61–78, doi:10.1111/j.1472-4669.2010.00257.x.

Crowe S.A., Døssing L.N., Beukes N.J., Bau M., Kruger S.J., Frei R. and Canfield D.E. (2013) Atmospheric oxygenation three billion years ago. *Nature*, **501**, 535–538, doi:10.1038/nature12426.

Cypionka H. (2000) Oxygen respiration by *Desulfovibrio* species. *Annual Review of Microbiology*, **54**, 827–848, doi:10.1146/annuremicro.54.1.827.

Czaja A.D., Beukes N.J. and Osterhout J.T, (2016) Sulfur-oxidizing bacteria prior to the Great Oxidation Event from the 2.52 Ga Gamohaan Formation of South Africa. *Geology*, **44**, 983–986, doi:10.1130/G38150.1.

https://doi.org/10.1180/gbi.2025.10003 Published online by Cambridge University Press

Dahl C., Friedrich C. and Kletzin A. (2008) Sulfur oxidation in Prokaryotes. In: *Encyclopedia of Life Sciences (ELS)*. John Wiley & Sons, Ltd, doi:10.1002/9780470015902.a0021155.

Daines S.J. and Lenton T.M. (2016) The effect of widespread early aerobic marine ecosystems on methane cycling and the Great Oxidation. *Earth and Planetary Science Letters*, **434**, 42–51, doi:10.1016/j.epsl.2015.11.021.

Dauphas N. (2017) The isotopic nature of the Earth's accreting material through time. *Nature*, **541**, 521–524, doi:10.1038/nature20830.

David L.A. and Alm E.J. (2011) Rapid evolutionary innovation during an Archaean genetic expansion. *Nature*, **469**, 93–96, doi:10.1038/nature09649.

Daye M., Klepac-Ceraj V., Pajusalu M., Rowland S., Farrell-Sherman A., Beukes N., Tamura N., Fournier G. and Bosak T. (2019) Light-driven anaerobic microbial oxidation of manganese. *Nature*, **576**, 311–314, doi:10.1038/s41586-019-1804-0.

Debaille V., O'Neill C., Brandon A.D., Haenecour P., Yin Q.-Z., Mattielli N. and Treiman A.H. (2013) Stagnant-lid tectonics in early Earth revealed by ^{142}Nd variations in late Archean rocks. *Earth and Planetary Science Letters*, **373**, 83–92, doi:10.1016/j.epsl.2013.04.016.

Delano J.W. (2001) Redox History of the Earth's Interior Since ~3900 Ma: Implications for Prebiotic Molecules. *Origins of Life and Evolution of Biospheres*, **31**, 311–341.

Dellwig O., Leipe T., März C., Glockzin M., Pollehne F., Schnetger B., Yakushev E.V., Böttcher M.E. and Brumsack H.-J. (2010) A new particulate Mn–Fe–P-shuttle at the redoxcline of anoxic basins. *Geochimica et Cosmochimica Acta*, **74**, 7100–7115, doi:10.1016/j.gca.2010.09.017.

Deng J., Du Z., Karki B.B., Ghosh D.B. and Lee K.K.M. (2020) A magma ocean origin to divergent redox evolutions of rocky planetary bodies and early atmospheres. *Nature Communications*, **11**, doi:10.1038/s41467-020-15757-0.

Derry L.A. (2015) Causes and consequences of mid-Proterozoic anoxia. *Geophysical Research Letters*, **42**, 8538–8546, doi:10.1002/2015GL065333.

Devol A.H. (1978) Bacterial oxygen uptake kinetics as related to biological processes in oxygen deficient zones of the oceans. *Deep Sea Research*, **25**, 137–146, doi:10.1016/0146-6291(78)90001-2.

Dick G.J., Grim S.L. and Klatt J.M. (2018) Controls on O_2 production in cyanobacterial mats and implications for Earth's oxygenation. *Annual Review of Earth and Planetary Sciences*, **46**, 123–147, doi:10.1146/annurev-earth-082517-010035.

Dodd M.S. *et al.* (2022) Abiotic anoxic iron oxidation, formation of Archean banded iron formations, and the oxidation of early Earth. *Earth and Planetary Science Letters*, **584**, 117469, doi:10.1016/j.epsl.2022.117469.

Dodd M.S., Papineau D., Grenne T., Slack J.F., Rittner M., Pirajno F., O'Neil J. and Little C.T.S. (2017) Evidence for early life in Earth's oldest hydrothermal vent precipitates. *Nature*, **543**, 60–64, doi:10.1038/nature21377.

Domagal-Goldman S.D., Kasting J.F., Johnston D.T. and Farquhar, J. (2008) Organic haze, glaciations and multiple sulfur isotopes in the Mid-Archean Era. *Earth and Planetary Science Letters*, **269**, 29–40, doi:10.1016/j.epsl.2008.01.040.

Dreher C.L., Schad M., Robbins L.J., Konhauser K.O., Kappler, A. and Joshi, P. (2021) Microbial processes during deposition and diagenesis of Banded Iron Formations. *PalZ*, **95**, 593–610, doi:10.1007/s12542-021-00598-z.

Druschel G.K., Emerson D., Sutka R., Suchecki P. and Luther G.W. (2008) Low-oxygen and chemical kinetic constraints on the geochemical niche of neutrophilic iron(II) oxidizing microorganisms. *Geochimica et Cosmochimica Acta*, **72**, 3358–3370, doi:10.1016/j.gca.2008.04.035.

Ducluzeau A.-L., Schoepp-Cothenet B., Van Lis R., Baymann F., Russell M.J. and Nitschke W. (2014) The evolution of respiratory O_2 /NO reductases: an out-of-the-phylogenetic-box perspective. *Journal of The Royal Society Interface*, **11**, 20140196, doi:10.1098/rsif.2014.0196.

Duncan M.S. and Dasgupta R. (2017) Rise of Earth's atmospheric oxygen controlled by efficient subduction of organic carbon. *Nature Geoscience*, **10**, 387–392, doi:10.1038/ngeo2939.

Eigenbrode J.L. and Freeman K.H. (2006) Late Archean rise of aerobic microbial ecosystems. *Proceedings of the National Academy of Sciences*, **103**, 15759–15764, doi:10.1073/pnas.0607540103.

Eigenbrode J.L., Freeman K.H. and Summons, R.E. (2008) Methylhopane biomarker hydrocarbons in Hamersley Province sediments provide evidence for Neoarchean aerobiosis. *Earth and Planetary Science Letters*, **273**, 323–331, doi:10.1016/j.epsl.2008.06.037.

Elling F.J. *et al.* (2025) A novel quinone biosynthetic pathway illuminates the evolution of aerobic metabolism. *Proceedings of the National Academy of Sciences*, **122**, e2421994122, doi:10.1073/pnas.2421994122.

Ernst R. and Bleeker W. (2010) Large igneous provinces (LIPs), giant dyke swarms, and mantle plumes: significance for breakup events within Canada and adjacent regions from 2.5 Ga to the Present. *Canadian Journal of Earth Sciences*, **47**, 695–739, doi:10.1139/E10-025.

Ershov B.G. (2021) Radiation-induced oxidation of iron in the ocean of the early Earth. *Precambrian Research*, **364**, 106360, doi:10.1016/j.precamres.2021.106360.

Evans G.N., Coogan L.A., Kaçar B. and Seyfried W.E. (2023) Molybdenum in basalt-hosted seafloor hydrothermal systems: Experimental, theoretical, and field sampling approaches. *Geochimica et Cosmochimica Acta*, **353**, 28–44, doi:10.1016/j.gca.2023.05.018.

Falkowski P.G. (1997) Evolution of the nitrogen cycle and its influence on the biological sequestration of CO_2 in the ocean. *Nature*, **387**, 272–275, doi:10.1038/387272a0.

Falkowski P.G., Fenchel T. and Delong E.F. (2008) The microbial engines that drive Earth's biogeochemical cycles. *Science*, **320**, 1034–1039, doi:10.1126/science.1153213.

Farquhar J. (2000) Atmospheric influence of Earth's earliest sulfur cycle. *Science*, **289**, 756–758, doi:10.1126/science.289.5480.756.

Farquhar J., Johnston D.T. and Wing B.A. (2007) Implications of conservation of mass effects on mass-dependent isotope fractionations: Influence of network structure on sulfur isotope phase space of dissimilatory sulfate reduction. *Geochimica et Cosmochimica Acta*, **71**, 5862–5875, doi:10.1016/j.gca.2007.08.028.

Farquhar J., Savarino J., Airieau S. and Thiemens M.H. (2001) Observation of wavelength-sensitive mass-independent sulfur isotope effects during SO_2 photolysis: Implications for the early atmosphere. *Journal of Geophysical Research*, **106**, 32829–32839.

Field C.B., Behrenfeld M.J., Randerson J.T. and Falkowski P. (1998) primary production of the biosphere: integrating terrestrial and oceanic components. *Science*, **281**, 237–240, doi:10.1126/science.281.5374.237.

Fischer R.A., Nakajima Y., Campbell A.J., Frost D.J., Harries D., Langenhorst F., Miyajima N., Pollok K. and Rubie D.C. (2015) High pressure metal–silicate partitioning of Ni, Co, V, Cr, Si, and O. *Geochimica et Cosmochimica Acta*, **167**, 177–194, doi:10.1016/j.gca.2015.06.026.

Fischer-Gödde M., Elfers B.-M., Münker C., Szilas K., Maier W.D., Messling N., Morishita T., Van Kranendonk M. and Smithies H. (2020) Ruthenium isotope vestige of Earth's pre-late-veneer mantle preserved in Archaean rocks. *Nature*, **579**, 240–244, doi:10.1038/s41586-020-2069-3.

Fischer-Gödde M. and Kleine T. (2017) Ruthenium isotopic evidence for an inner Solar System origin of the late veneer. *Nature*, **541**, 525–527, doi:10.1038/nature21045.

Flannery D.T., Allwood A.C., Summons R.E., Williford K.H., Abbey W., Matys E.D. and Ferralis N. (2018) Spatially-resolved isotopic study of carbon trapped in ~3.43 Ga Strelley Pool Formation stromatolites. *Geochimica et Cosmochimica Acta*, **223**, 21–35, doi:10.1016/j.gca.2017.11.028.

Foley S.F. (2011) A reappraisal of redox melting in the Earth's mantle as a function of tectonic setting and time. *Journal of Petrology*, **52**, 1363–1391, doi:10.1093/petrology/egq061.

Foley B.J. and Rizo H. (2017) Long-term preservation of early formed mantle heterogeneity by mobile lid convection: Importance of grainsize evolution. *Earth and Planetary Science Letters*, **475**, 94–105, doi:10.1016/j.epsl.2017.07.031.

Fournier G.P., Moore K.R., Rangel L.T., Payette J.G., Momper L. and Bosak T. (2021) The Archean origin of oxygenic photosynthesis and extant cyanobacterial lineages. *Proceedings of the Royal Society B: Biological Sciences*, **288**, 20210675, doi:10.1098/rspb.2021.0675.

François L.M. (1986) Extensive deposition of banded iron formations was possible without photosynthesis. *Nature*, **320**, 352–354, doi:10.1038/320352a0.

Frei R., Gaucher C., Poulton S.W. and Canfield D.E. (2009) Fluctuations in Precambrian atmospheric oxygenation recorded by chromium isotopes. *Nature*, **461**, 250–253, doi:10.1038/nature08266.

French K.L. *et al.* (2015) Reappraisal of hydrocarbon biomarkers in Archean rocks. *Proceedings of the National Academy of Sciences*, **112**, 5915–5920, doi:10.1073/pnas.1419563112.

Frost D.J., Liebske C., Langenhorst F., McCammon C.A., Trønnes R.G. and Rubie D.C. (2004) Experimental evidence for the existence of iron-rich metal in the Earth's lower mantle. *Nature*, **428**, 409–412, doi:10.1038/nature02413.

https://doi.org/10.1180/gbi.2025.10003 Published online by Cambridge University Press

Frost D.J., Mann U., Asahara Y. and Rubie D.C. (2008) The redox state of the mantle during and just after core formation. *Philosophical Transactions of the Royal Society A: Mathematical, Physical and Engineering Sciences*, **366**, 4315–4337, doi:10.1098/rsta.2008.0147.

Frost D.J. and McCammon C.A. (2008) The redox state of Earth's mantle. *Annual Review of Earth and Planetary Sciences*, **36**, 389–420, doi:10.1146/annureearth.36.031207.124322.

Füssel J., Lam P., Lavik G., Jensen M.M., Holtappels M., Günter M. and Kuypers M.M.M. (2012) Nitrite oxidation in the Namibian oxygen minimum zone. *The ISME Journal*, **6**, 1200–1209, doi:10.1038/ismej.2011.178.

Gaillard F., Bouhifd M.A., Füri E., Malavergne V., Marrocchi Y., Noack L., Ortenzi G., Roskosz, M. and Vulpius S. (2021) The diverse planetary ingassing/outgassing paths produced over billions of years of magmatic activity. *Space Science Reviews*, **217**, 22, doi:10.1007/s11214-021-00802-1.

Gaillard F., Scaillet B. and Arndt N.T. (2011) Atmospheric oxygenation caused by a change in volcanic degassing pressure. *Nature*, **478**, 229–232, doi:10.1038/nature10460.

Gaillard F., Scaillet B., Pichavant M. and Iacono-Marziano G. (2015) The redox geodynamics linking basalts and their mantle sources through space and time. *Chemical Geology*, **418**, 217–233, doi:10.1016/j.chemgeo.2015.07.030.

Garcia-Pichel F., Lombard J., Soule T., Dunaj S., Wu S.H. and Wojciechowski, M.F. (2019) Timing the evolutionary advent of cyanobacteria and the later Great Oxidation Event using gene phylogenies of a sunscreen. *mBio*, **10**, e00561–19, doi:10.1128/mBio.00561-19.

Garvin J., Buick R., Anbar A.D., Arnold G.L. and Kaufman A.J. (2009) Isotopic evidence for an aerobic nitrogen cycle in the Latest Archean. *Science*, **323**, 1045–1048, doi:10.1126/science.1165675.

Gessmann C.K., Rubie D.C. and McCammon C.A. (1999) Oxygen fugacity dependence of Ni, Co, Mn, Cr, V, and Si partitioning between liquid metal and magnesiowüstite at 9–18 GPa and 2200°C. *Geochimica et Cosmochimica Acta*, **63**, 1853–1863, doi:10.1016/S0016-7037(99)00059-9.

Girard J., Amulele G., Farla R., Mohiuddin A. and Karato S. (2016) Shear deformation of bridgmanite and magnesiowüstite aggregates at lower mantle conditions. *Science*, **351**, 144–147, doi:10.1126/science.aad3113.

Girguis P.R., Lee R.W., Desaulniers N., Childress J.J., Pospesel M., Felbeck H. and Zal F. (2000) Fate of nitrate acquired by the tubeworm *Riftia pachyptila*. *Applied and Environmental Microbiology*, **66**, 2783–2790, doi:10.1128/AEM.66.7.2783-2790.2000.

Godfrey L.V. and Falkowski P.G. (2009) The cycling and redox state of nitrogen in the Archaean ocean. *Nature Geoscience*, **2**, 725–729, doi:10.1038/ngeo633.

Goldblatt C., Lenton T.M. and Watson A.J. (2006) Bistability of atmospheric oxygen and the Great Oxidation. *Nature*, **443**, 683–686, doi:10.1038/nature05169.

Grandstaff D. (1980) Origin of uraniferous conglomerates at Elliot Lake, Canada and Witwatersrand, South Africa: Implications for oxygen in the Precambrian atmosphere. *Precambrian Research*, **13**, 1–26, doi:10.1016/0301-9268(80)90056-X.

Grettenberger C., Gold D.A. and Brown C.T. (2025) Distribution of early-branching Cyanobacteria and the potential habitats that gave rise to the earliest oxygenic phototrophs. *mSphere*, **10**, e01013–24, doi:10.1128/msphere.01013-24.

Grettenberger C.L. and Sumner D.Y. (2024) Physiology, not nutrient availability, may have limited primary productivity after the emergence of oxygenic photosynthesis. *Geobiology*, **22**, e12622, doi:10.1111/gbi.12622.

Grewal D.S., Dasgupta R., Sun C., Tsuno K. and Costin G. (2019) Delivery of carbon, nitrogen, and sulfur to the silicate Earth by a giant impact. *Science Advances*, **5**, eaau3669, doi:10.1126/sciadaau3669.

Gribaldo S., Talla E. and Brochier-Armanet C. (2009) Evolution of the haem copper oxidases superfamily: a rooting tale. *Trends in Biochemical Sciences*, **34**, 375–381, doi:10.1016/j.tibs.2009.04.002.

Gu T., Li M., McCammon C. and Lee K.K.M. (2016) Redox-induced lower mantle density contrast and effect on mantle structure and primitive oxygen. *Nature Geoscience*, **9**, 723–727, doi:10.1038/ngeo2772.

Guimond C.M., Noack L., Ortenzi G. and Sohl F. (2021) Low volcanic outgassing rates for a stagnant lid Archean earth with graphite-saturated magmas. *Physics of the Earth and Planetary Interiors*, **320**, 106788, doi:10.1016/j.pepi.2021.106788.

Gumsley A.P., Chamberlain K.R., Bleeker W., Söderlund U., de Kock M.O., Larsson E.R. and Bekker A. (2017) Timing and tempo of the Great Oxidation Event. *Proceedings of the National Academy of Sciences*, **114**, 1811–1816, doi:10.1073/pnas.1608824114.

Guo Q. *et al.* (2009) Reconstructing Earth's surface oxidation across the Archean-Proterozoic transition. *Geology*, **37**, 399–402, doi:10.1130/G25423A.1.

Gutzmer J. and Beukes N.J. (1996) Mineral paragenesis of the Kalahari manganese field, South Africa. *Ore Geology Reviews*, **11**, 405–428.

Guy B.M., Ono S., Gutzmer J., Kaufman A.J., Lin Y., Fogel M.L. and Beukes N.J. (2012) A multiple sulfur and organic carbon isotope record from non-conglomeratic sedimentary rocks of the Mesoarchean Witwatersrand Supergroup, South Africa. *Precambrian Research*, **216–219**, 208–231, doi:10.1016/j.precamres.2012.06.018.

Haggerty S.E. (1978) The redox state of planetary basalts. *Geophysical Research Letters*, **5**, 443–446, doi:10.1029/GL005i006p00443.

Halevy I. (2013) Production, preservation, and biological processing of mass-independent sulfur isotope fractionation in the Archean surface environment. *Proceedings of the National Academy of Sciences*, **110**, 17644–17649, doi:10.1073/pnas.1213148110.

Hansel C.M. (2017) Manganese in marine microbiology. Pp. 37–83 in *Advances in Microbial Physiology, Vol. 70* (R. K. Poole, editor), Elsevier, doi:10.1016/bs.ampbs.2017.01.005.

Hao J., Knoll A.H., Huang F., Hazen R.M. and Daniel I. (2020) Cycling phosphorus on the Archean Earth: Part I. Continental weathering and riverine transport of phosphorus. *Geochimica et Cosmochimica Acta*, **273**, 70–84, doi:10.1016/j.gca.2020.01.027.

Hao J., Liu W., Goff J.L., Steadman J.A., Large R.R., Falkowski P.G. and Yee N. (2022) Anoxic photochemical weathering of pyrite on Archean continents. *Science Advances*, **8**, eabn2226, doi:10.1126/sciadabn2226.

Haqq-Misra J., Kasting J.F. and Lee S. (2011) Availability of O_2 and H_2O_2 on Pre-Photosynthetic Earth. *Astrobiology*, **11**, 293–302, doi:10.1089/ast.2010.0572.

Harrison T.M., Schmitt A.K., McCulloch M.T. and Lovera O.M. (2008) Early (≥4.5 Ga) formation of terrestrial crust: Lu–Hf, $\delta^{18}O$, and Ti thermometry results for Hadean zircons. *Earth and Planetary Science Letters*, **268**, 476–486, doi:10.1016/j.epsl.2008.02.011.

Hayes J.M. (2001) Fractionation of the isotopes of carbon and hydrogen in biosynthetic processes. *Reviews in Mineralogy and Geochemistry* **43**, 225–277.

Hayes J.M. (1983) Geochemical evidence bearing on the origin of aerobiosis, a speculative interpretation. Pp. 93–134 in: *The Earth's Earliest Biosphere: Its Origin and Evolution* (J.W. Schopf, J.W. editor), Princeton University Press, Princeton.

Hayes J.M. (1994) Global methanotrophy at the Archean-Proterozoic transition. Pp. 220–236 in: *Early Life on Earth, Nobel Sympsosium* (S. Bengtson, editor). Columbia University Press, New York.

Hayes J.M. and Waldbauer J.R. (2006) The carbon cycle and associated redox processes through time. *Philosophical Transactions of the Royal Society B: Biological Sciences*, **361**, 931–950, doi:10.1098/rstb.2006.1840.

Hazen R.M., Papineau D., Bleeker W., Downs R.T., Ferry J.M., McCoy T.J., Sverjensky D.A. and Yang H. (2008) Mineral evolution. *American Mineralogist*, **93**, 1693–1720, doi:10.2138/am.2008.2955.

He H. *et al.* (2023) A mineral-based origin of Earth's initial hydrogen peroxide and molecular oxygen. *Proceedings of the National Academy of Sciences*, **120**, e2221984120, doi:10.1073/pnas.2221984120.

He H., Wu X., Xian H., Zhu J., Yang Y., Lv, Y., Li, Y. and Konhauser, K.O. (2021) An abiotic source of Archean hydrogen peroxide and oxygen that pre-dates oxygenic photosynthesis. *Nature Communications*, **12**, 6611, doi:10.1038/s41467-021-26916-2.

Head I.M. (2016) Geomicrobiology of fossil fuels. Pp. 565–622 in: *Ehrlich's Geomicrobiology* (H.L. Ehrlich, D.K. Newman and A. Kappler, editors). CRC Press, Boca Raton, pp. 635.

Heard A.W., Aarons S.M., Hofmann A., He X., Ireland T., Bekker A., Qin L. and Dauphas N. (2021) Anoxic continental surface weathering recorded by the 2.95 Ga Denny Dalton Paleosol (Pongola Supergroup, South Africa). *Geochimica et Cosmochimica Acta*, **295**, 1–23, doi:10.1016/j.gca.2020.12.005.

Heinrichs T.K. and Reimer T. (1977) A sedimentary barite deposit from the Archean Fig Tree Group of the Barberton Mountain Land (South Africa). *Economic Geology*, **72**, 1426–1441.

Hentschel U. and Felbeck H. (1993) Nitrate respiration in the hydrothermal vent tubeworm *Riftia pachyptila*. *Nature*, **366**, 338–340.

Herd C.D.K., Borg L.E., Jones J.H. and Papike J.J. (2002) Oxygen fugacity and geochemical variations in the Martian basalts: implications for Martian basalt petrogenesis and the oxidation state of the upper mantle of Mars. *Geochimica et Cosmochimica Acta*, **66**, 2025–2036, doi:10.1016/S0016-7037(02)00828-1.

Herd C.D., Papike J.J. and Brearley A.J. (2001) Oxygen fugacity of Martian basalts from electron microprobe oxygen and TEM-EELS analyses of Fe-Ti oxides. *American Mineralogist*, **86**, 1015–1024.

Herrmann A.J., Sorwat J., Byrne J.M., Frankenberg-Dinkel N. and Gehringer M. M. (2021) Diurnal Fe(II)/Fe(III) cycling and enhanced O_2 production in a simulated Archean marine oxygen oasis. *Nature Communications*, **12**, 2069, doi:10.1038/s41467-021-22258-1.

Herwartz D., Pack A., Krylov D., Xiao Y., Muehlenbachs K., Sengupta S., and Di Rocco T. (2015) Revealing the climate of snowball Earth from $\Delta^{17}O$ systematics of hydrothermal rocks. *Proceedings of the National Academy of Sciences*, **112**, 5337–5341.

Herwartz D., Pack A. and Nagel T.J. (2021) A CO_2 greenhouse efficiently warmed the early Earth and decreased seawater $^{18}O/^{16}O$ before the onset of plate tectonics. *Proceedings of the National Academy of Sciences*, **118**, e2023617118, doi:10.1073/pnas.2023617118.

Herwartz D. and Viehmann S. (2024) Does water transparency control the banding in shallow water iron formations? *South African Journal of Geology*, **127**, 379–390, doi:10.25131/sajg.127.0014.

Hinrichs K.-U. (2002) Microbial fixation of methane carbon at 2.7 Ga: Was an anaerobic mechanism possible? *Geochemistry, Geophysics, Geosystems*, **3**, 1–10, doi:10.1029/2001GC000286.

Hoffmann J.E. (2017) Oxygenation by a changing crust. *Nature Geoscience*, **10**, 713–714, doi:10.1038/ngeo3038.

Hofmann A., Bekker A., Rouxel O., Rumble D. and Master S. (2009) Multiple sulphur and iron isotope composition of detrital pyrite in Archaean sedimentary rocks: A new tool for provenance analysis. *Earth and Planetary Science Letters*, **286**, 436–445, doi:10.1016/j.epsl.2009.07.008.

Hofmann H.J., Grey K., Hickman A.H. and Thorpe R.I. (1999) Origin of 3.45 Ga coniform stromatolites in Warrawoona Group, Western Australia. *Geological Society of America Bulletin*, **111**, 1256–1262.

Holm G. (1989) The $^{13}C/^{12}C$ ratios of siderite and organic matter of a modern metalliferous hydrothermal sediment and their implications for banded iron formations. *Chemical Geology*, **77**, 41–45.

Holland H.D. (2006) The oxygenation of the atmosphere and oceans. *Philosophical Transactions of the Royal Society B: Biological Sciences*, **361**, 903–915, doi:10.1098/rstb.2006.1838.

Holland H.D. (2002) Volcanic gases, black smokers, and the great oxidation event. *Geochimica et Cosmochimica Acta*, **66**, 3811–3826, doi:10.1016/S0016-7037(02)00950-X.

Holloway J.R. and Blank J.G. (1994) Application of experimental results to C-O-H species in natural melts. Pp. 187–230 in: *Volatiles in Magmas* (M.R. Carroll and J.R. Holloway, editors). De Gruyter, doi:10.1515/9781501509674-012.

Holloway J.R., Pan V. and Gudmundsson G. (1992) High-pressure fluid-absent melting experiments in the presence of graphite: oxygen fugacity, ferric/ferrous ratio and dissolved CO_2. *European Journal of Mineralogy*, **4**, 105–114.

Homann M. (2019) Earliest life on Earth: Evidence from the Barberton Greenstone Belt, South Africa. *Earth-Science Reviews*, **196**, 102888, doi:10.1016/j.earscire2019.102888.

Homann M., Heubeck C., Airo A. and Tice M.M. (2015) Morphological adaptations of 3.22 Ga-old tufted microbial mats to Archean coastal habitats (Moodies Group, Barberton Greenstone Belt, South Africa). *Precambrian Research*, **266**, 47–64, doi:10.1016/j.precamres.2015.04.018.

Hopkins M., Harrison T.M. and Manning C.E. (2008) Low heat flow inferred from >4 Gyr zircons suggests Hadean plate boundary interactions. *Nature*, **456**, 493–496, doi:10.1038/nature07465.

Horan M.F., Carlson R.W., Walker R.J., Jackson M., Garçon M. and Norman M. (2018) Tracking Hadean processes in modern basalts with 142-Neodymium. *Earth and Planetary Science Letters*, **484**, 184–191, doi:10.1016/j.epsl.2017.12.017.

Hu G., Rumble D., and Wang P. (2003) An ultraviolet laser microprobe for the in situ analysis of multisulfur isotopes and its use in measuring Archean sulfur isotope mass-independent anomalies. *Geochimica et Cosmochimica Acta*, **67**, 3101–3118, doi:10.1016/S0016-7037(02)00929-8.

Huston D.L. and Logan G.A. (2004) Barite, BIFs and bugs: evidence for the evolution of the Earth's early hydrosphere. *Earth and Planetary Science Letters*, **220**, 41–55, doi:10.1016/S0012-821X(04)00034-2.

Ingalls M., Grotzinger J.P., Presen, T., Rasmussen B. and Fischer W.W. (2022) Carbonate-associated phosphate (CAP) indicates elevated phosphate availability in Neoarchean shallow marine environments. *Geophysical Research Letters*, **49**, e2022GL098100, doi:10.1029/2022GL098100.

Isson T. and Rauzi S. (2024) Oxygen isotope ensemble reveals Earth's seawater, temperature, and carbon cycle history. *Science*, **383**, 666–670, doi:10.1126/science.adg1366.

Jabłońska J. and Tawfik D.S. (2022) Innovation and tinkering in the evolution of oxidases. *Protein Science*, **31**, e4310, doi:10.1002/pro.4310.

Jabłońska J. and Tawfik D.S. (2021) The evolution of oxygen-utilizing enzymes suggests early biosphere oxygenation. *Nature Ecology & Evolution*, **5**, 442–448, doi:10.1038/s41559-020-01386-9.

Jamieson J.W., Wing B.A., Hannington M.D. and Farquhar J. (2006) Evaluating isotopic equilibrium among sulfide mineral pairs in Archean ore deposits: case study from the Kidd Creek VMS deposit, Ontario, Canada. *Economic Geology*, **101**, 1055–1061.

Javoy M. (1995) The integral enstatite chondrite model of the Earth. *Geophysical Research Letters*, **22**, 2219–2222, doi:10.1029/95GL02015.

Johnson J.E., Gerpheide A., Lamb M.P. and Fischer W.W. (2014) O_2 constraints from Paleoproterozoic detrital pyrite and uraninite. *GSA Bulletin*, **126**, 813–830.

Johnson J.E., Webb S.M., Thomas K., Ono S., Kirschvink J.L. and Fischer W.W. (2013) Manganese-oxidizing photosynthesis before the rise of cyanobacteria. *Proceedings of the National Academy of Sciences*, **110**, 11238–11243, doi:10.1073/pnas.1305530110.

Johnston D.T., Farquhar J., Summons R.E., Shen Y., Kaufman A.J., Masterson A. L., and Canfield D.E. (2008) Sulfur isotope biogeochemistry of the Proterozoic McArthur Basin. *Geochimica et Cosmochimica Acta*, **72**, 4278–4290, doi:10.1016/j.gca.2008.06.004.

Johnston D.T., Poulton S.W., Fralick P.W., Wing B.A., Canfield D.E. and Farquhar J. (2006) Evolution of the oceanic sulfur cycle at the end of the Paleoproterozoic. *Geochimica et Cosmochimica Acta*, **70**, 5723–5739, doi:10.1016/j.gca.2006.08.001.

Jones C., Crowe S.A., Sturm A., Leslie K.L., MacLean L.C.W., Katsev S., Henny C., Fowle D.A. and Canfield D.E. (2011) Biogeochemistry of manganese in ferruginous Lake Matano, Indonesia. *Biogeosciences*, **8**, 2977–2991, doi:10.5194/bg-8-2977-2011.

Jones C., Nomosatryo S., Crowe S.A., Bjerrum C.J. and Canfield D.E. (2015) Iron oxides, divalent cations, silica, and the early earth phosphorus crisis. *Geology*, **43**, 135–138, doi:10.1130/G36044.1.

Jørgensen B.B. and Gallardo A., 1999, *Thioploca* sp: filamentous sulfur bacteria with nitrate vacuoles. *FEMS Microbiology Ecology*, **28**, 301–313, doi:10.1111/j.1574-6941.1999.tb00585.x.

Kalvelage T. *et al.* (2015) Aerobic microbial respiration in oceanic oxygen minimum zones. *PLoS ONE*, **10**, e0133526, doi:10.1371/journal.pone.0133526.

Kalvelage T., Jensen M.M., Contreras S., Revsbech N.P., Lam P., Günter M., LaRoche J., Lavik G. and Kuypers M.M.M. (2011) Oxygen sensitivity of anammox and coupled N-cycle processes in oxygen minimum zones. *PLoS ONE*, **6**, e29299, doi:10.1371/journal.pone.0029299.

Kamber B.S. and Whitehouse M.J. (2007) Micro-scale sulphur isotope evidence for sulphur cycling in the late Archean shallow ocean. *Geobiology*, **5**, 5–17.

Kappler A., Bryce C., Mansor M., Lueder U., Byrne J.M. and Swanner E.D. (2021) An evolving view on biogeochemical cycling of iron. *Nature Reviews Microbiology*, **19**, 360–374, doi:10.1038/s41579-020-00502-7.

Kappler A. and Newman D.K. (2004) Formation of Fe(III)-minerals by Fe(II)-oxidizing photoautotrophic bacteria. *Geochimica et Cosmochimica Acta*, **68**, 1217–1226, doi:10.1016/j.gca.2003.09.006.

Kappler A., Pasquero C., Konhauser K.O. and Newman D.K. (2005) Deposition of banded iron formations by anoxygenic phototrophic Fe(II)-oxidizing bacteria. *Geology*, **33**, 865–868, doi:10.1130/G21658.1.

Kasting J.F. (1993) Earth's early atmosphere. *Science*, **259**, 920–926.

Kasting J.F. (1987) Theoretical constraints on oxygen and carbon dioxide concentrations in the Precambrian atmosphere. *Precambrian Research*, **34**, 205–229, doi:10.1016/0301-9268(87)90001-5.

https://doi.org/10.1180/gbi.2025.10003 Published online by Cambridge University Press

Kasting J.F. and Canfield D.E. (2012) The global oxygen cycle. Pp. 93–104 in *Fundamentals of Geobiology* (A. Knoll, D. Canfield and K.O. Konhauser, editors). Wiley-Blackwell, West-Sussex.

Kasting J.F., Eggler D.H. and Raeburn S.P. (1993) Mantle redox evolution and the oxidation state of the Archean atmosphere. *The Journal of Geology*, **101**, 245–257, doi:10.1086/648219.

Kasting J.F., Howard M.T., Wallmann K., Veizer J., Shields G. and Jaffrés J. (2006) Paleoclimates, ocean depth, and the oxygen isotopic composition of seawater. *Earth and Planetary Science Letters*, **252**, 82–93, doi:10.1016/j.epsl.2006.09.029.

Kasting J.F. and Siefert J.L. (2002) Life and the evolution of Earth's atmosphere. *Science*, **296**, 1066–1068, doi:10.1126/science.1071184.

Kaufman A.J., Johnston D.T., Farquhar J., Masterson A.L., Lyons T.W., Bates S., Anbar A.D., Arnold G.L., Garvin J. and Buick R. (2007) Late Archean biospheric oxygenation and atmospheric evolution. *Science*, **317**, 1900–1903, doi:10.1126/science.1138700.

Kemp A.I.S. and Hawkesworth C.J. (2014) Growth and differentiation of the continental crust from isotope studies of accessory minerals. Pp. 379–421 in *Treatise on Geochemistry*, 2nd edition. Elsevier, doi:10.1016/B978-0-08-095975-7.00312-0.

Kendall B. (2021) Recent advances in geochemical paleo-oxybarometers. *Annual Review of Earth and Planetary Sciences*, **49**, annurev-earth-071520-051637, doi:10.1146/annurev-earth-071520-051637.

Kendall B., Creaser R.A., Reinhard C.T., Lyons T.W. and Anbar A.D. (2015) Transient episodes of mild environmental oxygenation and oxidative continental weathering during the late Archean. *Science Advances*, **1**, e1500777, doi:10.1126/sciad1500777.

Kharecha P., Kasting J. and Siefert J. (2005) A coupled atmosphere-ecosystem model of the early Archean Earth. *Geobiology*, **3**, 53–76, doi:10.1111/j.1472-4669.2005.00049.x.

Kim K.M., Qin T., Jiang Y.-Y., Chen L.-L., Xiong M., Caetano-Anollés D., Zhang H.-Y. and Caetano-Anollés G. (2012) Protein domain structure uncovers the origin of aerobic metabolism and the rise of planetary oxygen. *Structure*, **20**, 67–76, doi:10.1016/j.str.2011.11.003.

Kipp M.A. and Stüeken E.E. (2017) Biomass recycling and Earth's early phosphorus cycle. *Science Advances*, **3**, eaao4795, doi:10.1126/sciadaao4795.

Kirschvink J.L., Gaidos E.J., Bertani L.E., Beukes N.J., Gutzmer J., Maepa L.N. and Steinberger R.E. (2000) Paleoproterozoic snowball Earth: Extreme climatic and geochemical global change and its biological consequences. *Proceedings of the National Academy of Sciences*, **97**, 1400–1405, doi:10.1073/pnas.97.4.1400.

Klatt J.M., Chennu A., Arbic B.K., Biddanda B.A. and Dick G.J. (2021) Possible link between Earth's rotation rate and oxygenation. *Nature Geoscience*, **14**, 564–570, doi:10.1038/s41561-021-00784-3.

Klein C. and Beukes N.J. (1992) Proterozoic iron formations. *Developments in Precambrian Geology*, **10**, 383–418.

Knittel K. and Boetius A. (2009) Anaerobic oxidation of methane: progress with an unknown process. *Annual Review of Microbiology*, **63**, 311–334, doi:10.1146/annuremicro.61.080706.093130.

Knoll A.H., Bergmann K.D. and Strauss J.V. (2016) Life: the first two billion years. *Philosophical Transactions of the Royal Society B: Biological Sciences*, **371**, 20150493, doi:10.1098/rstb.2015.0493.

Koehler M.C., Buick R., Kipp M.A., Stüeken E.E. and Zaloumis J. (2018) Transient surface ocean oxygenation recorded in the ∼2.66-Ga Jeerinah Formation, Australia. *Proceedings of the National Academy of Sciences*, **115**, 7711–7716, doi:10.1073/pnas.1720820115.

Konhauser K.O. *et al.* (2011) Aerobic bacterial pyrite oxidation and acid rock drainage during the Great Oxidation Event. *Nature*, **478**, 369–373, doi:10.1038/nature10511.

Konhauser K. (2007) *Introduction to Geomicrobiology*. Blackwell Pub, Malden, 425 pp.

Konhauser K.O. *et al.* (2017) Iron formations: A global record of Neoarchaean to Palaeoproterozoic environmental history. *Earth-Science Reviews*, **172**, 140–177, doi:10.1016/j.earscire2017.06.012.

Konhauser K.O. *et al.* (2018) Phytoplankton contributions to the trace-element composition of Precambrian banded iron formations. *GSA Bulletin*, **130**, 941–951, doi:10.1130/B31648.1.

Konhauser K.O., Amskold L., Lalonde S.V., Posth N.R., Kappler A. and Anbar A. (2007a) Decoupling photochemical Fe(II) oxidation from shallow-water BIF deposition. *Earth and Planetary Science Letters*, **258**, 87–100, doi:10.1016/j.epsl.2007.03.026.

Konhauser K.O., Hamade T., Raiswell R., Morris R.C., Ferris F.G., Southam G. and Canfield D.E. (2002) Could bacteria have formed the Precambrian banded iron formations? *Geology*, **30** (12), 1079–1082.

Konhauser K.O., Lalonde S.V., Amskold L. and Holland H.D. (2007b) Was there really an Archean phosphate crisis? *Science*, **315**, 1234–1234, doi:10.1126/science.1136328.

Konhauser K.O., Pecoits E., Lalonde S.V., Papineau D., Nisbet E.G., Barley M.E., Arndt N.T., Zahnle K. and Kamber B.S. (2009) Oceanic nickel depletion and a methanogen famine before the Great Oxidation Event. *Nature*, **458**, 750–753, doi:10.1038/nature07858.

Kopp R.E., Kirschvink J.L., Hilburn I.A. and Nash C.Z. (2005) The Paleoproterozoic snowball Earth: A climate disaster triggered by the evolution of oxygenic photosynthesis. *Proceedings of the National Academy of Sciences*, **102**, 11131–11136, doi:10.1073/pnas.0504878102.

Korenaga J. (2018) Estimating the formation age distribution of continental crust by unmixing zircon ages. *Earth and Planetary Science Letters*, **482**, 388–395, doi:10.1016/j.epsl.2017.11.039.

Kuang J., Morra G., Yuen D.A., Kusky T., Jiang S., Yao H. and Qi S. (2023) Metamorphic constraints on Archean tectonics. *Precambrian Research*, **397**, 107195, doi:10.1016/j.precamres.2023.107195.

Kump L.R., and Barley M.E. (2007) Increased subaerial volcanism and the rise of atmospheric oxygen 2.5 billion years ago. *Nature*, **448**, 1033–1036, doi:10.1038/nature06058.

Kump L.R., Kasting J.F. and Barley M.E. (2001) Rise of atmospheric oxygen and the upside-down Archean mantle. *Geochemistry, Geophysics, Geosystems*, **2**, 2000GC000114.

Kurzweil F., Wille M., Gantert N., Beukes N.J. and Schoenberg R. (2016) Manganese oxide shuttling in pre-GOE oceans – evidence from molybdenum and iron isotopes. *Earth and Planetary Science Letters*, **452**, 69–78, doi:10.1016/j.epsl.2016.07.013.

Laakso T.A. and Schrag D.P. (2014) Regulation of atmospheric oxygen during the Proterozoic. *Earth and Planetary Science Letters*, **388**, 81–91, doi:10.1016/j.epsl.2013.11.049.

Lalonde S.V. and Konhauser K.O. (2015) Benthic perspective on Earth's oldest evidence for oxygenic photosynthesis. *Proceedings of the National Academy of Sciences*, **112**, 995–1000, doi:10.1073/pnas.1415718112.

Lam P., Lavik G., Jensen M.M., Van De Vossenberg J., Schmid M., Woebken D., Gutiérrez D., Amann R., Jetten M.S.M. and Kuypers M.M.M. (2009) Revising the nitrogen cycle in the Peruvian oxygen minimum zone. *Proceedings of the National Academy of Sciences*, **106**, 4752–4757, doi:10.1073/pnas.0812444106.

Lammer H. *et al.* (2018) Origin and evolution of the atmospheres of early Venus, Earth and Mars. *The Astronomy and Astrophysics Review*, **26**, 2, doi:10.1007/s00159-018-0108-y.

Latysheva N., Junker L., Palmer W.J., Codd G.A. and Barker D. (2012) The evolution of nitrogen fixation in cyanobacteria. *Bioinformatics*, **28**, 603–606, doi:10.1093/bioinformatics/bts008.

Learman D.R., Voelker B.M., Vazquez-Rodriguez A.I. and Hansel C.M. (2011) Formation of manganese oxides by bacterially generated superoxide. *Nature Geoscience*, **4**, 95–98, doi:10.1038/ngeo1055.

Lee C.-T.A., Brandon A.D. and Norman M. (2003) Vanadium in peridotites as a proxy for paleo-fO_2 during partial melting: Prospects, limitations, and implications. *Geochimica et Cosmochimica Acta*, **67**, 3045–3064.

Lee C.-T.A., Yeung L.Y., McKenzie N.R., Yokoyama Y., Ozaki K. and Lenardic A. (2016) Two-step rise of atmospheric oxygen linked to the growth of continents. *Nature Geoscience*, **9**, 417–424, doi:10.1038/ngeo2707.

Lee S.H., Youn H., Kang S.G. and Lee H.S. (2019) Oxygen-mediated growth enhancement of an obligate anaerobic archaeon *Thermococcus onnurineus* NA1. *Journal of Microbiology*, **57**, 138–142, doi:10.1007/s12275-019-8592-y.

Lepot K. (2020) Signatures of early microbial life from the Archean (4 to 2.5 Ga) eon. *Earth-Science Reviews*, **209**, 103296, doi:10.1016/j.earscire2020.103296.

Lepot K., Williford K.H., Philippo, P., Thomazo C., Ushikubo T., Kitajima K., Mostefaoui S. and Valley J.W. (2019) Extreme ^{13}C-depletions and organic sulfur content argue for S-fueled anaerobic methane oxidation in 2.72 Ga old

stromatolites. *Geochimica et Cosmochimica Acta*, **244**, 522–547, doi:10.1016/j.gca.2018.10.014.

Li Y.-L., Konhauser K.O. and Zhai M. (2017) The formation of magnetite in the early Archean oceans. *Earth and Planetary Science Letters*, **466**, 103–114, doi:10.1016/j.epsl.2017.03.013.

Li Z.-X.A. and Lee C.-T.A. (2004) The constancy of upper mantle fO_2 through time inferred from V/Sc ratios in basalts. *Earth and Planetary Science Letters*, **228**, 483–493, doi:10.1016/j.epsl.2004.10.006.

Little C.T.S. *et al.* (2021) A late Paleoproterozoic (1.74 Ga) deep-sea, low-temperature, iron-oxidizing microbial hydrothermal vent community from Arizona, USA. *Geobiology*, **19**, 228–249, doi:10.1111/gbi.12434.

Liu W., Hao J., Elzinga E.J., Piotrowiak P., Nanda V., Yee N. and Falkowski P.G. (2020) Anoxic photogeochemical oxidation of manganese carbonate yields manganese oxide. *Proceedings of the National Academy of Sciences*, **117**, 22698–22704, doi:10.1073/pnas.2002175117.

Loucks R.R., Fiorentini M.L. and Henríquez G.J. (2020) New magmatic oxybarometer using trace elements in zircon. *Journal of Petrology*, **61**, egaa034, doi:10.1093/petrology/egaa034.

Lowe D.R., Drabon N. and Byerly G.R. (2019) Crustal fracturing, unconformities, and barite deposition, 3.26–3.23 Ga, Barberton Greenstone Belt, South Africa. *Precambrian Research*, **327**, 34–46, doi:10.1016/j.precamres.2019.02.024.

Luo G., Ono S., Beukes N.J., Wang D.T., Xie S. and Summons R.E. (2016) Rapid oxygenation of Earth's atmosphere 2.33 billion years ago. *Science Advances*, **2**, e1600134, doi:10.1126/sciad1600134.

Luther G.W., Findlay A.J., MacDonald D.J., Owings S.M., Hanson T.E., Beinart R.A. and Girguis P.R. (2011) Thermodynamics and kinetics of sulfide oxidation by oxygen: A look at inorganically controlled reactions and biologically mediated processes in the environment. *Frontiers in Microbiology*, **2**, doi:10.3389/fmicb.2011.00062.

Luther G.W., Sundby B., Lewis B.L., Brendel P.J. and Silverberg N. (1997) Interactions of manganese with the nitrogen cycle. Alternative pathways to dinitrogen. *Geochimica et Cosmochimica Acta*, **61**, 4043–4052, doi:10.1016/S0016-7037(97)00239-1.

Lyons T.W., Diamond C.W., Planavsky N.J., Reinhard C.T. and Li C. (2021) Oxygenation, life, and the planetary system during Earth's middle history: An overview. *Astrobiology*, **21**, 906–923, doi:10.1089/ast.2020.2418.

Lyons T.W., Reinhard C.T. and Planavsky N.J. (2014) The rise of oxygen in Earth's early ocean and atmosphere. *Nature*, **506**, 307–315, doi:10.1038/nature13068.

Lyons T.W., Tino C.J., Fournier G.P., Anderson R.E., Leavitt W.D., Konhauser K.O. and Stüeken E.E. (2024) Co-evolution of early Earth environments and microbial life. *Nature Reviews Microbiology*, doi:10.1038/s41579-024-01044-y.

Maisch M., Lueder U., Laufer K., Scholze C., Kappler A. and Schmidt C. (2019) Contribution of microaerophilic iron(II)-oxidizers to iron(III) mineral formation. *Environmental Science & Technology*, **53**, 8197–8204, doi:10.1021/acs.est.9b01531.

Mänd K., Robbins L.J., Planavsky N.J., Bekke, A. and Konhauser K.O. (2021) *iron formations as palaeoenvironmental archives in:* Elements in Geochemical Tracers in Earth System Science. Cambridge University Press.

Mandernack K.W., Mills C.T., Johnson C.A., Rahn T. and Kinney C. (2009) The $\delta^{15}N$ and $\delta^{18}O$ values of N_2O produced during the co-oxidation of ammonia by methanotrophic bacteria. *Chemical Geology*, **267**, 96–107, doi:10.1016/j.chemgeo.2009.06.008.

Mao H.K. and Bell P.M. (1977) Disproportionation equilibrium in iron-bearing systems at pressures above 100 kbar with applications to chemistry of the Earth's mantle. Pp. 236–249 in: *Energetics of Geological Processes: Hans Ramberg on his 60th birthday* (S.K. Saxena, S. Bhattacharji, H. Annersten and O. Stephansson, editors). Springer, Berlin Heidelberg, doi:10.1007/978-3-642-86574-9_12.

Mariotti A., Germon J.C., Hubert P., Kaiser P., Letolle R., Tardieux A. and Tardieux P. (1981) Experimental determination of nitrogen kinetic isotope fractionation: Some principles; illustration for the denitrification and nitrification processes. *Plant and Soil*, **62**, 413–430, doi:10.1007/BF02374138.

Martin A.N., Stüeken E.E., Michaud J.A.-S., Münker C., Weyer S., Van Hees E.H.P. and Gehringer M.M. (2024) Mechanisms of nitrogen isotope fractionation at an ancient black smoker in the 2.7 Ga Abitibi greenstone belt, Canada. *Geology*, **52**, 181–186, doi:10.1130/G51689.1.

Marty B. (2012) The origins and concentrations of water, carbon, nitrogen and noble gases on Earth. *Earth and Planetary Science Letters*, **313–314**, 56–66, doi:10.1016/j.epsl.2011.10.040.

McAllister S.M., Moore R.M., Gartman A., Luther G.W., Emerson D. and Chan C.S. (2019) The Fe(II)-oxidizing *Zetaproteobacteria* : historical, ecological and genomic perspectives. *FEMS Microbiology Ecology*, **95**, doi:10.1093/femsec/fiz015.

McCammon C. (2005) The paradox of mantle redox. *Science*, **308**, 807–808, doi:10.1126/science.1110532.

Meadows S. *et al.* (2018) Exoplanet biosignatures: Understanding oxygen as a biosignature in the context of its environment. *Astrobiology*, **18**, 630–662, doi:10.1089/ast.2017.1727.

Mhlanga X.R., Tsikos H., Lee B., Rouxel O.J., Boyce A.C., Harris C. and Lyons T.W. (2023) The Palaeoproterozoic Hotazel BIF-Mn formation as an archive of Earth's earliest oxygenation. *Earth-Science Reviews*, **240**, 104389, doi:10.1016/j.earscire2023.104389.

Mikhail S. and Sverjensky D.A. (2014) Nitrogen speciation in upper mantle fluids and the origin of Earth's nitrogen-rich atmosphere. *Nature Geoscience*, **7**, 816–819, doi:10.1038/ngeo2271.

Mills D.B., Boyle R.A., Daines S.J., Sperling E.A., Pisani D., Donoghue P.C.J. and Lenton T.M. (2022) Eukaryogenesis and oxygen in Earth history. *Nature Ecology & Evolution*, **6**, 520–532, doi:10.1038/s41559-022-01733-y.

Milucka J., Kirf M., Lu L., Krupke A., Lam P., Littmann S., Kuypers M.M. and Schubert C.J. (2015) Methane oxidation coupled to oxygenic photosynthesis in anoxic waters. *The ISME Journal*, **9**, 1991–2002, doi:10.1038/ismej.2015.12.

Mloszewska A.M., Cole D.B., Planavsky N.J., Kappler A., Whitford D.S., Owttrim G.W. and Konhauser K.O. (2018) UV radiation limited the expansion of cyanobacteria in early marine photic environments. *Nature Communications*, **9**, 3088, doi:10.1038/s41467-018-05520-x.

Mojzsis S.J., Arrhenius G., McKeegan K.D., Harrison T.M., Nutman A.P, and Friend C.R.L. (1996) Evidence for life on Earth before 3,800 million years ago. *Nature*, **384**, 55–59, doi:10.1038/384055a0.

Mojzsis S.J., Coath C.D., Greenwood J.P., McKeegan K.D. and Harrison T.M. (2003) Mass-independent isotope effects in Archean (2.5 to 3.8 Ga) sedimentary sulfides determined by ion microprobe analysis. *Geochimica et Cosmochimica Acta*, **67**, 1635–1658, doi:10.1016/S0016-7037(03)00059-0.

Muhling J.R. and Rasmussen B. (2020) Widespread deposition of greenalite to form Banded Iron Formations before the Great Oxidation Event. *Precambrian Research*, **339**, 105619, doi:10.1016/j.precamres.2020.105619.

Mukhopadhyay S. (2012) Early differentiation and volatile accretion recorded in deep-mantle neon and xenon. *Nature*, **486**, 101–104, doi:10.1038/nature11141.

Mulder A., Graaf A.A., Robertson L.A. and Kuenen J.G. (1995) Anaerobic ammonium oxidation discovered in a denitrifying fluidized bed reactor. *FEMS Microbiology Ecology*, **16**, 177–184, doi:10.1111/j.1574-6941.1995.tb00281.x.

Mundl A., Touboul M., Jackson M.G., Day J.M.D., Kurz M.D., Lekic V., Helz R.T. and Walker R.J. (2017) Tungsten-182 heterogeneity in modern ocean island basalts. *Science*, **356**, 66–69, doi:10.1126/science.aal4179.

Mundl-Petermeier A., Viehmann S., Tusch J., Bau M., Kurzweil F. and Münker C. (2022) Earth's geodynamic evolution constrained by ^{182}W in Archean seawater. *Nature Communications*, **13**, 2701, doi:10.1038/s41467-022-30423-3.

Nabhan S., Marin-Carbonne J., Mason P.R.D. and Heubeck C. (2020) In situ S-isotope compositions of sulfate and sulfide from the 3.2 Ga Moodies Group, South Africa: A record of oxidative sulfur cycling. *Geobiology*, **18**, 426–444, doi:10.1111/gbi.12393.

Navarro-González R., Molina M.J. and Molina L.T. (1998) Nitrogen fixation by volcanic lightning in the early Earth. *Geophysical Research Letters*, **25**, 3123–3126.

Nealson K.H., Tebo B.M. and Rosson R.A. (1988) Occurrence and mechanisms of microbial oxidation of manganese. Pp. 279–318 in: *Advances in Applied Microbiology*, Vol. **33**, Elsevier, doi:10.1016/S0065-2164(08)70209-0.

Nicklas R.W., Puchtel I.S. and Ash R.D. (2016) High-precision determination of the oxidation state of komatiite lavas using vanadium liquid-mineral partitioning. *Chemical Geology*, **433**, 36–45, doi:10.1016/j.chemgeo.2016.04.011.

Nicklas R.W., Puchtel I.S. and Ash R.D. (2018) Redox state of the Archean mantle: Evidence from V partitioning in 3.5–2.4 Ga komatiites. *Geochimica et Cosmochimica Acta*, **222**, 447–466, doi:10.1016/j.gca.2017.11.002.

Nicklas R.W., Puchtel I.S., Ash R.D., Piccoli P.M., Hanski E., Nisbet E.G., Waterton P., Pearson D.G. and Anbar A.D. (2019) Secular mantle oxidation

across the Archean-Proterozoic boundary: Evidence from V partitioning in komatiites and picrites. *Geochimica et Cosmochimica Acta*, **250**, 49–75, doi:10.1016/j.gca.2019.01.037.

Nims C., Lafond J., Alleon J., Templeton A.S. and Cosmidis J. (2021) Organic biomorphs may be better preserved than microorganisms in early Earth sediments. *Geology*, **49**, 629–634, doi:10.1130/G48152.1.

Ohmoto H., Watanabe Y., Ikemi, H., Poulson S.R. and Taylor B.E. (2006a) Sulphur isotope evidence for an oxic Archaean atmosphere. *Nature*, **442**, 908–911.

Ohmoto H., Watanabe Y., Yamaguchi K.E., Naraoka H., Haruna M., Kakegawa T., Hayashi K. and Kato Y. (2006b) Chemical and biological evolution of early Earth: Constraints from banded iron formations in: *Evolution of Early Earth's Atmosphere, Hydrosphere, and Biosphere – Constraints from Ore Deposits*. Geological Society of America, doi:10.1130/2006.1198(17).

Olson H.C., Drabon N. and Johnston D.T. (2022) Oxygen isotope insights into the Archean ocean and atmosphere. *Earth and Planetary Science Letters*, **591**, 117603, doi:10.1016/j.epsl.2022.117603.

O'Neill H.St.C. (1991) The origin of the moon and the early history of the earth —A chemical model. Part 2: The earth. *Geochimica et Cosmochimica Acta*, **55**, 1159–1172, doi:10.1016/0016-7037(91)90169-6.

O'Neill C. and Aulbach S. (2022) Destabilization of deep oxidized mantle drove the Great Oxidation Event. *Science Advances*, **8**, eabg1626, doi:10.1126/sciadabg1626.

O'Neill H.St.C. and Wall J. (1987) The olivine–orthopyroxene–spinel oxygen geobarometer, the nickel precipitation curve, and the oxygen fugacity of the Earth's upper mantle. *Journal of Petrology*, **28**, 1169–1191, doi:10.1093/petrology/28.6.1169.

Ono S. (2017) Photochemistry of sulfur dioxide and the origin of mass-independent isotope fractionation in earth's atmosphere. *Annual Review of Earth and Planetary Sciences*, **45**, 301–329, doi:10.1146/annurev-earth-060115-012324.

Ono S., Beukes N.J. and Rumble D. (2009) Origin of two distinct multiple-sulfur isotope compositions of pyrite in the 2.5Ga Klein Naute Formation, Griqualand West Basin, South Africa. *Precambrian Research*, **169**, 48–57, doi:10.1016/j.precamres.2008.10.012.

Ono S., Beukes N.J., Rumble D. and Fogel M.L. (2006) Early evolution of atmospheric oxygen from multiple-sulfur and carbon isotope records of the 2.9 Ga Mozaan Group of the Pongola Supergroup, Southern Africa. *South African Journal of Geology*, **109**, 97–108.

Ono S., Eigenbrode J.L., Pavlov A.A., Kharecha P., Rumble D., Kasting J.F. and Freeman K.H., (2003) New insights into Archean sulfur cycle from mass-independent sulfur isotope records from the Hamersley Basin, Australia. *Earth and Planetary Science Letters*, **213**, 15–30, doi:10.1016/S0012-821X(03)00295-4.

Ortenzi G. *et al.* (2020) Mantle redox state drives outgassing chemistry and atmospheric composition of rocky planets. *Scientific Reports*, **10**, 10907, doi:10.1038/s41598-020-67751-7.

Ossa Ossa F. *et al.* (2022) Moderate levels of oxygenation during the late stage of Earth's Great Oxidation Event. *Earth and Planetary Science Letters*, **594**, 117716, doi:10.1016/j.epsl.2022.117716.

Ossa Ossa F., Hofmann A., Spangenberg J.E., Poulton S.W., Stüeken E.E., Schoenberg R., Eickmann B., Wille M., Butler M., and Bekker A. (2019) Limited oxygen production in the Mesoarchean ocean. *Proceedings of the National Academy of Sciences*, **116**, 6647–6652, doi:10.1073/pnas.1818762116.

Ossa Ossa F., Hofmann A., Vidal O., Kramers J.D., Belyanin G. and Cavalazzi B. (2016) Unusual manganese enrichment in the Mesoarchean Mozaan Group, Pongola Supergroup, South Africa. *Precambrian Research*, **281**, 414–433, doi:10.1016/j.precamres.2016.06.009.

Ossa Ossa F., Hofmann A., Wille M., Spangenberg J.E., Bekker A., Poulton S.W., Eickmann B. and Schoenberg R. (2018) Aerobic iron and manganese cycling in a redox-stratified Mesoarchean epicontinental sea. *Earth and Planetary Science Letters*, **500**, 28–40, doi:10.1016/j.epsl.2018.07.044.

Ostrander C.M., Johnson A.C. and Anbar A.D. (2021) Earth's First Redox Revolution. *Annual Review of Earth and Planetary Sciences*, **49**, 337–366, doi:10.1146/annurev-earth-072020-055249.

Ostrander C.M., Nielsen S.G., Owens J.D., Kendall B., Gordon G.W., Romaniello S.J. and Anbar A.D. (2019) Fully oxygenated water columns over continental shelves before the Great Oxidation Event. *Nature Geoscience*, **12**, 186–191, doi:10.1038/s41561-019-0309-7.

Oswald K., Milucka J., Brand A., Littmann S., Wehrli B., Kuypers M.M.M. and Schubert C.J. (2015) Light-dependent aerobic methane oxidation reduces methane emissions from seasonally stratified lakes. *PLoS ONE*, **10**, e0132574, doi:10.1371/journal.pone.0132574.

Ozaki K., Thompson K.J., Simister R.L., Crowe S.A. and Reinhard C.T. (2019) Anoxygenic photosynthesis and the delayed oxygenation of Earth's atmosphere. *Nature Communications*, **10**, 3026, doi:10.1038/s41467-019-10872-z.

Pahlevan K., Schaefer L. and Hirschmann M.M. (2019) Hydrogen isotopic evidence for early oxidation of silicate Earth. *Earth and Planetary Science Letters*, **526**, 115770, doi:10.1016/j.epsl.2019.115770.

Papineau D., Mojzsis S.J., Coath C.D., Karhu J.A. and McKeegan K.D. (2005) Multiple sulfur isotopes of sulfides from sediments in the aftermath of Paleoproterozoic glaciations. *Geochimica et Cosmochimica Acta*, **69**, 5033–5060, doi:10.1016/j.gca.2005.07.005.

Papineau D., Mojzsis S.J. and Schmitt A.K. (2007) Multiple sulfur isotopes from Paleoproterozoic Huronian interglacial sediments and the rise of atmospheric oxygen. *Earth and Planetary Science Letters*, **255**, 188–212, doi:10.1016/j.epsl.2006.12.015.

Papineau D., She Z., Dodd M.S., Iacoviello F., Slack J.F., Hauri E., Shearing P. and Little C.T.S. (2022) Metabolically diverse primordial microbial communities in Earth's oldest seafloor-hydrothermal jasper: *Science Advances*, **8**, eabm2296, doi:10.1126/sciadabm2296.

Parsons C., Stüeken E.E., Rosen C.J., Mateos K. and Anderson R.E. (2021) Radiation of nitrogen-metabolizing enzymes across the tree of life tracks environmental transitions in Earth history. *Geobiology*, **19**, 18–34, doi:10.1111/gbi.12419.

Partridge M.A., Golding S.D., Baublys K.A. and Young E. (2008) Pyrite paragenesis and multiple sulfur isotope distribution in late Archean and early Paleoproterozoic Hamersley Basin sediments. *Earth and Planetary Science Letters*, **272**, 41–49, doi:10.1016/j.epsl.2008.03.051.

Pavlov A.A., Brown L.L. and Kasting J.F. (2001) UV shielding of NH_3 and O_2 by organic hazes in the Archean atmosphere. *Journal of Geophysical Research: Planets*, **106**, 23267–23287, doi:10.1029/2000JE001448.

Pavlov A.A. and Kasting J.F. (2002) Mass-independent fractionation of sulfur isotopes in Archean sediments: Strong evidence for an anoxic Archean atmosphere. *Astrobiology*, **2**, 27–41, doi:10.1089/153110702753621321.

Peck W.H., Valley J.W., Wilde S.A. and Graham C.M. (2001) Oxygen isotope ratios and rare earth elements in 3.3 to 4.4 Ga zircons: Ion microprobe evidence for high $\delta^{18}O$ continental crust and oceans in the Early Archean. *Geochimica et Cosmochimica Acta*, **65**, 4215–4229.

Pecoits E., Smith M.L., Catling D.C., Philippot P., Kappler A. and Konhauser K.O. (2015) Atmospheric hydrogen peroxide and Eoarchean iron formations. *Geobiology*, **13**, 1–14, doi:10.1111/gbi.12116.

Pellerin A., Thomazo C., Ader, M., Marin-Carbonne J., Alleon J., Vennin E. and Hofmann A. (2023) Iron-mediated anaerobic ammonium-oxidation recorded in the early Archean ferruginous ocean. *Geobiology*, **21**, 277–289.

Pellerin A., Thomazo C., Ader M., Rossignol C., Rego E.S., Busigny V. and Philippot P. (2024) Neoarchaean oxygen-based nitrogen cycle en route to the Great Oxidation Event. *Nature*, **633**, 365–370, doi:10.1038/s41586-024-07842-x.

Philippot P., Van Zuilen M., Lepot K., Thomazo C., Farquhar J. and Van Kranendonk M.J., (2007) Early Archaean microorganisms preferred elemental sulfur, not sulfate. *Science*, **317**, 1534–1537, doi:10.1126/science.1145861.

Picard A., Kappler A., Schmid G., Quaroni L. and Obst M. (2015) Experimental diagenesis of organo-mineral structures formed by microaerophilic Fe(II)-oxidizing bacteria. *Nature Communications*, **6**, 6277, doi:10.1038/ncomms7277.

Pirajno F. and Yu H.-C. (2021) Cycles of hydrothermal activity, precipitation of chemical sediments, with special reference to Algoma-type BIF. *Gondwana Research*, **100**, 251–260, doi:10.1016/j.gr.2021.02.012.

Planavsky N.J. *et al.* (2014) Evidence for oxygenic photosynthesis half a billion years before the Great Oxidation Event. *Nature Geoscience*, **7**, 283–286, doi:10.1038/ngeo2122.

Postgate J.R. (1998) *Nitrogen fixation*. Cambridge University Press, London.

Poulton S.W., Bekker A., Cumming M., Zerkle A.L., Canfield D.E. and Johnston, D.T. (2021) A 200-million-year delay in permanent atmospheric oxygenation. *Nature*, **592**, 232–236, doi:10.1038/s41586-021-03393-7.

Ramdohr P. (1958) New observations of the ores of the Witwatersrand in South Africa and their genetic significance. *Geological Society of South Africa Transactions*, **61**, 1–50.

https://doi.org/10.1180/gbi.2025.10003 Published online by Cambridge University Press

Rasmussen B. and Buick R. (1999) Redox state of the Archean atmosphere: Evidence from detrital heavy minerals in ca. 3250–2750 Ma sandstones from the Pilbara Craton, Australia. *Geology*, **27**, 115, doi:10.1130/0091-7613(1999)027<0115:RSOTAA>2.3.CO;2.

Rasmussen B., Fletcher I.R., Brocks J.J. and Kilburn M.R. (2008) Reassessing the first appearance of eukaryotes and cyanobacteria. *Nature*, **455**, 1101–1104, doi:10.1038/nature07381.

Rasmussen B., Muhling J.R., Suvorova A. and Fischer W.W. (2021) Apatite nanoparticles in 3.46–2.46 Ga iron formations: Evidence for phosphorus-rich hydrothermal plumes on early Earth. *Geology*, **49**, 647–651, doi:10.1130/G48374.1.

Rasmussen B., Muhling J.R., Tosca N.J. and Fischer W.W. (2023) Did nutrient-rich oceans fuel Earth's oxygenation? *Geology*, **51**(5), 444–448, doi:10.1130/G50835.1.

Reinhard C.T. and Planavsky N.J. (2011) Mineralogical constraints on Precambrian pCO_2. *Nature*, **474**, E1, doi:10.1038/nature09959.

Reinhard C.T. and Planavsky N.J. (2022) The History of Ocean Oxygenation. *Annual Review of Marine Science*, **14**, 331–353, doi:10.1146/annurev-marine-031721-104005.

Reinhard C.T., Planavsky N.J., Gill B.C., Ozaki K., Robbins L.J., Lyons T.W., Fischer W.W., Wang C., Cole D.B. and Konhauser K.O. (2017) Evolution of the global phosphorus cycle. *Nature*, **541**, 386–389, doi:10.1038/nature20772.

Reinhard C.T., Raiswell R., Scott C., Anbar A.D. and Lyons T.W. (2009) A Late Archean sulfidic sea stimulated by early oxidative weathering of the continents. *Science*, **326**, 713–716, doi:10.1126/science.1176711.

Righter K. and Drake M.J., (1996) Core formation in Earth's Moon, Mars, and Vesta. *Icarus*, **124**, 513–529, doi:10.1006/icar.1996.0227.

Righter K., Yang H., Costin G. and Downs R.T. (2008) Oxygen fugacity in the Martian mantle controlled by carbon: New constraints from the nakhlite MIL 03346. *Meteoritics & Planetary Science*, **43**, 1709–1723, doi:10.1111/j.1945-5100.2008.tb00638.x.

Ringwood A.E. (1979) *Origin of the Earth and Moon*. Springer Science & Business Media, New York, 295 pp.

Rios-Del Toro E.E., Valenzuela E.I., López-Lozano N.E., Cortés-Martínez M.G., Sánchez-Rodríguez M.A., Calvario-Martínez O., Sánchez-Carrillo S. and Cervantes F.J. (2018) Anaerobic ammonium oxidation linked to sulfate and ferric iron reduction fuels nitrogen loss in marine sediments. *Biodegradation*, **29**, 429–442, doi:10.1007/s10532-018-9839-8.

Rizo H., Boyet M., Blichert-Toft J. and Rosing M.T. (2013) Early mantle dynamics inferred from ^{142}Nd variations in Archean rocks from southwest Greenland. *Earth and Planetary Science Letters*, **377–378**, 324–335, doi:10.1016/j.epsl.2013.07.012.

Rizo H., Walker R.J., Carlson R.W., Horan M.F., Mukhopadhyay S., Manthos V., Francis D. and Jackson M.G. (2016a) Preservation of Earth-forming events in the tungsten isotopic composition of modern flood basalts. *Science*, **352**, 809–812, doi:10.1126/science.aad8563.

Rizo H., Walker R.J., Carlson R.W., Touboul M., Horan M.F., Puchtel I.S., Boyet M. and Rosing M.T. (2016b) Early Earth differentiation investigated through ^{142}Nd, ^{182}W, and highly siderophile element abundances in samples from Isua, Greenland. *Geochimica et Cosmochimica Acta*, **175**, 319–336, doi:10.1016/j.gca.2015.12.007.

Robbins L.J. *et al.* (2023) Manganese oxides, Earth surface oxygenation, and the rise of oxygenic photosynthesis. *Earth-Science Reviews*, **239**, 104368, doi:10.1016/j.earscire2023.104368.

Roger A.J. and Susko E. (2018) Molecular clocks provide little information to date methanogenic Archaea. *Nature Ecology & Evolution*, **2**, 1676–1677, doi:10.1038/s41559-018-0687-z.

Rollinson H., Adetunji J., Lenaz D. and Szilas K. (2017) Archaean chromitites show constant $Fe^{3+}/\Sigma Fe$ in Earth's asthenospheric mantle since 3.8 Ga. *Lithos*, **282–283**, 316–325, doi:10.1016/j.lithos.2017.03.020.

Rubie D.C., Frost D.J., Mann U., Asahara Y., Nimmo F., Tsuno K., Kegler P., Holzheid A. and Palme, H. (2011) Heterogeneous accretion, composition and core–mantle differentiation of the Earth. *Earth and Planetary Science Letters*, **301**, 31–42, doi:10.1016/j.epsl.2010.11.030.

Rubie D.C., Jacobson S.A., Morbidelli A., O'Brien D.P., Young E.D., De Vries J., Nimmo F., Palme H. and Frost D.J. (2015) Accretion and differentiation of the terrestrial planets with implications for the compositions of early-formed Solar System bodies and accretion of water. *Icarus*, **248**, 89–108, doi:10.1016/j.icarus.2014.10.015.

Ruff S.E. *et al.* (2023) Hydrogen and dark oxygen drive microbial productivity in diverse groundwater ecosystems. *Nature Communications*, **14**, 3194, doi:10.1038/s41467-023-38523-4.

Runge E.A., Mansor M., Kappler A. and Duda J.-P. (2023) Microbial biosignatures in ancient hydrothermal sulfides. *Geobiology*, **21**, 355–377.

Rush J.D. and Bielski B.H.J. (1985) Pulse radiolytic studies of the reaction of perhydroxyl/superoxide O_2- with iron(II)/iron(III) ions. The reactivity of HO_2/O_2- with ferric ions and its implication on the occurrence of the Haber–Weiss reaction. *The Journal of Physical Chemistry*, **89**, 5062–5066, doi:10.1021/j100269a035.

Rye R. and Holland H.D. (1998) Paleosols and the evolution of atmospheric oxygen: a critical review. *American Journal of Science*, **298**, 621–672.

Sánchez-Baracaldo P. (2015) Origin of marine planktonic cyanobacteria. *Scientific Reports*, **5**, 17418, doi:10.1038/srep17418.

Sánchez-Baracaldo P., Bianchini G., Di Cesare A., Callieri C. and Chrismas N.A.M. (2019) Insights Into the Evolution of Picocyanobacteria and Phycoerythrin Genes (mpeBA and cpeBA). *Frontiers in Microbiology*, **10**, 45, doi:10.3389/fmicb.2019.00045.

Sánchez-Baracaldo P., Raven J.A., Pisani D. and Knoll A.H. (2017) Early photosynthetic eukaryotes inhabited low-salinity habitats. *Proceedings of the National Academy of Sciences*, **114**, doi:10.1073/pnas.1620089114.

Sánchez-Baracaldo P., Ridgwell A. and Raven J.A. (2014) A Neoproterozoic Transition in the Marine Nitrogen Cycle. *Current Biology*, **24**, 652–657, doi:10.1016/j.cub.2014.01.041.

Scaillet B. and Gaillard F. (2011) Redox state of early magmas. *Nature*, **480**, 48–49, doi:10.1038/480048a.

Schaefer L. and Elkins-Tanton L.T. (2018) Magma oceans as a critical stage in the tectonic development of rocky planets. *Philosophical Transactions of the Royal Society A: Mathematical, Physical and Engineering Sciences*, **376**, 20180109, doi:10.1098/rsta.2018.0109.

Schidlowski M. (2001) Carbon isotopes as biogeochemical recorders of life over 3.8 Ga of Earth history: evolution of a concept. *Precambrian Research*, **106**, 117–134, doi:10.1016/S0301-9268(00)00128-5.

Schidlowski M. (1981) Uraniferous constituents of the Witwatersrand conglomerates: ore-microscopic observations and implications for the Witwatersrand metallogeny.

Schippers A., Neretin L.N., Lavik G., Leipe T. and Pollehne F. (2005) Manganese (II) oxidation driven by lateral oxygen intrusions in the western Black Sea. *Geochimica et Cosmochimica Acta*, **69**, 2241–2252, doi:10.1016/j.gca.2004.10.016.

Schirrmeister B.E., Gugger M. and Donoghue P.C.J. (2015) Cyanobacteria and the Great Oxidation Event: evidence from genes and fossils. *Palaeontology*, **58**, 769–785, doi:10.1111/pala.12178.

Schirrmeister B.E., Sanchez-Baracaldo P. and Wacey D. (2016) Cyanobacterial evolution during the Precambrian. *International Journal of Astrobiology*, **15**, 187–204, doi:10.1017/S1473550415000579.

Schönbächler M., Carlson R.W., Horan M.F., Mock T.D. and Hauri E.H. (2010) Heterogeneous accretion and the moderately volatile element budget of Earth. *Science*, **328**, 884–887, doi:10.1126/science.1186239.

Schopf J.W. (1993) Microfossils of the Early Archean Apex Chert: New evidence of the antiquity of life. *Nature*, **260**, 640–646.

Schröder S., Bedorf D., Beukes N.J. and Gutzmer J. (2011) From BIF to red beds: Sedimentology and sequence stratigraphy of the Paleoproterozoic Koegas Subgroup (South Africa). *Sedimentary Geology*, **236**, 25–44, doi:10.1016/j.sedgeo.2010.11.007.

Schwieterman E.W. *et al.* (2018) Exoplanet biosignatures: a review of remotely detectable signs of Life. *Astrobiology*, **18**, 663–708, doi:10.1089/ast.2017.1729.

Scott C.T., Bekker A., Reinhard C.T., Schnetger B., Krapež B., Rumble D. and Lyons T.W. (2011) Late Archean euxinic conditions before the rise of atmospheric oxygen. *Geology*, **39**, 119–122, doi:10.1130/G31571.1.

Scott C., Lyons T.W., Bekker A., Shen Y., Poulton S.W., Chu X. and Anbar A.D. (2008) Tracing the stepwise oxygenation of the Proterozoic ocean. *Nature*, **452**, 456–459, doi:10.1038/nature06811.

Segerer A., Neuner A., Kristjansson J.K. and Stetter K.O. (1986) *Acidianus infernus gen. nov.*, sp. nov., and *Acidianus brierleyi Comb. nov.*: Facultatively aerobic, extremely acidophilic thermophilic sulfur-metabolizing

Archaebacteria. *International Journal of Systematic Bacteriology*, **36**, 559–564, doi:10.1099/00207713-36-4-559.

Sekine Y. *et al.* (2011) Manganese enrichment in the Gowganda Formation of the Huronian Supergroup: A highly oxidizing shallow-marine environment after the last Huronian glaciation: *Earth and Planetary Science Letters*, **307**, 201–210, doi:10.1016/j.epsl.2011.05.001.

Sengupta S. and Pack A. (2018) Triple oxygen isotope mass balance for the Earth's oceans with application to Archean cherts. *Chemical Geology*, **495**, 18–26, doi:10.1016/j.chemgeo.2018.07.012.

Sharp Z.D., McCubbin F.M. and Shearer C.K. (2013) A hydrogen-based oxidation mechanism relevant to planetary formation. *Earth and Planetary Science Letters*, **380**, 88–97, doi:10.1016/j.epsl.2013.08.015.

Shen Y., Farquhar J., Masterson A., Kaufman A.J. and Buick R. (2009) Evaluating the role of microbial sulfate reduction in the early Archean using quadruple isotope systematics. *Earth and Planetary Science Letters*, **279**, 383–391, doi:10.1016/j.epsl.2009.01.018.

Sherwood Lollar B. and McCollom T.M. (2006) Biosignatures and abiotic constraints on early life. *Nature*, **444**, E18, doi:10.1038/nature05499.

Shi T. and Falkowski P.G. (2008) Genome evolution in cyanobacteria: The stable core and the variable shell. *Proceedings of the National Academy of Sciences*, **105**, 2510–2515, doi:10.1073/pnas.0711165105.

Shibuya T., Komiya T., Nakamura K., Takai K. and Maruyama S. (2010) Highly alkaline, high-temperature hydrothermal fluids in the early Archean ocean. *Precambrian Research*, **182**, 230–238, doi:10.1016/j.precamres.2010.08.011.

Siebert J., Badro J., Antonangeli D. and Ryerson F.J. (2013) Terrestrial accretion under oxidizing conditions. *Science*, **339**, 1194–1197, doi:10.1126/science.1227923.

Smart K.A., Tappe S., Stern R.A., Webb S.J. and Ashwal L.D. (2016) Early Archaean tectonics and mantle redox recorded in Witwatersrand diamonds. *Nature Geoscience*, **9**, 255–259, doi:10.1038/ngeo2628.

Smit M.A. and Mezger K. (2017) Earth's early O_2 cycle suppressed by primitive continents. *Nature Geoscience*, **10**, 788–792, doi:10.1038/ngeo3030.

Smith A.J.B. (2018) The iron formations of Southern Africa. Pp. 469–491 in: *Geology of Southwest Gondwana* (S. Siegesmund, M.A.S. Basei, P. Oyhantçabal, and S. Oriolo, editors), Springer International Publishing, Cham, doi:10.1007/978-3-319-68920-3_17.

Smith A.J.B. and Beukes N.J. (2023) The paleoenvironmental implications of pre-Great Oxidation Event manganese deposition in the Mesoarchean Ijzermijn Iron Formation Bed, Mozaan Group, Pongola Supergroup, South Africa. *Precambrian Research*, **384**, 106922, doi:10.1016/j.precamres.2022.106922.

Smithies R.H., Champion D.C., Van Kranendonk M.J., Howard H.M. and Hickman A.H. (2005) Modern-style subduction processes in the Mesoarchaean: Geochemical evidence from the 3.12 Ga Whundo intra-oceanic arc. *Earth and Planetary Science Letters*, **231**, 221–237, doi:10.1016/j.epsl.2004.12.026.

Søgaard E.G., Medenwaldt R. and Abraham-Peskir J.V. (2000) Conditions and rates of biotic and abiotic iron precipitation in selected Danish freshwater plants and microscopic analysis of precipitate morphology. *Water Research*, **34**, 2675–2682, doi:10.1016/S0043-1354(00)00002-6.

Sommer T. *et al.*, (2017) Bacteria-induced mixing in natural waters. *Geophysical Research Letters*, **44**, 9424–9432.

Soo R.M., Hemp J., Parks D.H., Fischer W.W. and Hugenholtz P. (2017) On the origins of oxygenic photosynthesis and aerobic respiration in Cyanobacteria. *Science*, **355**, 1436–1440, doi:10.1126/science.aal3794.

Stagno V., and Aulbach S. (2021) Redox processes before, during, and after Earth's accretion affecting the deep carbon cycle in: *Magma Redox Geochemistry* (R. Moretti and D.R. Neuville, editors), *Geophysical Monograph Series* Vol. **266**, AGU & Wiley, Hoboken, USA.

Stagno V. and Fei Y. (2020) The redox boundaries of Earth's interior. *Elements*, **16**, 167–172, doi:10.2138/gselements.16.3.167.

Stockey R.G., Cole D.B., Farrell U.C., Agić H., Boag T.H., Brocks J.J., Canfield D.E., Cheng M., Crockford P.W., Cui H., Dahl T.W., Del Mouro L., Dewing K., Dornbos S.Q., Emmings J.F., Gaines R.R., Gibson T.M., Gill B.C., Gilleaudeau G.J. … Sperling E.A. (2024) Sustained increases in atmospheric oxygen and marine productivity in the Neoproterozoic and Palaeozoic eras. *Nature Geoscience*, **17**(7), 667–674. https://doi.org/10.1038/s41561-024-01479-1.

Stolper D.A., Revsbech N.P. and Canfield D.E. (2010) Aerobic growth at nanomolar oxygen concentrations. *Proceedings of the National Academy of Sciences*, **107**, 18755–18760, doi:10.1073/pnas.1013435107.

Stone J., Edgar J.O., Gould J.A. and Telling J. (2022) Tectonically-driven oxidant production in the hot biosphere. *Nature Communications*, **13**, 4529, doi:10.1038/s41467-022-32129-y.

Stüeken E.E., Boocock T.J., Robinson A., Mikhail S. and Johnson B.W. (2021) Hydrothermal recycling of sedimentary ammonium into oceanic crust and the Archean ocean at 3.24 Ga. *Geology*, **49**, 822–826, doi:10.1130/G48844.1.

Stüeken E.E. and Buick R. (2018) Environmental control on microbial diversification and methane production in the Mesoarchean. *Precambrian Research*, **304**, 64–72, doi:10.1016/j.precamres.2017.11.003.

Stüeken E.E., Buick R., Anderson R.E., Baross J.A., Planavsky N.J. and Lyons T.W. (2017) Environmental niches and metabolic diversity in Neoarchean lakes. *Geobiology*, **15**, 767–783, doi:10.1111/gbi.12251.

Stüeken E.E., Buick R., Guy B.M. and Koehler M.C. (2015a) Isotopic evidence for biological nitrogen fixation by molybdenum-nitrogenase from 3.2 Gyr. *Nature*, **520**, 666–669, doi:10.1038/nature14180.

Stüeken E.E., Buick R. and Schauer A.J. (2015b) Nitrogen isotope evidence for alkaline lakes on late Archean continents. *Earth and Planetary Science Letters*, **411**, 1–10, doi:10.1016/j.epsl.2014.11.037.

Stüeken E.E., Kipp M.A., Koehler M.C. and Buick R. (2016) The evolution of Earth's biogeochemical nitrogen cycle. *Earth-Science Reviews*, **160**, 220–239, doi:10.1016/j.earscire2016.07.007.

Stüeken E.E., Pellerin A., Thomazo C., Johnson B.W., Duncanson S. and Schoepfer S.D. (2024) Marine biogeochemical nitrogen cycling through Earth's history. *Nature Reviews Earth & Environment*, doi:10.1038/s43017-024-00591-5.

Sun L., Lechte M., Shi X., Zhou X., Zhou L., Feng H., Xie B., Wu M. and Tang D. (2022) Hexagonal magnetite in Algoma-type banded iron formations of the ca. 2.52 Ga Baizhiyan Formation, North China: Evidence for a green rust precursor? *American Mineralogist*, **107**, 970–984.

Swanner E.D., Mloszewska A.M., Cirpka O.A., Schoenberg R., Konhauser K.O. and Kappler A. (2015a) Modulation of oxygen production in Archaean oceans by episodes of Fe(II) toxicity. *Nature Geoscience*, **8**, 126–130, doi:10.1038/ngeo2327.

Swanner E.D., Wu W., Hao L., Wüstner M.L., Obst M., Moran D.M., McIlvin M.R., Saito M.A. and Kappler A. (2015b) Physiology, Fe(II) oxidation, and Fe mineral formation by a marine planktonic cyanobacterium grown under ferruginous conditions. *Frontiers in Earth Science*, **3**, doi:10.3389/feart.2015.00060.

Tamaura Y., Yoshida T. and Katsura T. (1984) The synthesis of green rust II ($FeIII_1$-$FeII_2$) and its spontaneous transformation into Fe_3O_4. *Bulletin of the Chemical Society of Japan*, **57**, 2411–2416.

Tatzel M., Frings P.J., Oelze M., Herwartz D., Lünsdorf N.K. and Wiedenbeck M. (2022) Chert oxygen isotope ratios are driven by Earth's thermal evolution. *Proceedings of the National Academy of Sciences*, **119**, e2213076119, doi:10.1073/pnas.2213076119.

Tebo B.M. (1991) Manganese(II) oxidation in the suboxic zone of the Black Sea. *Deep Sea Research Part A. Oceanographic Research Papers*, **38**, S883–S905, doi:10.1016/S0198-0149(10)80015-9.

Tebo B.M., Bargar J.R., Clement B.G., Dick G.J., Murray K.J., Parker D., Verity R. and Webb, S.M. (2004) Biogenic manganese oxides: properties and mechanisms of formation. *Annual Review of Earth and Planetary Sciences*, **32**, 287–328, doi:10.1146/annureearth.32.101802.120213.

Tebo B.M., Johnson H.A., McCarthy J.K. and Templeton A.S. (2005) Geomicrobiology of manganese(II) oxidation. *Trends in Microbiology*, **13**, 421–428, doi:10.1016/j.tim.2005.07.009.

Thamdrup, B., Dalsgaard, T. and Revsbech, N.P. (2012) Widespread functional anoxia in the oxygen minimum zone of the Eastern South Pacific. *Deep Sea Research Part I: Oceanographic Research Papers*, **65**, 36–45, doi:10.1016/j.dsr.2012.03.001.

Thomazo C., Ader M., Farquhar J. and Philippot P. (2009a) Methanotrophs regulated atmospheric sulfur isotope anomalies during the Mesoarchean (Tumbiana Formation, Western Australia). *Earth and Planetary Science Letters*, **279**, 65–75, doi:10.1016/j.epsl.2008.12.036.

Thomazo C., Ader M. and Philippot P. (2011) Extreme ^{15}N-enrichments in 2.72-Gyr-old sediments: evidence for a turning point in the nitrogen cycle. *Geobiology*, **9**, 107–120.

Thomazo C., Pinti D.L., Busigny V., Ader M., Hashizume K. and Philippot P. (2009b) Biological activity and the Earth's surface evolution: Insights from

carbon, sulfur, nitrogen and iron stable isotopes in the rock record. *Comptes Rendus Palevol*, **8**, 665–678, doi:10.1016/j.crp2009.02.003.

Thompson K.J. *et al.* (2019) Photoferrotrophy, deposition of banded iron formations, and methane production in Archean oceans. *Science Advances*, **5**, eaav2869, doi:10.1126/sciadaav2869.

Thorpe R.I. (1979) A sedimentary barite deposit from the Archean Fig Tree Group of the Barberton Mountain Land (South Africa); discussion. *Economic Geology*, **74**, 700–702.

Towe K.M. (1990) Aerobic respiration in the Archaean? *Nature*, **348**, 54–56, doi:10.1038/348054a0.

Trail D., Watson E.B. and Tailby N.D. (2011) The oxidation state of Hadean magmas and implications for early Earth's atmosphere. *Nature*, **480**, 79–82, doi:10.1038/nature10655.

Trendall A.F. (2002) The significance of iron-formation in the Precambrian stratigraphic record. Pp. 33–66 in: *Precambrian Sedimentary Environments* (W. Altermann and P.L. Corcoran, editors), Wiley, doi:10.1002/9781444304312.ch3.

Tsikos H., Beukes N.J., Moore J.M. and Harris C. (2003) Deposition, diagenesis, and secondary enrichment of metals in the Paleoproterozoic Hotazel Iron Formation, Kalahari manganese field, South Africa. *Economic Geology*, **98**, 1449–1462.

Tusch J., Hoffmann J.E., Hasenstab E., Fischer-Gödde M., Marien C.S., Wilson A.H. and Münker C. (2022) Long-term preservation of Hadean protocrust in Earth's mantle. *Proceedings of the National Academy of Sciences*, **119**, e2120241119, doi:10.1073/pnas.2120241119.

Tusch J., Münker C., Hasenstab E., Jansen M., Marien C.S., Kurzweil F., Van Kranendonk M.J., Smithies H., Maier W. and Garbe-Schönberg D. (2021) Convective isolation of Hadean mantle reservoirs through Archean time. *Proceedings of the National Academy of Sciences*, **118**, e2012626118, doi:10.1073/pnas.2012626118.

Ueno Y., Ono S., Rumble D. and Maruyama S. (2008) Quadruple sulfur isotope analysis of ca. 3.5Ga Dresser Formation: New evidence for microbial sulfate reduction in the early Archean. *Geochimica et Cosmochimica Acta*, **72**, 5675–5691, doi:10.1016/j.gca.2008.08.026.

Ueno Y., Yamada K., Yoshida N., Maruyama S. and Isozaki Y., 2006, Evidence from fluid inclusions for microbial methanogenesis in the early Archaean era: *Nature*, **440**, 516–519, doi:10.1038/nature04584.

Valley J.W., Peck W.H., King E.M. and Wilde S.A. (2002) A cool early Earth. *Geology*, **30**, 351–354.

Van De Graaf A.A., Mulder A., De Bruijn P., Jetten M.S., Robertson L.A. and Kuenen J.G. (1995) Anaerobic oxidation of ammonium is a biologically mediated process. *Applied and Environmental Microbiology*, **61**, 1246–1251, doi:10.1128/aem.61.4.1246-1251.1995.

Van Kranendonk M.J. (2011) Onset of Plate Tectonics. *Science*, **333**, 413–414, doi:10.1126/science.1208766.

Van Kranendonk M.J., Smithies H.R., Hickman A.H. and Champion D.C. (2007) Review: secular tectonic evolution of Archean continental crust: interplay between horizontal and vertical processes in the formation of the Pilbara Craton, Australia. *Terra Nova*, **19**, 1–38, doi:10.1111/j.1365-3121.2006.00723.x.

Wacey D., Saunders M., Brasier M.D. and Kilburn M.R. (2011) Earliest microbially mediated pyrite oxidation in ~3.4 billion-year-old sediments. *Earth and Planetary Science Letters*, **301**, 393–402, doi:10.1016/j.epsl.2010.11.025.

Wade J. and Wood B.J. (2005) Core formation and the oxidation state of the Earth. *Earth and Planetary Science Letters*, **236**, 78–95, doi:10.1016/j.epsl.2005.05.017.

Wade J. and Wood B.J. (2001) The Earth's 'missing' niobium may be in the core. *Nature*, **409**, 75–78, doi:10.1038/35051064.

Wadhwa M. (2008) Redox conditions on small bodies, the Moon and Mars. *Reviews in Mineralogy and Geochemistry*, **68**, 493–510.

Wadhwa M. (2001) Redox state of Mars' upper mantle and crust from Eu anomalies in shergottite pyroxenes. *Science*, **291**, 1527–1530, doi:10.1126/science.1057594.

Waldbauer J.R., Sherman L.S., Sumner D.Y. and Summons R.E. (2009) Late Archean molecular fossils from the Transvaal Supergroup record the antiquity of microbial diversity and aerobiosis. *Precambrian Research*, **169**, 28–47, doi:10.1016/j.precamres.2008.10.011.

Wallmann K. (2001) The geological water cycle and the evolution of marine $\delta^{18}O$ values. *Geochimica et Cosmochimica Acta*, **65**, 2469–2485.

Walter M.R., Buick R., and Dunlop J.S.R. (1980) Stromatolites 3,400–3,500 Myr old from the North Pole area, Western Australia. *Nature*, **284**, 443–445, doi:10.1038/284443a0.

Walton C.R., Ewens S., Coates J.D., Blake R.E., Planavsky N.J., Reinhard C., Ju P., Hao J. and Pasek M.A. (2023) Phosphorus availability on the early Earth and the impacts of life. *Nature Geoscience*, **16**, 399–409, doi:10.1038/s41561-023-01167-6.

Wang X. *et al.* (2018) A Mesoarchean shift in uranium isotope systematics. *Geochimica et Cosmochimica Acta*, **238**, 438–452, doi:10.1016/j.gca.2018.07.024.

Wang M., Jiang Y.-Y., Kim K.M., Qu G., Ji H.-F., Mittenthal J.E., Zhang H.-Y. and Caetano-Anollés G. (2011) A universal molecular clock of protein folds and its power in tracing the early history of aerobic metabolism and planet oxygenation. *Molecular Biology and Evolution*, **28**, 567–582, doi:10.1093/molbev/msq232.

Wang X., Ossa Ossa F., Hofmann A., Agangi A., Paprika D. and Planavsky N.J. (2020) Uranium isotope evidence for Mesoarchean biological oxygen production in shallow marine and continental settings. *Earth and Planetary Science Letters*, **551**, 116583, doi:10.1016/j.epsl.2020.116583.

Wänke H., Dreibus G. and Jagoutz E. (1984) Mantle chemistry and accretion history of the Earth. Pp. 1–24 in: *Archaean Geochemistry* (A. Kröner, G.N. Hanson, and A.M. Goodwin, editors). Springer, Berlin, Heidelberg, doi:10.1007/978-3-642-70001-9_1.

Warke M.R., Di Rocco T., Zerkle A.L., Lepland A., Prave A.R., Martin A.P., Ueno Y., Condon D.J. and Claire M.W. (2020) The Great Oxidation Event preceded a Paleoproterozoic 'snowball Earth'. *Proceedings of the National Academy of Sciences*, **117**, 13314–13320, doi:10.1073/pnas.2003090117.

Watanabe Y. and Tajika E. (2021) Atmospheric oxygenation of the early earth and earth-like planets driven by competition between land and seafloor weathering. *Earth, Planets and Space*, **73**, 188, doi:10.1186/s40623-021-01527-9.

Whitehill A.R. and Ono S. (2012) Excitation band dependence of sulfur isotope mass-independent fractionation during photochemistry of sulfur dioxide using broadband light sources. *Geochimica et Cosmochimica Acta*, **94**, 238–253, doi:10.1016/j.gca.2012.06.014.

Whitehill A.R., Xie C., Hu X., Xie D., Guo H. and Ono S. (2013) Vibronic origin of sulfur mass-independent isotope effect in photoexcitation of SO_2 and the implications to the early earth's atmosphere. *Proceedings of the National Academy of Sciences*, **110**, 17697–17702, doi:10.1073/pnas.1306979110.

Whitehouse M.J., Kamber B.S., Fedo C.M. and Lepland, A. (2005) Integrated Pb- and S-isotope investigation of sulphide minerals from the early Archaean of southwest Greenland. *Chemical Geology*, **222**, 112–131, doi:10.1016/j.chemgeo.2005.06.004.

Williams R.J.P. and Fraústo Da Silva J.J.R. (2003) Evolution was chemically constrained. *Journal of Theoretical Biology*, **220**, 323–343, doi:10.1006/jtbi.2003.3152.

Wolfe J.M. and Fournier G.P. (2018) Horizontal gene transfer constrains the timing of methanogen evolution. *Nature Ecology & Evolution*, **2**, 897–903, doi:10.1038/s41559-018-0513-7.

Wong M.L., Charnay B.D., Gao P., Yung Y.L. and Russell M.J. (2017) Nitrogen oxides in early Earth's atmosphere as electron acceptors for life's emergence. *Astrobiology*, **17**, 975–983, doi:10.1089/ast.2016.1473.

Wood B.J., Bryndzia L.T. and Johnson K.E. (1990) Mantle oxidation state and its relationship to tectonic environment and fluid speciation. *Science*, **248**, 337–345, doi:10.1126/science.248.4953.337.

Wood B.J. and Virgo D. (1989) Upper mantle oxidation state: Ferric iron contents of lherzolite spinels by ^{57}Fe Mössbauer spectroscopy and resultant oxygen fugacities. *Geochimica et Cosmochimica Acta*, **53**, 1277–1291.

Xu D., Qin Z., Wang X., Li J., Shi X., Tang D. and Liu J. (2023) Extensive sea-floor oxygenation during the early Mesoproterozoic. *Geochimica et Cosmochimica Acta*, **354**, 186–196, doi:10.1016/j.gca.2023.06.007.

Yang X., Liu H. and Zhang K. (2022) Redox geodynamics in Earth's interior. *Science China Earth Sciences*, **65**, 624–640, doi:10.1007/s11430-021-9864-8.

Yang W.H., Weber K.A. and Silver W.L. (2012) Nitrogen loss from soil through anaerobic ammonium oxidation coupled to iron reduction. *Nature Geoscience*, **5**, 538–541, doi:10.1038/ngeo1530.

Yu H. and Leadbetter J.R., (2020) Bacterial chemolithoautotrophy via manganese oxidation. *Nature*, **583**, 453–458, doi:10.1038/s41586-020-2468-5.

https://doi.org/10.1180/gbi.2025.10003 Published online by Cambridge University Press

Zahnle K., Claire M. and Catling D. (2006) The loss of mass-independent fractionation in sulfur due to a Palaeoproterozoic collapse of atmospheric methane. *Geobiology*, **4**, 271–283.

Zakharov D.O., Bindeman I.N., Tanaka R., Friðleifsson G.Ó., Reed, M.H. and Hampton, R.L., (2019) Triple oxygen isotope systematics as a tracer of fluids in the crust: A study from modern geothermal systems of Iceland. *Chemical Geology*, **530**, 119312, doi:10.1016/j.chemgeo.2019.119312.

Zehr J.P. and Kudela R.M. (2011) Nitrogen cycle of the open ocean: from genes to ecosystems. *Annual Review of Marine Science*, **3**, 197–225, doi:10.1146/annurev-marine-120709-142819.

Zerkle A.L., House C.H., Cox R.P. and Canfield D.E. (2006) Metal limitation of cyanobacterial N_2 fixation and implications for the Precambrian nitrogen cycle. *Geobiology*, **4**, 285–297, doi:10.1111/j.1472-4669.2006.00082.x.

Zhang X., Shu D., Han J., Zhang Z., Liu J. and Fu D. (2014) Triggers for the Cambrian explosion: Hypotheses and problems. *Gondwana Research*, **25**, 896–909, doi:10.1016/j.gr.2013.06.001.

Zhao M., Mills B.J.W., Homoky W.B. and Peacock, C.L. (2023) Oxygenation of the Earth aided by mineral–organic carbon preservation. *Nature Geoscience*, **16**, 262–267, doi:10.1038/s41561-023-01133-2.

https://doi.org/10.1180/gbi.2025.10003 Published online by Cambridge University Press